A Study of the Brass Instrument Lip Reed Mechanism using Artificial Lips and Lattice Boltzmann Flow Simulations

Mark Neal

A thesis submitted in fulfilment of the requirements

for the degree of Doctor of Philosophy

to the

University of Edinburgh

2002

Abstract

The lips of a brass player form a complex mechanical oscillator which has a non-harmonic set of resonance frequencies. In order for the lips to create a note when a player starts to play a brass instrument there must be interactions between the mechanical resonances of the lips, the fluid dynamics of the air passing between the lips, and the acoustic pressures which surround the lips. In this thesis studies are made of these interactions utilising an artificial lip and mouth to perform experimental measurements and Lattice Boltzmann fluid simulations to study the flow of air between the lips.

By taking mechanical response measurements of the artificial lips, the mechanical resonances of the lips have been examined. The effects of both air flow between the lips and the presence of acoustic resonators, both in the form of an instrument on the downstream side of the lips and the mouth cavity on the upstream side of the lips have been studied. Results of these measurements have shown that the lips of a brass player can behave in either of two lip reed operating regimes (inward or outward striking), depending on the relationship between the resonance frequency of the lips and that of the resonator. The behaviour of the lips during the transition between inward and outward striking regimes has been studied in order that improved models of the lip reed can be constructed.

Numerical simulations of the flow in a pipe with a constriction which is based

on the shape of a player's lips both with and without a mouthpiece downstream of the lips have provided information on how the jet formation by the lips occurs. By using the data from these simulations the sizes of the forces which lead to the inward and outward striking behaviour of the lips have been estimated and a clearer picture of the physics behind the operation of a brass player's lips obtained.

Declaration

I do hereby declare that this thesis was composed by myself and that the work described within is my own, except where explicitly stated otherwise.

Mark Neal

3rd Sept 2002

Acknowledgements

I would like to thank my supervisors Murray Campbell and Clive Greated for their advice and guidance during this research programme. I would also like to thank Joel Gilbert for his discussions and advice on the experimental work. Particular thanks also go to John Cullen for help with experimenal techniques and provision of analysis programs and to Jim Buick for help with the Lattice Boltzmann programs. Thanks also to Ted Schlicke for much useful assistance with programming, Alison Frydman for proof reading and to all my other colleagues in the University of Edinburgh Acoustics and Fluids group; Jim Buick, Dawn Rockliff, Susan Jack, Orlando Richards, Maarten Van Walstijn, Steven Tonge, David Skulina, Jonathan Kemp, David Sharp, Alix Thomas, Scott Coltman, Calum Gray, Thomas MacGillvary, David Forehand, Alan Marson, Sandra Carral and John Cosgrove.

Finacial support was provided by EPSRC.

Thanks also to all my friends who helped me keep going and keep moderately sane especially all the musicians who I have played with: Andrew, Jonathan, Mike, Colin and Kit. Finally thanks to all my family: Mum, Dad and Julie.

Contents

List of Figures

Chapter 1

Introduction

1.1 A review of brass instrument acoustics

The act of a musician playing a note on brass wind instruments comes about through the coupling between the motion of the player's lips, which act as a flow control valve, and an acoustic resonator in the form of an instrument. The lips of a brass player act in many ways like the reed of a woodwind instrument, giving a rapidly oscillating passage into the instrument through which the air blown by the player passes. For reed or lip reed driven wind instruments, the reed behaviour can be categorised into two main categories as originally defined by Helmholtz [35], inward and outward striking. Inward striking reeds are those where an increase in the blowing pressure leads to closing of the reed, whereas outward striking reeds are those where an increase in blowing pressure opens the

reed. In this simple classification the reed can be considered as a single mass on a spring referred to as the 'one mass model'. This model of the lips was first set out in the work of Elliott and Bowsher [27] which is also extensively discussed by Campbell and Greated [15]. Since Helmholtz's initial classification of these two reed types, various studies have been done into aspects of the lip reed, further refining the lip models thorough both experimental work [18] [20] [52] and refining of the mathematical models used to understand the lips [2] [1] [29] [46]. These studies have shown that reed behaviour of a brass player's lips cannot be simply classified as either inward or outward striking, but rather a more advanced model of the lip reed is needed. Precise measurement of the behaviour of the lips during playing has remained difficult due to the inaccessibility of the lips during playing and the complications involved with measuring the properties of the lips, due to the large variety of changes which a player can make through muscular activity.

The development of an artificial lip capable of playing brass instruments by Gilbert and Petiot [33] greatly increased the possibilities of studying of the lip motion during the playing of brass instruments. This artificial lip enables measurements to be taken over extended periods of time without the problems associated with real player measurements such as the variability of the lip parameters with time as the player becomes tired. The artificial lips also enable experimental configurations which would not be possible using a real player, in addition to avoiding any psychological problems of the player "correcting" for poor sounding or out of tune notes. The design of this artificial lip was extended by Cullen [21],

[22], increasing the control over some of the limited number of lip parameters which can be adjusted on the artificial lips. Cullen performed experiments using the artificial lips, looking into how the behaviour and playing characteristics are affected by changes in lip parameters, mouth over pressure and coupling to the acoustic resonances of an instrument. Much of this current work is a direct extension following on from the work of Cullen.

The acoustics of brass instrument resonators has been extensively studied [6], [27], [30], [31] and there are well established experimental and theoretical models for the acoustic behaviour of the resonator and the radiation of sound from the instrument. In terms of the simple models of lip reed behaviour which are used in the following work, only a limited view of the acoustic resonator need be considered. For the simple one mass model, only a single resonant mode of the instrument which is in close proximity to the frequency of the note played need be considered. Even when this model is extended to enable transitions between inward and outward behaviour of the lip reed, only two or three of the resonant modes of the instrument need to be taken into account.

1.2 Techniques for studying brass instruments

The structure of the brass player's lips means that the lips have a series of non-harmonic mechanical resonances which can be changed by the player by altering

the tension and pressure of the lips. Using the artificial lips a limited number of these lip parameters such as the pressure of the teeth on the back of the lips, pressing them against the mouthpiece rim and relative position of the lips to each other can be adjusted. In order to measure the effect of changing these parameters on the resonant frequencies of the lips, measurements of the mechanical response of the lips to a set acoustic field can be made. For these measurements the lips are driven from one side with an acoustic signal of known frequency and amplitude; the amplitude and phase response of the lips to this driving signal can then be measured. By performing this type of measurement over a range of frequencies a graph showing the lip resonances along with the phase response of the lips at each frequency can be obtained.

Measurements of the playing properties of the lips can also be measured by taking simultaneous signals from microphones placed in the mouth cavity, in the mouthpiece and at the bell of the instrument, as well as signals from sensors measuring the motion of the lips. The amplitude and phase response of these signals can be compared to give a greater understanding of the behaviour of the lips when playing.

Acoustic properties of the instrument used during these experiments can best be obtained from acoustic input impedance measurements. In this study these measurements were done using a setup based on that suggested by Backus [6]. By comparing the acoustic resonance frequency of the instrument with the lip

resonance frequency and the frequency of the note produced by the instrument, and using the simple one mass model analogy the reed behaviour of the lips can, within the limitations of the model, be determined.

In addition to these measurements on the artificial lips, an experimental technique devised by Ayers [4] using a mouthpiece with a hole bored in the side can be used to compare the lip resonance frequencies of real players with those obtained using the artificial lips.

1.3 Numerical modeling of fluid flows

Computational fluid dynamics (CFD) is an area of research which has been growing rapidly over recent years due to the large increase in computational power available. Most methods for performing CFD have involved numerically solving the Navier-Stokes equation using finite difference or finite element approaches [19]. These methods work well for simple flows, but can be considerably more difficult if complicated flows or flow boundaries are required.

An alternative way to simulate flow is to use an approach deriving from molecular dynamics. These techniques come from the idea that if each molecule of the fluid is simulated with the correct inter-molecular interactions then the model will behave like a fluid. This method of fluid simulation has the disadvantage that it takes a large amount of computational power to make a significant simulation,

as a large number of molecules must be simulated and the time steps between successive calculations must be very small. These problems limit the possibilities for molecular dynamics simulations.

The molecular dynamics model can be extended to consider a number of 'fluid particles' which, although much larger than the molecules in the fluid, are still much smaller than the smallest length scale in the simulation. This is the method used in the Lattice Gas Model [32]. Using the Lattice Gas Model simulations of a much larger scale can be simulated while still retaining the advantages of being fairly simple to simulate complicated flow and boundary configurations. The Lattice Boltzmann Model is a further extension of the lattice gas model, made to overcome some of the shortcomings of the Lattice Gas Model. The Lattice Boltzmann model utilizes particle distribution functions at the nodes of the simulation grid which can travel along the vertices of the grid at each time step. After the particle distributions have streamed along the vertices, a collision operation is performed on the different particles arriving at each node using the Boltzmann equation (1.1)

$$\frac{\partial f}{\partial t} + \mathbf{c} \cdot \frac{\partial f}{\partial r} + \mathbf{F} \cdot \frac{\partial f}{\partial c} = \Omega(f) \tag{1.1}$$

where $f(\mathbf{r}, \mathbf{c}, t)$ is the distribution function, $\mathbf{c}(\mathbf{r}, t)$ is the particle velocity, $\mathbf{F}(\mathbf{r}, t)$ is the force per unit mass and $\Omega(f)$ is a collision function.

The Lattice Boltzmann Method retains the advantages of easy handling of

complicated flows and boundary shapes, while also keeping interactions such that at any time step the particle distribution at a certain node can only be affected by its nearest neighbours. This makes the Lattice Boltzmann Method particularly suitable for running on parallel computers as the simulation can be easily divided up into different regions, with the computation in each region performed by a different processor.

The Lattice Boltzmann simulations are run using a rectangular grid shape, with the simulation code reading in files containing the initialisation parameters and the wall boundaries of the flow. The creation of these files containing the initialisation parameters and wall boundaries is done using another program, in which the boundaries can be drawn by the user on a computer screen. This graphical interface enables simulations of different flow profiles to be quickly set up and run and the flow velocities and grid sizes changed as required.

1.4 Aims and contents of thesis

The aims of this study are:

1. Develop and extend experimental setup and analysis software used for measuring mechanical response and playing characteristics of the artificial lips.

2. Measure the effects of resonator changes on the mechanical response of the artificial lips both with and without mouth over pressure.

3. Measure lip motion and acoustic pressure on both sides of the lips during playing.

4. Investigate the effects of mouth cavity volume on brass instrument playing.

5. Make experimental comparisons between the artificial lips and real players.

6. Develop and verify a numerical simulation for fluid flow using the Lattice Boltzmann technique.

7. Develop a graphical interface to enable simple operation of the Lattice Boltzmann simulation code.

8. Simulate flow though various static lip models both with and without the presence of a mouthpiece.

This study is done in two main sections. The first section in Chapters 2 to 4 is concerned with experimental work, using the artificial lips to understand the playing characteristics of the brass players lips. The second section in Chapters 5 and 6 is concerned with the study of flow models using Lattice Boltzmann computational simulations.

Chapter 2 presents the basic concepts of brass instrument acoustics, starting with a brief discussion of a brass instrument resonator both from the theoretical side and from measurements of real instruments. Some of the non-linear effects present in the playing of brass instruments are then explained, leading on to a

discussion of the lip reed mechanism using a one mass model of the lips. Finally the interactions between all of these different parts of the brass instrument are discussed.

In Chapter 3 a description of the artificial lips is given along with the other apparatus used in measuring the playing characteristics of the lips. The experimental method and analysis software used for obtaining the mechanical response of the lips is then described, and the various different methods for obtaining the mechanical response compared. Finally, results obtained from mechanical response measurements using a variable length tube as a resonator are presented. These results are analysed and compared to those obtained in previous work.

Chapter 4 extends these mechanical response measurements into a discussion on the behaviour of the lip under playing conditions. Starting by looking at the threshold playing of the lips at various pipe extensions, both in terms of the threshold playing pressure and the frequency produced by the instrument when played by the artificial lips. Following this, measurements showing the effect of mouth cavity volume changes on both the mechanical response and the played note are presented. The chapter then finishes with the results from experiments which allow comparison between the playing of the artificial lips and those of a real player.

Chapter 5 introduces the Lattice Boltzmann fluid simulation technique, starting with the formulation of the model and then presenting the techniques for

handing the various different boundary conditions which are applied at the walls, inflow and outflow points of the simulation. A series of different methods for handling the outflow boundary are then presented along with some of the simulation results obtained using these different methods. The graphical interfacing program used to edit the simulation parameter and grid is then presented. This section finishes with the validation results used to test the Lattice Boltzmann code against fluid flows with a known theoretical result.

Chapter 6 presents the simulation results obtained using the Lattice Boltzmann code. These simulations start with a simple step pipe expansion. Results are presented from three pipe expansions, all having the same expansion ratio and inflow parameters but each with a different corner shape at the expansion point. Following the step expansion simulations, results of various static lip models are shown. A set of seven lip models are used, and for each model the results are presented as a series of vorticity maps for different time steps of the simulation. Results from the seven different lip models are shown, both for the case of the lip models placed part way along a constant diameter pipe, and for the lip models placed in the pipe with a constriction in the shape of a brass instrument mouthpiece placed after the lips. The chapter ends with a discussion on the application of these simulation results to the behaviour of the lips during the playing of a brass instrument.

This thesis concludes in Chapter 7 with a review of the findings obtained and some ideas for further extension of this work.

Chapter 2

Lip-flow interactions in brass instruments

2.1 Introduction

When a brass player plays a note on an instrument, the sound produced is a result of many complex interactions between the player, the instrument and the flow of air. A subtle change in any of the lip, mouth or instrument parameters can lead to a considerable change in the sound of the note produced, due to the highly non-linear nature of these interactions. This inherent complexity has led to the fact that although the physics of brass instruments has been a subject of investigation for many decades, there are still many features of the playing of brass instruments which are not understood.

Much of the complication inherent in the playing of brass instruments is due to the nature of the lip reed mechanism. The lips of a brass player form two continuous mechanical damped oscillators. Each of these has a non-harmonic set of resonances, and especially at larger oscillation amplitudes, the lips have both a non-linear response to the driving forces and close completely for part of the oscillation cycle. When this is taken into consideration along with the coupled acoustic resonators of the instrument, the mouthpiece and the mouth of the player, it is unsurprising that the exact physics behind the playing of brass instruments has remained intractable. To overcome some of the problems of understanding the working of brass instruments the system can be simplified by breaking it down into four main parts: the air supply system (lungs, trachea, mouth), the flow control valve (lips), the mouthpiece and the instrument resonator. Each of these parts can then be modelled in varying degrees of sophistication to provide an overall model of the physics behind the playing of brass instruments.

A brief description of the acoustic resonator in the brass family of instruments and some of the main physical properties of such resonators is given in section 2.2, along with some discussion of how the resonator contributes to the "brassy" sound of these instruments. The lips of a brass player are then examined in section 2.3. Firstly, the action of the lip in playing is presented, followed by some of the models which can be used to provide understanding of the action of the lips. These models give varying degrees of convergence with the real working of the players lips, but even the simpler models can be useful in the understanding

of the working of brass instruments. The interaction of the lips with the acoustic fields and the flow of air is introduced in section 2.4 by analysing the air column and lips as two coupled single mass oscillators. This leads to the classification of different types of lip operation, and these modes of operation are then examined in the context of more complex models of the lips and air column resonances.

2.2 Sound propagation inside a brass instrument

2.2.1 The brass instrument family

The brass wind family of musical instruments all have a common construction in that they have an acoustic resonator which is driven by an oscillating valve mechanism in the form of the player's lips pressed against a mouthpiece. Thus a generic brass instrument can be described as an air supply system, an oscillatory flow control valve and a resonator as shown in Figure 2.1. In this simple model the air supply system can be assumed to provide a static pressure behind the flow control valve (the mouth over pressure P_m) which is higher than the atmospheric pressure. Air can then pass through the lips, which act as a flow control valve, controlling the volume flow by the size of the opening area between them. A feedback mechanism is provided, as the lips respond to the pressure in the mouthpiece, i.e. a high pressure in the mouthpiece may cause the lips to open wider, thus giving increased flow into the mouthpiece and providing a means for

sustained oscillation. The acoustic resonator of a normal brass instrument such as the trumpet or trombone is made up of the mouthpiece, a cylindrical bore pipe containing valves or slide mechanism. This mechanism enables changes in the resonator length, and at the end of the resonator is a bell which provides partial impedance matching to the outside environment allowing some acoustic radiation of sound from within the instrument. This simple model for a brass instruments is sufficient to model much of the physical behaviour of a brass instrument.

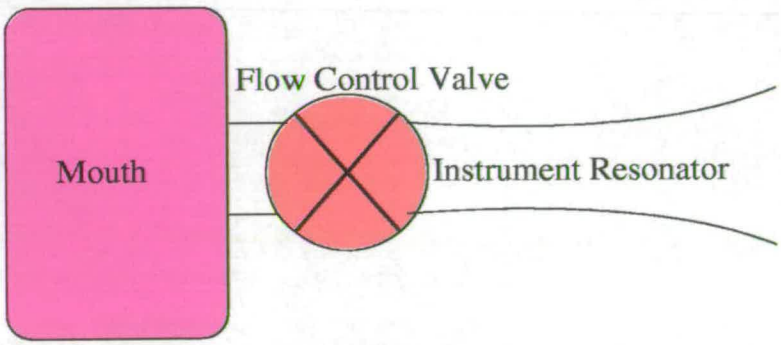

Figure 2.1: Schematic of a brass instrument

2.2.2 Air column resonances in brass instruments

There is a considerable body of literature about the properties of musical instrument bore shapes and accurate measurement techniques of the acoustic resonances [5], [47], and good theoretical models [31] are available. The air columns of most modern brass instruments [53] can be approximated by a section of cylindrical tubing followed by a flared horn, usually in the form of a Bessel horn, where the bore radius of the horn (a) is given by:

$$a = b(x + x_0)^{-\gamma} \tag{2.1}$$

The constants b and x_0 are chosen to give the correct radii at the small and large ends of the horn and γ defines the rate of flare of the horn. A value of γ of around 0.7 gives a bell shape which resembles that of a modern trumpet or trombone [53]. For the case where $\gamma = 0$ we have a cylindrical tube which, if the mouth end of the instrument is taken to act like a closed end, provides a series of odd harmonics given by:

$$f_n = \frac{c(2n-1)}{4l} \tag{2.2}$$

where f_n is the resonant frequency of mode n, l is the length of the resonator and c is the speed of sound. For the case where $\gamma \neq 0$ Benade [8] showed that the resonance frequencies of the horn can be given by:

$$f_n \approx \left[\frac{c}{4(l+x_0)}\right]\left[(2n-1) + \beta\left[\gamma(\gamma+1)\right]^{1/2}\right] \tag{2.3}$$

In addition to the horn at the open end of the instrument, there is also the mouthpiece which has a considerable effect on the characteristics of the resonator [6]. An example of the shape of a brass mouthpiece can be seen in Figure 2.2. The size and shape of the mouthpiece varies between different brass instruments

to a lesser extent on the player's choice, with the important characteristics being the cup volume and the throat diameter. A simple measurement of the mouthpiece acoustics is given by the "popping" frequency. This is the note obtained when the rim of the mouthpiece is slapped against the palm of the hand, causing the mouthpiece to sound a note at its Helmholtz resonance frequency. It should be noted that the popping frequency is strongly dependent on the mouthpiece backbore and shank which are of minor significance in terms of the playability of the instrument. Rather the popping frequency can be used as a very basic measurement to compare like mouthpieces.

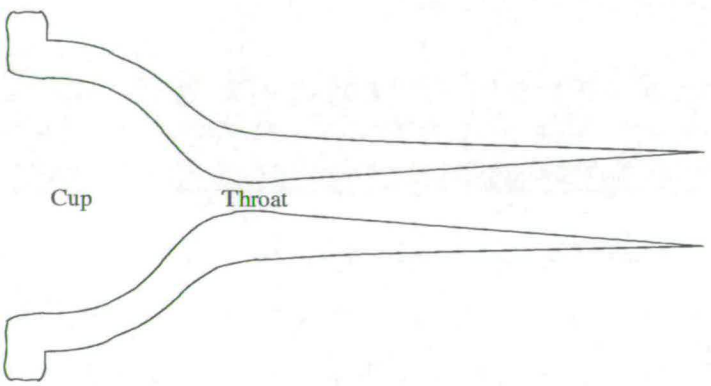

Figure 2.2: Cross section of a typical brass instrument mouthpiece

The combination of these different parts of the instrument act together to give each instrument a characteristic acoustic impedance curve such as the one shown in Figure 2.3. The player will most easily be able to play a note which has a fundamental frequency in close proximity to an impedance maximum of this curve. The shape and frequency of these impedance maxima can be changed con-

by altering the bore shape of the instrument. For example, a narrower bore will give a higher Q factor for the impedance maxima than would occur with a wider bore instrument [7]. A narrower bore instrument will tend to play notes which are very close to an impedance maximum, whereas on a wider bore instrument it will be easier to 'bend' the note away from an impedance maximum.

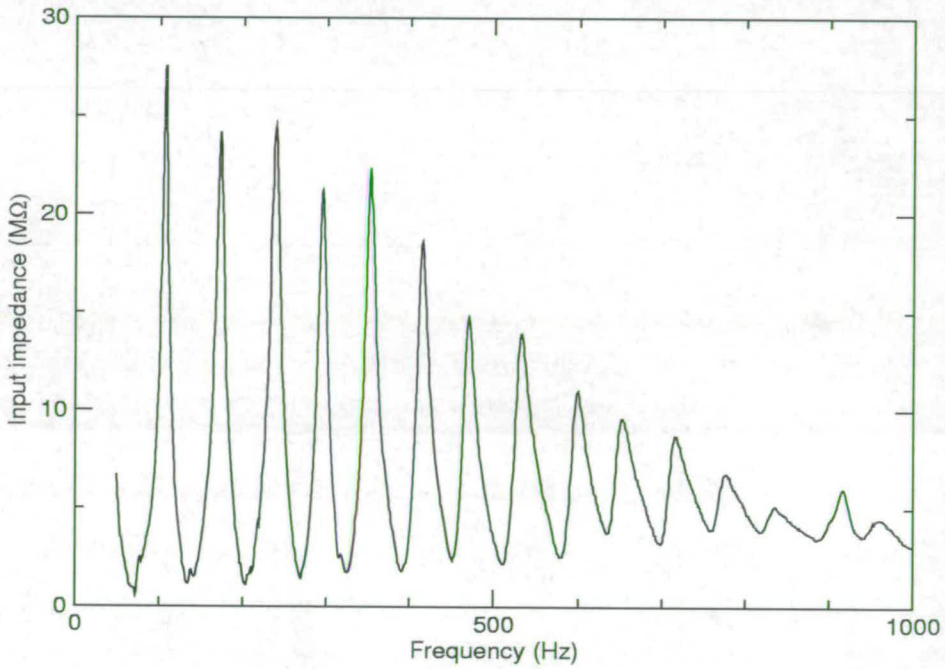

Figure 2.3: Input impedance curve from a trombone

Although the shape of the resonator of a brass instrument can have a considerable effect on the tone quality and playability of the instrument, for most of the following work the very simplest approximation of a brass instrument is sufficient. The measurements performed here in the most part consider only the single fundamental frequency of the played note and thus only the nearest impedance

maxima to this fundamental frequency need be considered. Most of the measurements are done using a telescopic cylindrical tube with a mouthpiece attached rather than an actual trombone. The frequencies of the second to fifth impedance maxima of the telescopic pipe with mouthpiece are shown as a function of pipe length in Figure 2.4. These measurements are found using input impedance measuring apparatus at the University of Edinburgh [13] and the calculated values also shown in this figure are given by Eqn. 2.2. This data shows that the simple equation for the acoustic resonances of a pipe (Eqn.2.2) has a fairly close resemblance to the actual values obtained from impedance measurements. This simple equation is considered sufficiently accurate in most of the following work and is used as part of the theoretical model for the telescopic tube with mouthpiece, especially as the artificial lips are only able to play notes utilising the 2nd or 3rd acoustic mode of the telescopic pipe, for which the measured impedance only deviates by a few Hz from the theoretical value.

2.2.3 Non-linear effects in brass instrument playing

Much of the complexity in the physics of playing brass instruments, which in many ways leads to their musicality, stems from the way in which the different parts of the instrument interact often in a very non-linear fashion. Two of the main examples of this non-linear interaction are the sound propagation in the instrument resonator at high volumes and the motion of the player's lips.

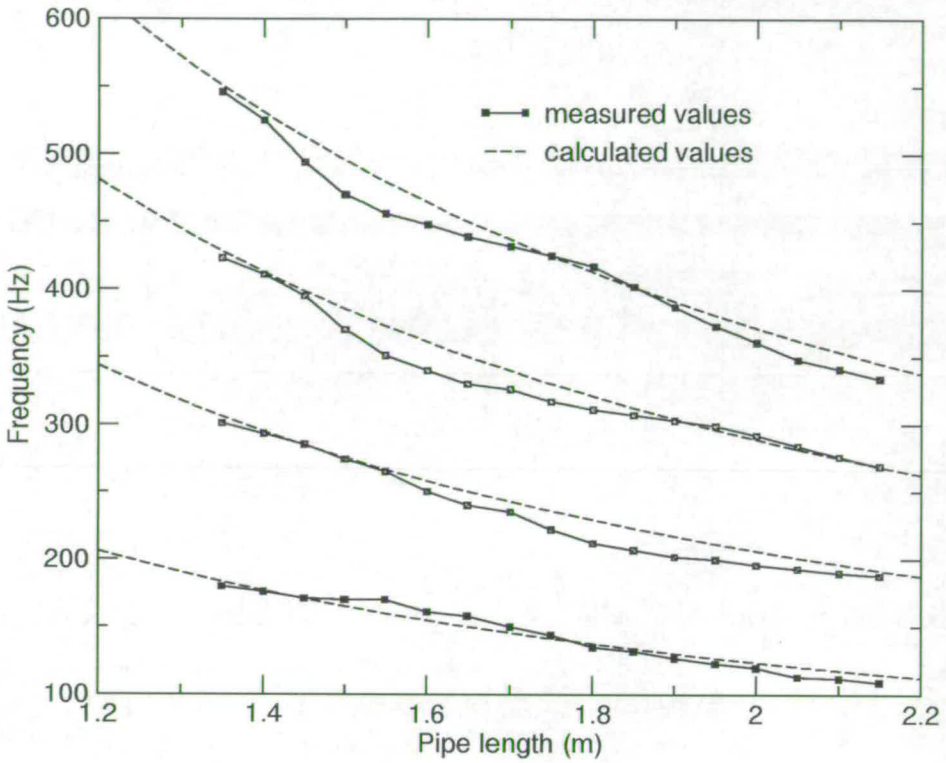

Figure 2.4: 2nd to 5th mode frequencies of a cylindrical pipe with mouthpiece.

The first of these examples, the sound propagation in the instrument leads to one of the most distinctive characteristics of the brass instrument family, the ability to change the sound from a smooth rounded tone at lower volumes to the well known bright 'brassy' tone at higher volume levels. This effect is not, as often supposed, caused by the material from which the instrument is made but rather from shock wave formation in the bore of the instrument [36]. These shock waves develop if the resonator is suitably long and also if the sound pressure level in the resonator is sufficiently high. The sound level inside brass instruments can reach particularly high levels (up to 170 dB). At these sound pressure levels, non-

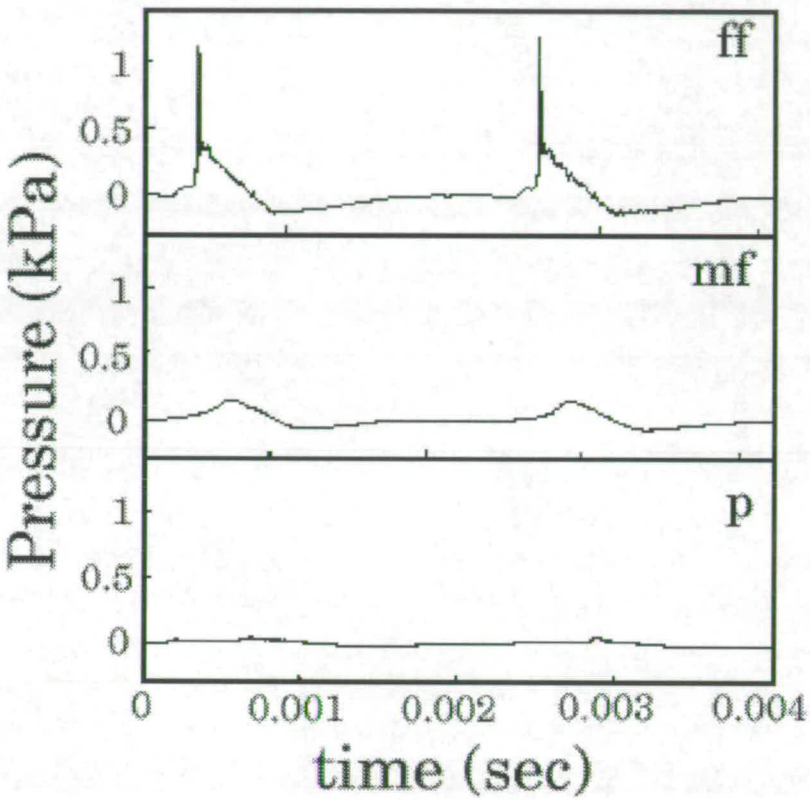

Figure 2.5: Acoustic pressure measured just outside the bell for three different playing amplitudes.

linear propagation effects lead to a speed of sound which depends on the pressure amplitude, thus the crest of the wave travels slightly faster than the trough and so there is a steepening of the wave front. This means that with a suitably long resonator, the rising part of the wave can become almost instantaneous, thus creating a shock wave as can be seen in Figure 2.5 [36].

A second example of non-linear effects in brass instruments more closely related to the current work is the motion of the player's lips. An initial understand-

ing of the lips can be gained by starting with a very simplified model of the lips which assumes that the lips act like a simple mass on a spring with one degree of freedom (Figure 2.6). At low oscillation amplitudes, i.e. near the threshold playing level, this model has a very linear behaviour acting as a classical, driven single harmonic oscillator; but even for this simple model where the lips are assumed to have a single resonance frequency and a linear response to the driving force, non-linear characteristics become apparent when the oscillation amplitude rises. For example, at playing levels above threshold level there can be a collision of the lips, causing a considerable part of the oscillation cycle to occur with the lips completely closed and no air flow from the mouth into the mouthpiece. If this is the case then the driving force for the air column no longer has the form of a regular sinusoid, but rather has more of a pulse form often with zero flow for a considerable part of the cycle and only a short open time [52]. This can be seen in the example mouthpiece pressure waveform shown in Figure 2.7.

The real brass player's lips are obviously much more complicated than this simple one mass model, having multiple resonance frequencies and damping which is dependent on the oscillation amplitude of the lips. Despite these complications many interesting results can be obtained from modelling the driving mechanism of the trombone with a single mass [21].

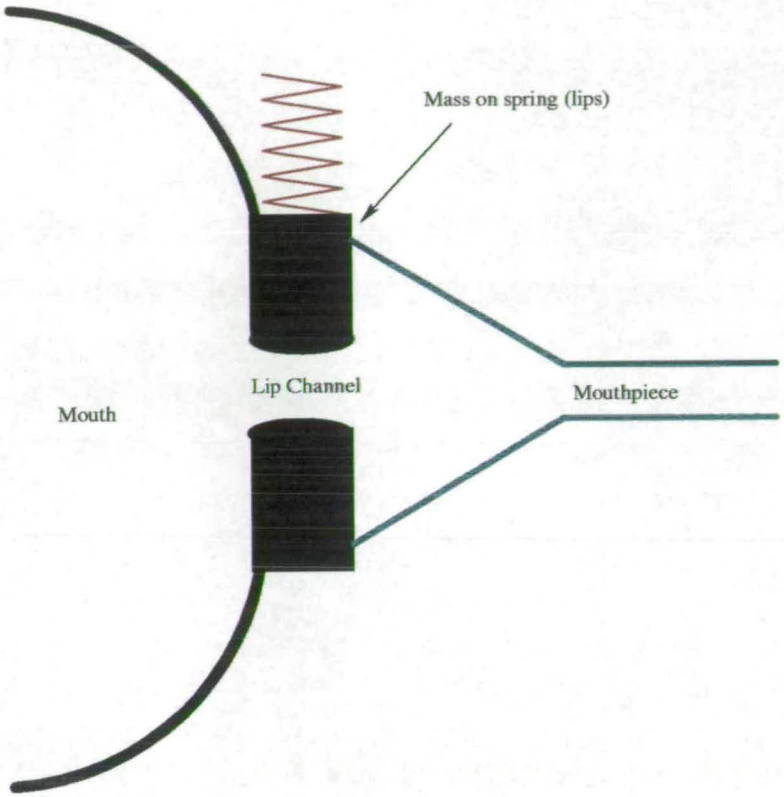

Figure 2.6: The simple one mass model.

2.3 The player's lips

As shown in the above example, the brass player's lips are one of the most complicated parts of the brass instrument. Many different models for describing the lips have been suggested by Cullen [21], Adachi [2] and others [25], [51]. In addition to this there is a considerable body of literature about glottal modelling in voice synthesis [42], [9] which in many ways is a similar problem to that of the brass player's lips.

The lips consist of two flexible masses which are suspended between the teeth,

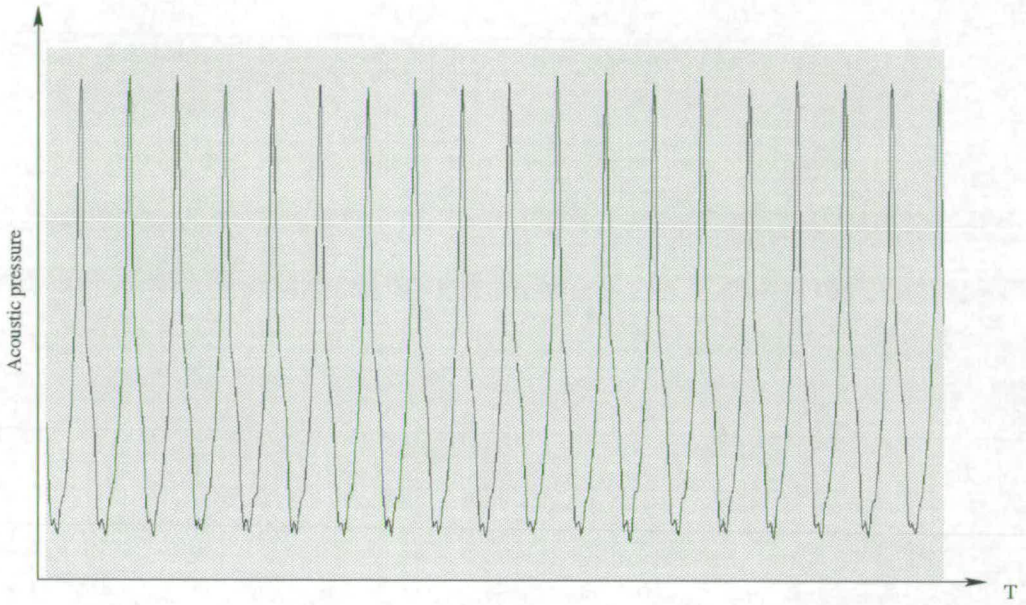

Figure 2.7: Pressure signal in mouthpiece for a loudly played note.

which press on the back of them, and the mouthpiece rim, which presses on the front. The motion of the lips is driven by fluid dynamical forces acting upon them created by a static over pressure in the mouth and an alternating acoustic pressure in the mouthpiece, leading to varying flow between the lips. There are two main forces which the pressure and related flow exert on the lips. These forces lead to two different oscillation regimes: "outward" and "inward" and striking.

The first of these regimes is known as the "outward striking" or "swinging door" model. In this regime the driving forces on the lips come mainly from the pressure in the mouth pushing the lips open, and the pressure in the mouthpiece opposing the opening of the lips as can be seen in Figure 2.8. For the initial analysis the pressure in the mouth can be assumed to have a constant value with

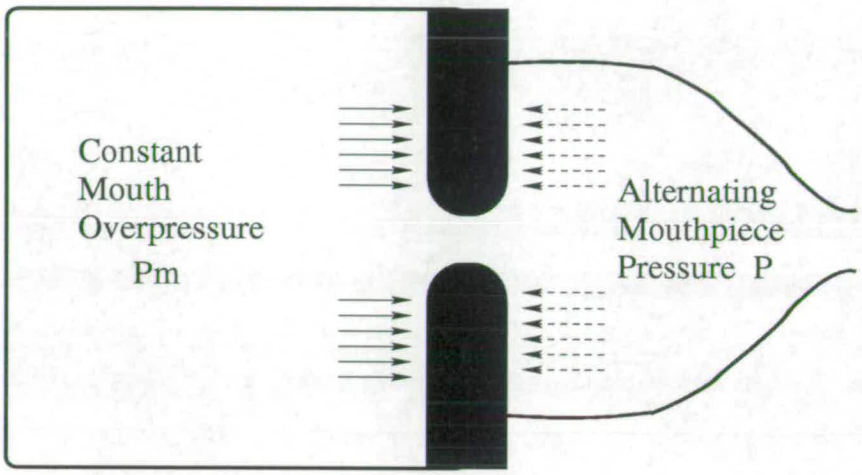

Figure 2.8: The outward striking forces on the lips.

a steady over pressure (P_m) and an alternating pressure in the mouthpiece (P). This leads to a pressure difference (ΔP) across the lips. When there is a low pressure in the mouthpiece, there is a greater force on the back of the lips than there is on the front and the lips are pushed open, whereas when there is a high pressure in the mouthpiece the lips are pushed closed.

The other regime is known as the "inward striking" or "sliding door" model. In some literature two regimes, "inward striking" and "sideways striking" are presented as two distinct cases [2]. If the mouth pressure is taken to have a constant value, as is the case in the following simple analysis, both the inward striking and the sideways striking model are identical and so shall be considered equivalent in the following work. The inward striking regime is primarily due to Bernoulli forces acting on the faces of the lips parallel to the direction of the air flow (Figure 2.9). In the inward striking regime, a low pressure in the mouthpiece

causes an increased air flow between the lips which due to the Bernoulli forces (equation 2.4) causes a pressure drop in the area between the lips and thus the lips are drawn together. From this it can be seen that the extent of the flow separation, and thus the pressure recovery on the downstream side of the lips is very important in the magnitude of the Bernoulli force on the lips.

$$\frac{1}{2}\rho q^2 + p = \text{constant along a streamline} \tag{2.4}$$

where q: velocity magnitude along any streamline.

It should be noted that there cannot be complete pressure recovery on the downstream side of the lips as this would mean that size of the lip opening (h) would have no effect on the flow into the mouthpiece.

These two regimes of operation have opposite responses to a pressure change in the mouthpiece, but as the lips act as a driven harmonic oscillator, there is in general a phase lag in the response of the lips to the driving pressure. Figures 2.10, 2.11 illustrate this effect, showing the response of the lips to an acoustic driving frequency in the mouthpiece. For there to be energy input to the system and thus the possibility of self sustaining feedback to the lips, there must be a phase difference between the lip opening and the mouthpiece pressure such that the maximum opening of the lips occurs at some point within $\pm\pi/2$ of the maximum of the acoustic mouthpiece pressure. It can also be seen that for the inward striking reed driven at a frequency well below its resonance, a maximum

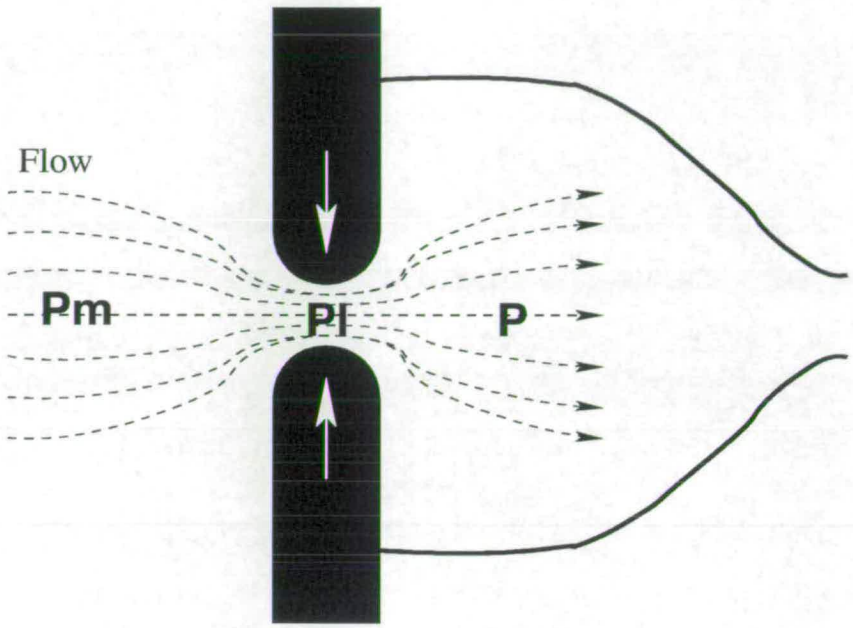

Figure 2.9: The inward striking forces on the lips.

acoustic pressure in the mouthpiece must occur at the same time as a maximum in the lip opening. As the frequency is increased a lag in the response of the lips occurs and so the maximum acoustic pressure in the mouthpiece is followed by a maximum in the lip opening. Thus for a playing inward striking reed the lip opening must have a phase lag behind the mouthpiece pressure of between 0 and $+\pi/2$. For the outward striking reed this is reversed, and so the lip opening must have a phase lag on the lip opening of between $3\pi/2$ and 2π which can more easily be expressed as between $-\pi/2$ and 0. The response of the lips $C(\omega)$ to a pressure difference ΔP across them, is given by:

$$C(\omega) = \frac{h(\omega)}{\Delta P(\omega)} \tag{2.5}$$

and thus the phase difference between the lip opening and the pressure difference across the lips is given by:

$$\angle C(\omega) = \angle h(\omega) - \angle \Delta P(\omega). \tag{2.6}$$

It should be noted that the minimum in the pressure difference ΔP occurs when there is a maximum in the mouthpiece pressure, thus there is a phase difference of π between the phase measured using $\Delta P(\omega)$ and that measured using the mouthpiece acoustic pressure P. By measuring the value of $\angle C(\omega)$ the reed type behaviour of the lips can be determined. The above definition of $C(\omega)$ helps to avoid some of the confusion given when changing from upstream to downstream driving of the lips. Cullen [21] used the pressure in the mouth (Pm) as the driving force on the lips, which gives the same phase as when using ΔP, which is defined as:

$$\Delta P = P_m - P. \tag{2.7}$$

Using the above calculations for $\angle C(\omega)$, it can be seen that for the inward striking reed regeneration is possible when $\angle C(\omega)$ has a value between $\pi/2$ and π, whereas for the outward striking reed, regeneration is possible when $\angle C(\omega)$ as a value between $-\pi/2$ and $-\pi$.

If a single resonance of the lips is considered to act as a damped single mass on a spring with a driving force $F_0 cos(\omega t)$ of frequency ω, the equation of motion

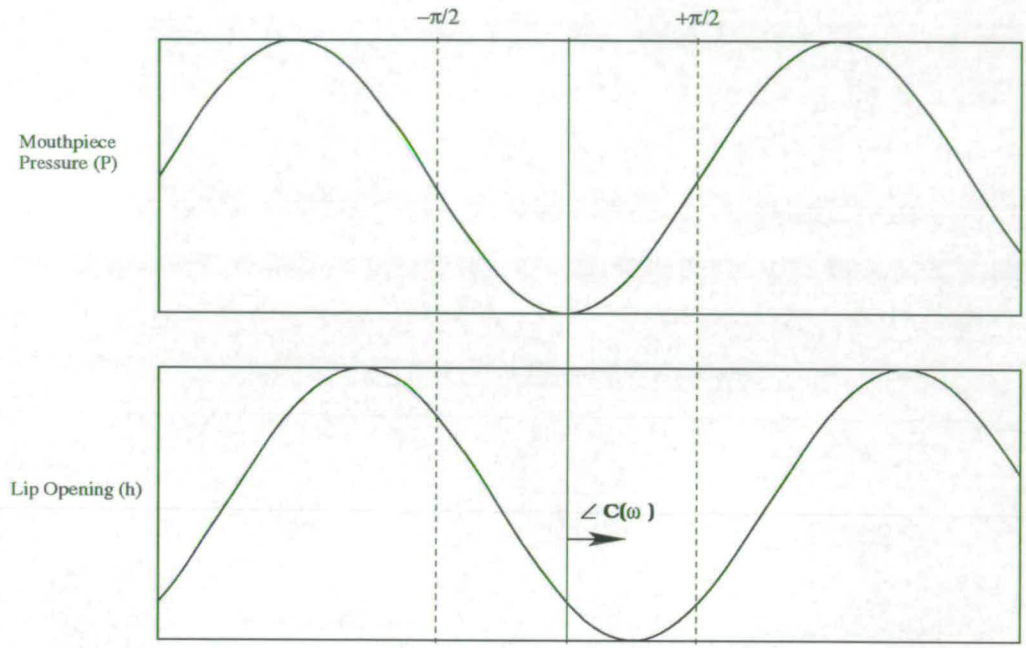

Figure 2.10: Response of lip opening to mouthpiece pressure for inward striking reed.

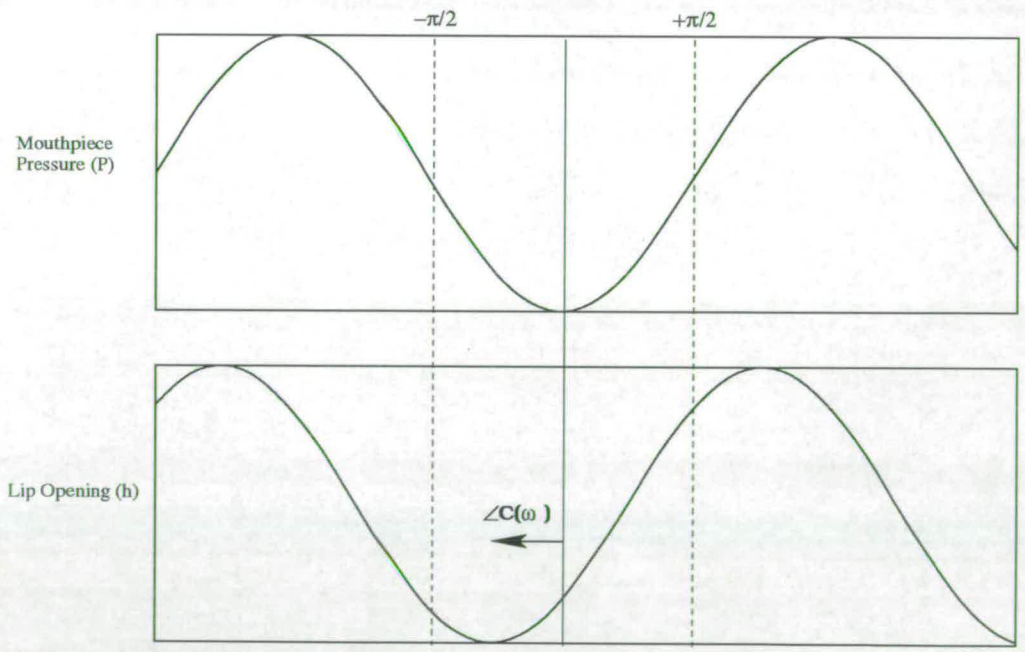

Figure 2.11: Response of lip opening to mouthpiece pressure for outward striking reed.

is given by:

$$\frac{d^2x}{dt^2} + \gamma\frac{dx}{dt} + \omega_0^2 x = \frac{F_0}{m}cos(\omega t) \tag{2.8}$$

The magnitude response of the mass to the driving frequency is given by equation 2.9 and the phase response is given by equation 2.10.

$$C(\omega) = \frac{F_0/m}{[(\omega_0^2 - \omega^2)^2 + (\omega\omega_0/Q)^2]^{1/2}} \tag{2.9}$$

$$tan[\angle C(\omega)] = \frac{\omega\omega_0/Q}{\omega_0^2 - \omega^2} \tag{2.10}$$

Using equation 2.10 it can be seen that there is a phase response of the lips to the driving force $F_0cos(\omega t)$ of $\pi/2$ when driving force is at the resonance frequency ω_0 of the lips. The driving force on the lips is created by the alternating acoustic presure in the mouthpiece which creates a pressure difference across the lips (ΔP). In the above discussion it was noted that for the inward striking reed well below resonance the maximum in acoustic pressure in the mouthpiece (P), which is equivalent to a minimum in the pressure difference (ΔP), occurs when there is a maximum lip opening, i.e. there is a phase $\angle C(\omega) = \pi$ whereas for the outward striking reed well below resonance, the maximum in mouthpiece pressure and thus the minimum in ΔP occurs when there is a minimum lip opening so

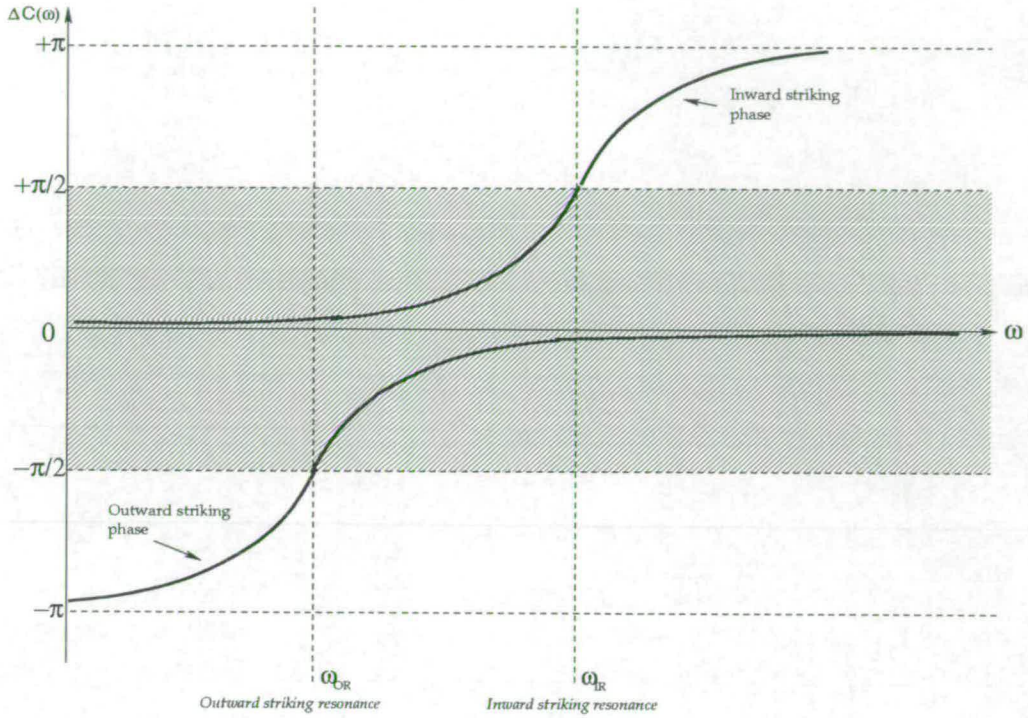

Figure 2.12: Phase response of outward and inward lip resonances as calculated from a single mass model.

$\angle C(\omega) = 0$. Thus for a single mass model of the inward striking reed with a driving force:

$$\Delta P \sim cos(\omega t) \tag{2.11}$$

the phase response $\Delta C(\omega)$ is given by equation 2.10, whereas for the outward striking reed the phase response is given by:

$$tan[\angle C(\omega)] = \frac{\omega\omega_0/Q}{\omega_0^2 - \omega^2} - \pi. \tag{2.12}$$

Figure 2.12 shows the phase response curves as given by the single mass models for two lip resonances, the lower frequency one having a outward striking behaviour and the higher frequency one having an inward striking behaviour, as is often shown to be the case in the measurements on the artificial lips. The shaded area shows the region in which the phase response of the lip reed is within $\pm\pi/2$ of the mouth phase, and so sustained oscillation is possible. It can be seen from this figure that the lower outward striking resonance can only sustain oscillations when the playing frequency is above the reed resonance, as for frequencies below the reed resonance the phase response of the lips is such that the maximum opening of the lips occurs when there is a low pressure in the mouthpiece. In a similar way the higher inward striking reed cannot sustain oscillation if the playing frequency is above the reed resonance. This means there is a region between the two lip resonances where it is possible for either the outward or inward striking lip resonance to play, although as shown above there is a different phase response of the lips for either case. This simple mass on a spring model can be compared with the results shown by Cullen [22] of the playing frequency against slide extension for inward and outward lip models for the trombone. In that case it can be seen that for the outward model the playing frequency is always above both the lip resonance and the acoustic resonance of the instrument, whereas for the inward model the playing frequency is always below the lip resonance and the instrument resonance. Extensions of this model [44] show the playing frequency crossing the acoustic resonance as the slide is extended, as happens for

the real instrument measurements. In a similar way, it is expected that the phase response of the lips will change from being very close to the single mass model theory when playing close to one of the lip resonances with a smooth transition in phase response between the two cases as the playing frequency is changed.

2.4 Interactions between the lips, player and instrument

As shown in the above discussions, the lips form a non-linear oscillator with various different regimes of oscillation, but this is only a small part of the overall system which enables a player to create notes on a brass instrument. The instrument resonator is responsible for the intensity and form of the pressure wave formed in the mouthpiece which in turn drives the motion of the lips, but there is also the DC component of the flow through the instrument, starting as a jet from between the lips into the mouthpiece, the form of which depends on the profile of the lips at the exit into the mouthpiece as well as the flow velocity. The shape of this jet and the way in which the jet dissipates in the mouthpiece changes the strength of the Bernoulli force on the lips. If the air flow between the lips is completely laminar, as is shown schematically in Figure 2.13, there will be complete pressure recovery on the instrument side of the lips and the Bernoulli force will be larger than it is for the case where the flow separates from the lips and forms a

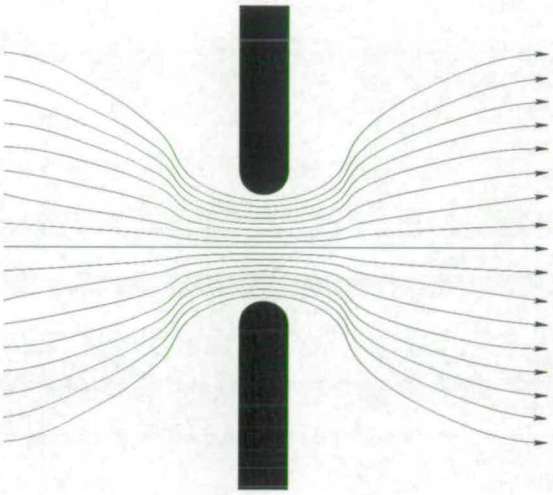

Figure 2.13: Laminar flow between lips.

jet (Figure 2.14). In this case there is no pressure recovery and the energy in the jet is dissipated through turbulence. The actual jet formation during real playing is somewhere between these two cases. Jet formation can also occur where there are rapid changes in the bore profile of the instrument such as the throat of the mouthpiece, which can have the effect of decoupling the mouthpiece and instrument resonators.

The vocal tract of the player may also have some effect on the playing of the instrument, although as previously stated the pressure changes in the mouth of the player are shown in experiments to be much lower than those in the mouthpiece. They are therefore insignificant for the basic single mass model type analysis shown above. Pressure oscillations in the mouth do occur and therefore the acoustic impedance of the mouth and vocal tract may have some effect on the playing of the instrument. It is has been suggested that it is the acoustic

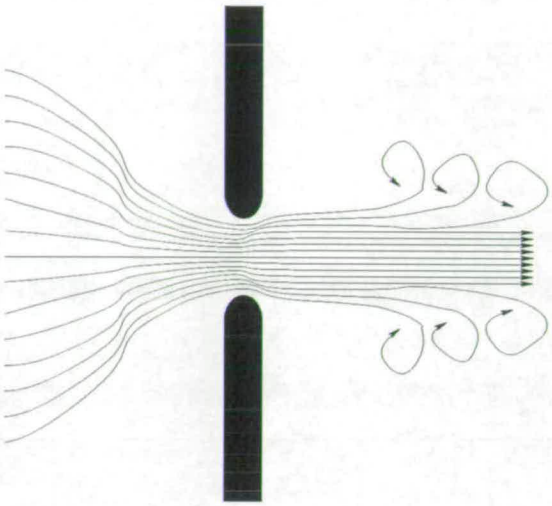

Figure 2.14: Jet formation between lips.

impedance of the mouth which creates the acoustic feedback necessary to enable buzzing of the lips without an instrument present [31]. A brief investigation into the effect of the mouth cavity on playing was done by Cullen [21] and theoretical models including the mouth impedance have been made [46] but much further work is needed into this effect, some of which is presented in Chapter 4.

Chapter 3

Studies of the mechanical response of lips

3.1 Introduction

Experiments on the brass player's lips have proved notoriously difficult, due to both the nature of the lips and the inaccessibility of the lips while playing. Some experiments have been done using real player's lips [20], [46], [52], [4] but many of the results from these experiments have been limited due to difficulties in experimental procedure, repeatability or limited data leading to an unclear overall picture.

As an alternative to using real players in experiments, an artificial mouth and

lips can be used to play the instruments while the experiments are performed. Using an artificial mouth for the experiments avoids some of the problems associated with experiments on real players, such as repeatability. Real players are often not able to keep their lips constant over a long period and have great problems with playing in exactly the same way if there is a change in note or instruments being played. In addition there are psychological effects which can affect real player's ability to play for some of the experiments as there is a tendency to compensate for out of tune or poor sounding notes. The artificial mouth enables extended experiments to be performed, both when long playing times are required and also in the case where many notes of instruments need to be played with a constant embouchure. The main problem with using the artificial mouth for experiments is the question of whether measurements taken are applicable to the real playing situation, a subject which is addressed in Chapter 4.

3.2 The artificial lips

The artificial mouth used for these experiments is based on a design by Gilbert and Petiot [33]. This original design was then altered by Cullen [22] to allow some further adjustment to the lips through changing the water pressure in the lips and an improvement in the adjustment for pressing the lips against the mouthpiece rim. A schematic diagram of the artificial mouth viewed from the side is shown in Figure 3.1 and a top view in Figure 3.2. A photograph of the mouth as viewed

through the rear viewing window is shown in Figure 3.3. Some of the experiments in Section 4.4 were also performed on a third generation of artificial mouth design, where the lips are mounted on the outside of the mouth box to give easier access and further adjustment possibilities.

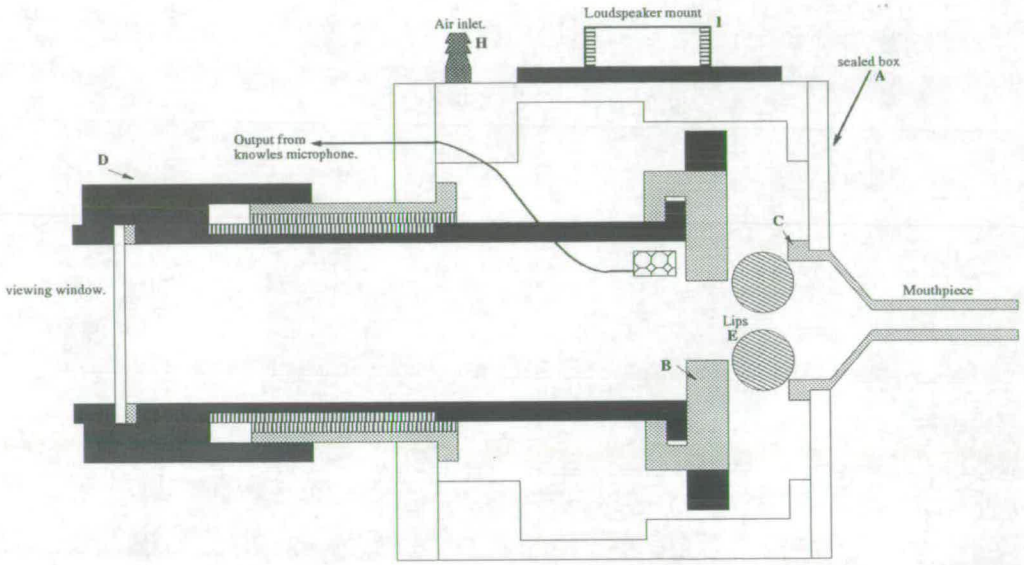

Figure 3.1: Schematic diagram of the artificial lips viewed from the side

The artificial mouth used in the main experiments (Figure 3.1) is constructed of a clear perspex hermetically sealed box (A), with the artificial lips mounted at the front just between the teeth plate (B) and the mouthpiece rim (C). The teeth plate can be moved using the screw adjustment (D) on the back of the mouth so as to change the pressure of the lips against the mouthpiece rim. The lips (E) are made of latex rubber tubing stretched between hollow brass mounting rods (F) at either side of the mouth which are fixed at one side of the mouth and have threaded adjusters (G) at the other side. Water can be pumped through these

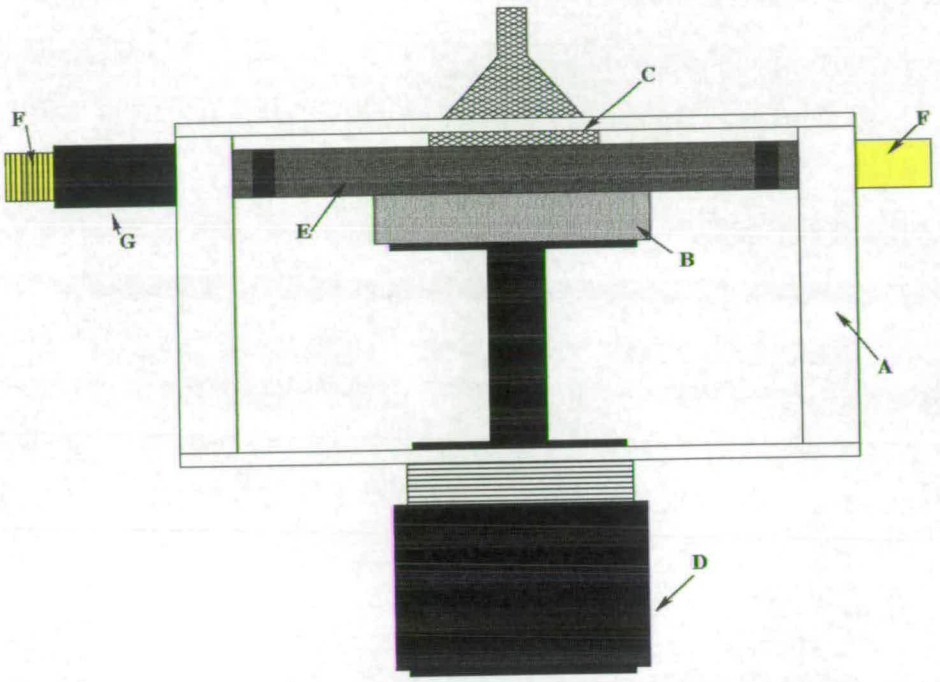

Figure 3.2: Schematic diagram of the artificial lips viewed from the top

mounting rods allowing water pressure in the lips to be increased or decreased. Experiments were done using various different thicknesses of latex tubing but the best results and reliability were given by latex tubing with an internal diameter of 16mm and a wall thickness of 0.3mm, although tubing with 0.1mm and 0.2mm wall thicknesses were also used. The embouchure of the lips can be adjusted in three different ways. The teeth plate can be moved forward and backwards by screwing the adjuster at the rear of the mouth (D). The water pressure in the lips can be changed by pumping water through the mounting rod on which the lips are mounted and the tension of the lips can be changed by tightening or loosening the threaded collar on the mounting rods.

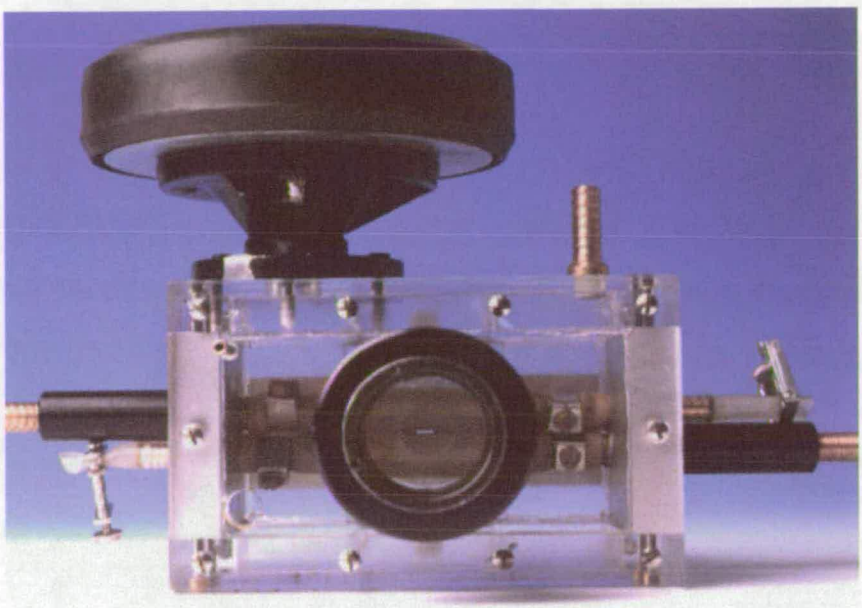

Figure 3.3: Photograph of the artificial mouth

The mouthpiece used was constructed to be similar to a Denis Wick 6BS trombone mouthpiece, with a removable rim enabling access to the lips without dismantling any of the mouth. This mouthpiece has a total volume of 12.7ml and a Helmholtz resonance frequency of 518 Hz. The dimensions of this mouthpiece are shown in Figure 3.4.

Air is supplied to the mouth via flexible tubing connected to the inlet point on the top back corner of the mouth (H) and an air pump (type: Air Control Industries MS11). Between the air pump and the mouth there is a ten turn control valve to enable continuous variation in the mouth overpressure. The static overpressure in the mouth was measured using a Digitron P200UL piezoceramic manometer connected to a small port on the rear of the mouth. Alternating

pressure in the mouth is measured using a miniature microphone (Knowles BT-1759 or B&K 1/4" type 4938) placed just behind the lips.

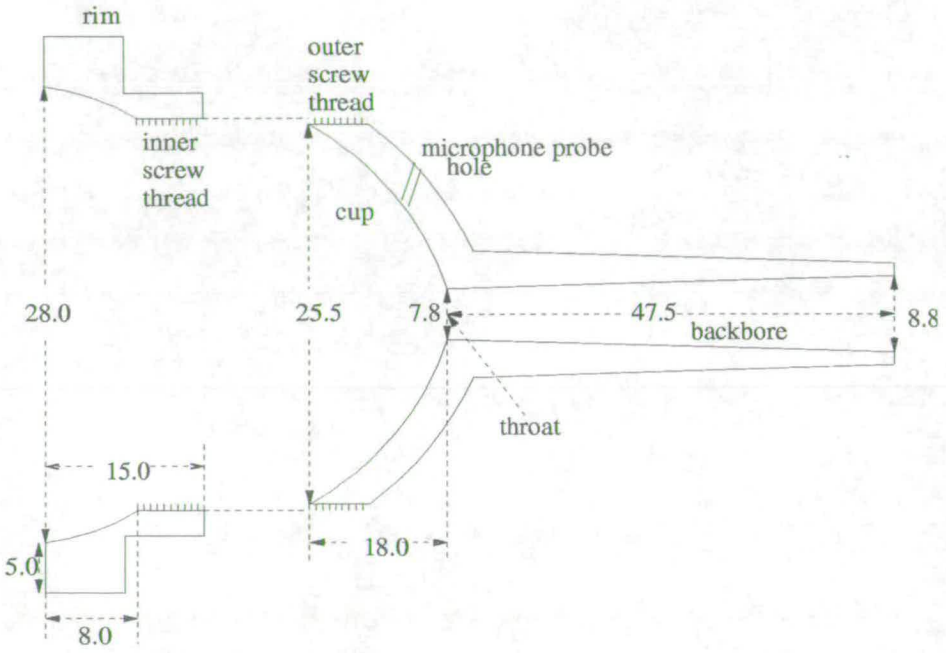

Figure 3.4: Cross-section of the mouthpiece with removable rim

To enable the creation of a specific acoustic pressure in the mouth there is a threaded loudspeaker mount (I) on the top of the artificial mouth. A loudspeaker can be screwed onto this when required or the port blocked off with a stopper when not required. For high frequency measurement a FANE NF100 8Ω horn mounting loudspeaker was used as seen in the photograph in Figure 3.3, but for most of the experiments a Monacore SPH-100C $3\frac{1}{2}''$ cone speaker was used with special adapter enabling it to be fitted onto the threaded loudspeaker mounting. The pressure in the mouthpiece was measured using a B&K 1/2" type 4192 microphone fitted with a 20mm long 2mm diameter probe which can be inserted

through the hole bored in the side of the mouthpiece cup (Figure 3.4). All the B&K microphones were used in conjunction with a B&K Nexus two channel signal conditioning pre-amplifier.

3.3 Mechanical response measurements

The lips of a brass player form a mechanical oscillator which has complex behaviour. In order to understand the properties of the lips when playing the instruments, the mechanical properties of the lips must be known. One of the most fundamental properties of the lips is the frequency of the mechanical resonances. The resonances of the lips can be determined through performing mechanical response measurements. In normal self-sustained playing, the lips are driven by the alternating acoustic pressure in the mouthpiece P, with the energy input to the system coming from interaction between the lips and the overpressure P_m in the mouth. In a basic model of the lips it is assumed that there is no alternating pressure in the mouth during normal playing, an assumption which is at least partially borne out by measurements which show that pressure fluctuations in the mouth are on average at least 20-30dB less than those in the mouthpiece.

3.3.1 Experimental setup

Mechanical response measurements are done by creating a known acoustic pressure difference across the lips at a single frequency. The level of this acoustic field is considerably lower that that which occurs during self-sustained oscillation of the lips. The lips respond to this driving acoustic field by oscillating at the same frequency. This motion of the lips is measured and so the amplitude and phase response of the lips to a known amplitude acoustic pressure can be calculated. Measurements can then be taken in frequency steps across the required range and so a mechanical response curve is obtained. For mechanical response measurements on the artificial lips the pressure difference across the lips is usually created by an acoustic pressure in the mouth cavity rather than on the mouthpiece side due to the greater experimental simplicity. If the response of the lips is assumed to be purely an effect of the pressure difference across the lips, thus any effects due to air flow direction or non-linear flow ignored, the side from which the lips are driven should not have any effect on the results. As the acoustic pressure used to drive the lips in mechanical response measurement is fairly low, the acoustic flow velocity between the lips should remain clear of the non-linear flow regime and so this assumption should be valid. This assumption was experimentally verified in section 3.3.4.

The acoustic pressure in the mouth is created by a loudspeaker mounted on top of the artificial mouth, driven by a standard hi-fi amplifier with the signal

sourced from a .wav file played back on a computer. The loudspeaker is driven with a sine wave signal which is stepped in small frequency intervals over the required frequency range. The microphone placed behind the lips inside the mouth cavity is used to give a reference signal of the amplitude and phase of the acoustic signal driving the lips. The gain of the input signal to the loudspeaker is adjusted on the amplifier so that there is an approximately constant acoustic pressure at each driving frequency. The size of the opening between the lips is measured by directing an expanded laser beam from a Melles Griot helium neon 5mW laser onto the lips and collecting the transmitted light via collimating optics using a photo diode (EG&G HFD-1100) as seen in Figure 3.5. Neutral density filters are used to optimise the light intensity falling on the diode so as to give maximum signal to noise ratio. The optics are adjusted so that the spot from the laser falling on the lips has a size which is as large as possible while still being able to pass through the mouthpiece throat. The opening between the lips is much wider than it is long (approximately 10-15mm wide and around 1mm high), so as long as the spot from the laser is considerably larger than 1mm the amount of light passed through the lips is directly proportional to the height of the opening between the lips.

Signals from the microphone in the mouth and the diode are fed through identical Kemo VBF/3 band pass filters type set with low pass frequencies of 20 Hz and a high pass frequency of 3kHz. These signals are then sampled using an IOTech DacBook/200 or WaveBook/512 multi channel A/D converters at a

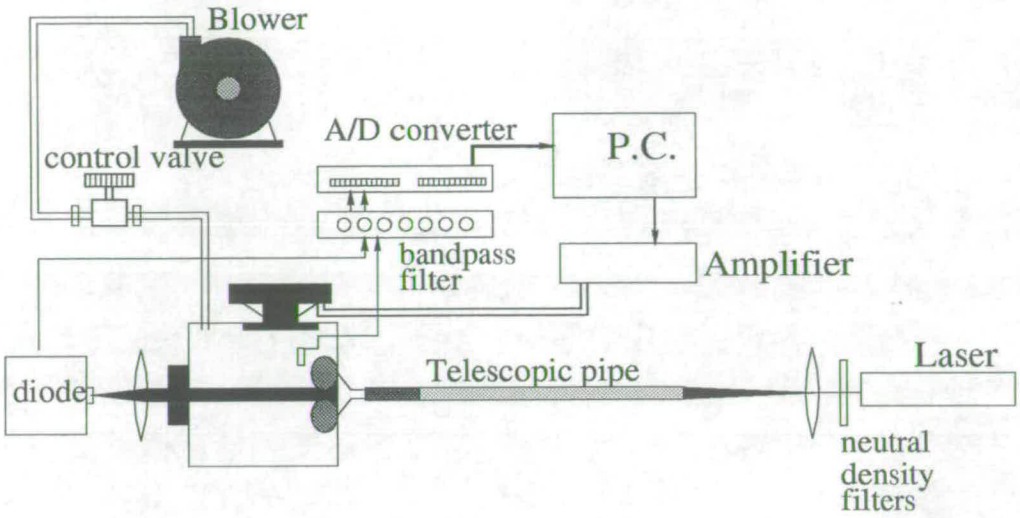

Figure 3.5: Experimental setup for mechanical response measurements.

sample rate of 4096Hz, with the resulting data being stored on a computer for later analysis. A typical measurement will involve driving the loudspeaker with sine wave signals of 1 second duration stepped in 5 Hz intervals from 50 Hz up to 600 Hz. For more precise measurements the step size can be reduced, as is sometimes necessary when lip resonances have high Q values. The laser, telescopic pipe, mouth, lenses and diode assemblies are all mounted on an optical bench to enable precise alignment.

The mechanical response of the lips to an acoustic pressure difference across the lips $\Delta P(\omega)$ is calculated using equation 2.5. The magnitude and phase of $C(\omega)$ can then be plotted to give a clear representation of the resonance properties of the lips.

3.3.2 Measurement calibration

The lip opening measurement setup using the helium neon 5mW laser was calibrated using an adjustable slit situated in place of the lips on the same optical bench as the experiments were performed. Using this setup, the voltage output from the diode was measured as a function of slit opening. The results of this measurement are shown in Figure 3.6. It can be seen from this graph that the voltage output from the diode is directly proportional to the slit opening for an opening height of up to 2mm, and even up to an opening of 3mm the voltage output from the diode remains almost linear. At an opening of greater than 3mm there is a saturation, as the slit height becomes comparable with the size of the spot produced by the laser at the plane of the lips. The diode is mounted in a box containing the power supply and amplifying circuitry needed as shown in Figure 3.7.

Throughout most of the work done here, the absolute calibration of the diode is not necessary as the main information required from the mechanical response measurements is the frequency of the response maxima of the lips and the corresponding phase of these maxima. Due to this it is only important that the diode has a linear response to the incoming illumination, which in turn is directly proportional to the lip opening as shown above. The HFD-1100 diode has a frequency response of up to 1.2 MHz and can measure down to D.C. so phase inaccuracies at the frequencies of interest (50Hz to 1KHz) are insignificant.

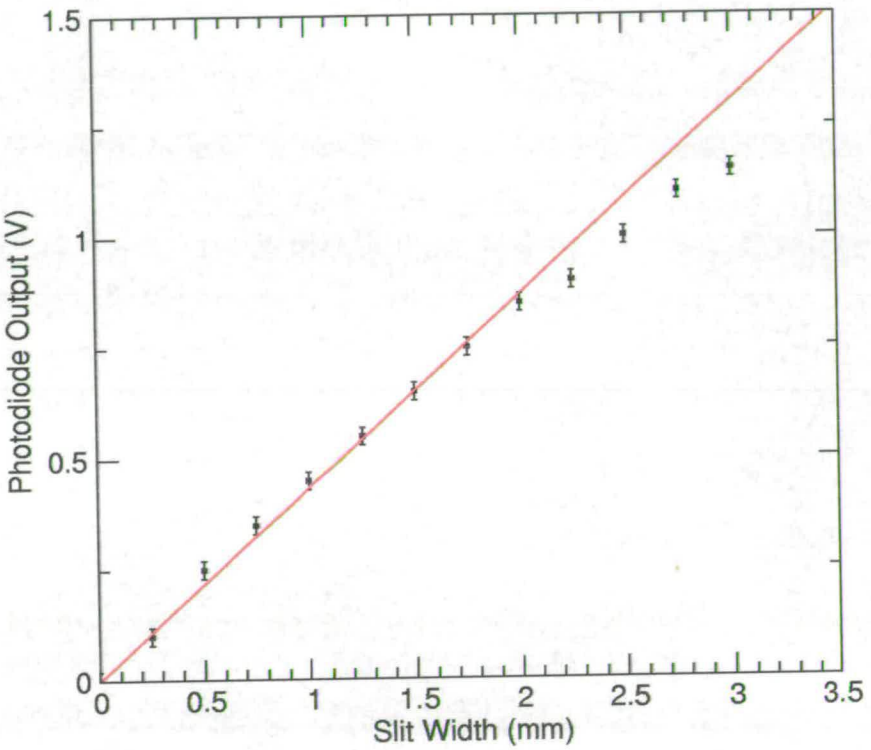

Figure 3.6: Diode voltage against slit opening height.

Three microphones were used for measurements during the experiments. A Knowles type BT-1759 microphone was used in the artificial mouth for measurements of the alternating component of the mouth pressure and a B&K type 4192 $\frac{1}{2}$" microphone with a 20mm probe fitted was used for measurements of alternating pressure in the mouthpiece. Some measurements of the mouth pressure were also done using a B&K type 4938 $\frac{1}{4}$" microphone. Both the Knowles and the probe microphones need to be calibrated to enable accurate analysis of the amplitude and phase of the acoustic signals. The B&K microphones when used

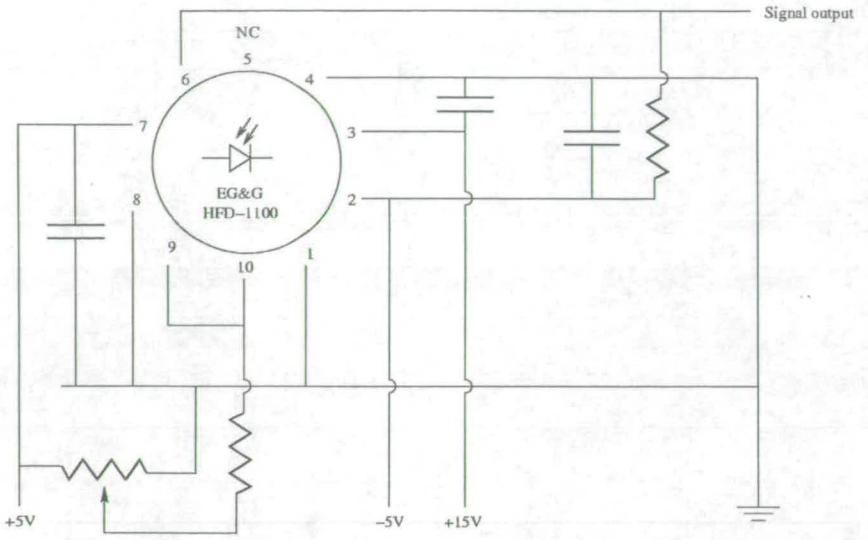

Figure 3.7: Circuit diagram for diode signal amplifier.

without probes have both phase and magnitude responses which are constant over the measurement range and can be used as calibration references for other microphones.

The B&K probe microphone was calibrated using a coupling device containing the probe microphone and a second B&K 1/2" microphone as a reference, as seen in Figure 3.8. The coupling device contains a ear-piece which generates an acoustic signal when driven by an amplifier connected to a PC producing sine waves stepped in 5Hz intervals between 50Hz and 2kHz. Signals from both microphones are sampled using an IOtech WaveBook/512 or DaqBook/200 A/D converter and stored for analysis using the auto.c analysis program.

Due to the lack of a suitable coupling device the Knowles microphone could not be calibrated against the 1/2" reference microphone, but instead was calibrated

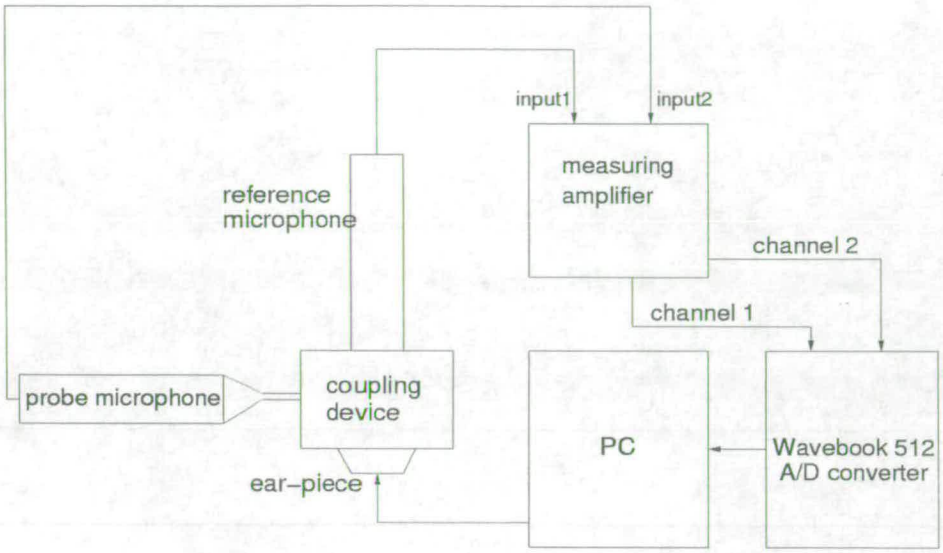

Figure 3.8: Microphone calibration setup.

by replacing the 1/2" reference microphone in the coupler with the Knowles microphone and using the calibrated probe microphone as a reference. The calibration data for the B&K type 4192 microphone fitted with the 20mm probe is shown in figure 3.9, and the calibration data for the Knowles BT-1759 microphone is shown in Figure 3.10.

It can be seen from these calibration graphs that the Knowles BT-1759 microphone has a phase response which has an approximately constant value of $+6^o$ over the frequency range used for mechanical response measurements of 50Hz to around 600 Hz, although as can be seen in Figure 3.10 the phase response in the lower frequencies changes rapidly. The magnitude response of the Knowles microphone is also fairly constant in the range of 50-600Hz. The B&K probe microphone has considerable variation in both phase and magnitude due to resonance

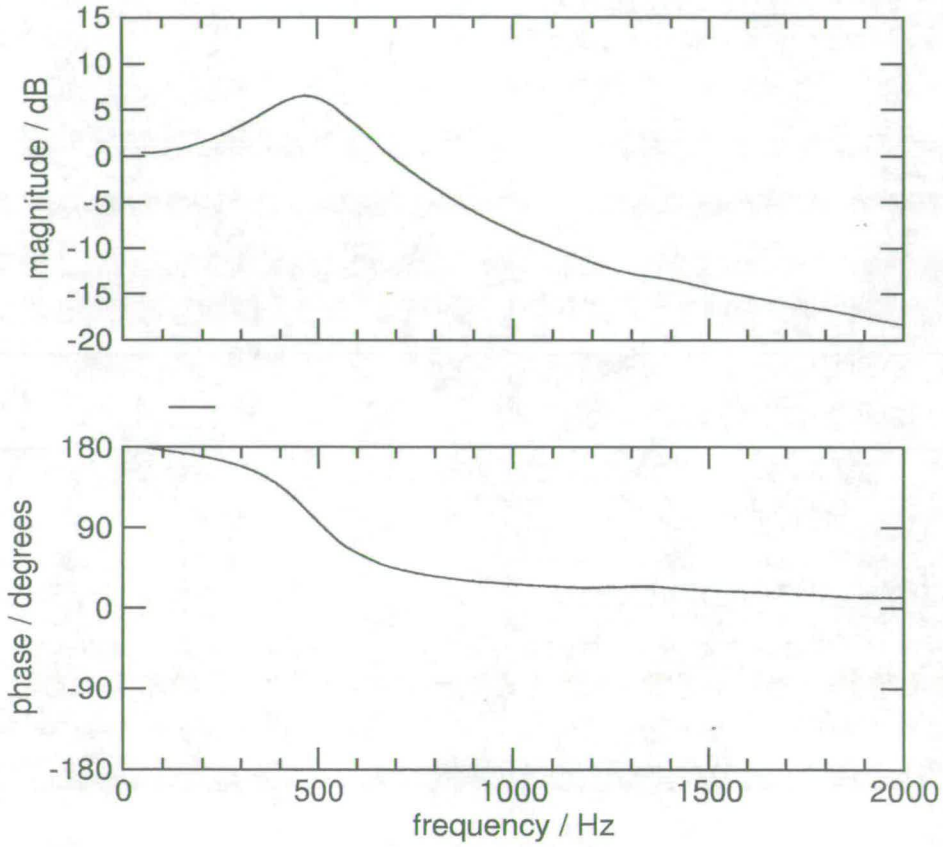

Figure 3.9: Calibration amplitude and phase for the B&K 25mm probe microphone.

properties of the probe attachment, which is needed to enable the microphone to measure pressure variations inside the mouthpiece. Corrections for the response of both of these microphones used are done after the measurements are taken by utilising the calibration data in the analysis software.

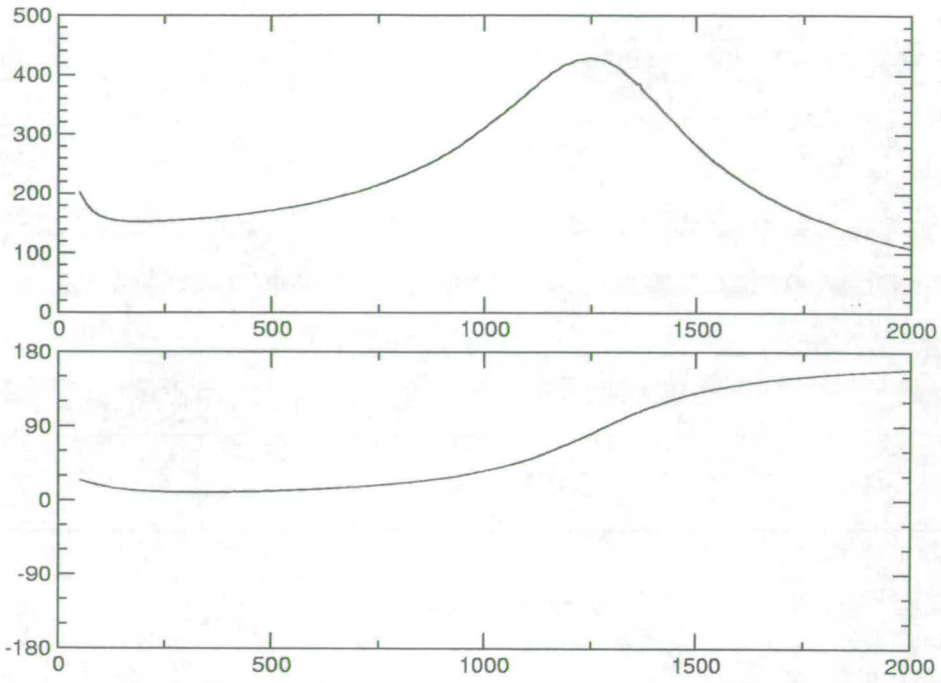

Figure 3.10: Calibration amplitude and phase for the Knowles BT-1759 microphone.

3.3.3 Analysis of mechanical response data

Analysis of the mechanical response and the calibration data was done using a program called 'auto.c' written in the C programming language. This program is a further developed version of the program of the same name used by Cullen [21]. Full details of the 'auto.c' program can be found in Appendix B. The program is written so as to be able to perform multiple types of analysis on signals from the microphones and diode, including microphone calibration and mechanical response using various measurement configurations. For analysis of the standard mechanical response data, the 'auto.c' program reads in the sampled data in the form of a two column ascii file, with the first column being the sampled data

from the Knowles microphone in the mouth and the second column being the sampled data from the diode signal. The program can also take data where there are signals from both the mouth and the mouthpiece microphones calculating the acoustic pressure difference across the lips before performing the mechanical response analysis. To perform the analysis, discrete fast Fourier transforms (FFT) are applied to the microphone signal and the main frequency component of the signal is identified. The diode signal is then analysed at this frequency and the magnitude and phase differences between the two signals is calculated using equations 3.1, 3.2.

$$| C(\omega) | = \frac{| h(\omega) |}{| P_m(\omega) |} \tag{3.1}$$

$$\angle C(\omega) = \angle h(\omega) - \angle P_m(\omega) \tag{3.2}$$

It should be noted that in this case the pressure difference across the lips ΔP is equivalent to P_m as there is no pressure on the mouthpiece side of the lips. The 'auto.c' program can analyse a file containing either a single frequency measurements or a number of different frequencies, such as is obtained from doing the mechanical response measurements using a .wav file containing 1 second sections of signal stepped in 5 Hz intervals. It does this by taking each frequency section in turn and performing the analysis on this section before proceeding to

the next. The 'auto.c' program, working in this way, creates an output file which contains frequency, magnitude and phase difference for each frequency section on the input signal. An example output from a mechanical response measurement can be seen in Figure 3.11.

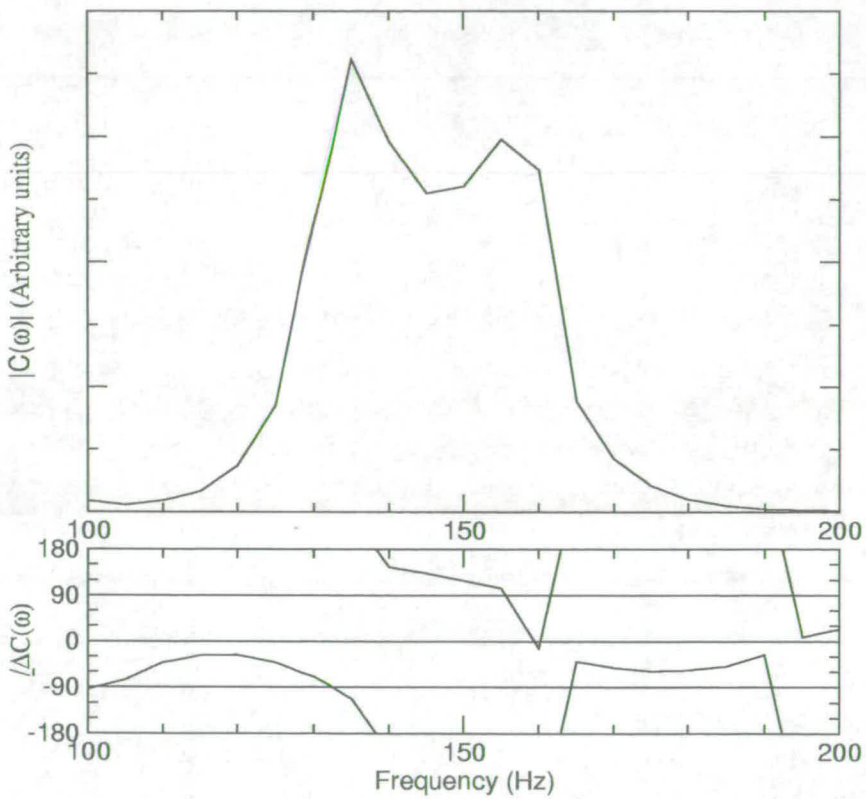

Figure 3.11: Mechanical response measurement of the artificial lips.

In this example of a mechanical response measurement, two lip resonances can be seen clearly on the amplitude response graph with frequencies of 135Hz and 155Hz. The lower frequency resonance at 135Hz has a corresponding phase response of $-\pi/2$, meaning that this resonance behaves as an outward striking

reed, whereas the higher resonance at 155Hz has a phase response of $+\pi/2$ and therefore behaves as an inward striking reed.

Mechanical response measurements can be done both with and without a mouth overpressure. If mechanical response measurements are taken with a mouth overpressure, it must have a value which is below the threshold pressure sufficient for the onset of auto-oscillation. By comparison between a mechanical response measurement done with no mouth overpressure and another done using the same lip settings but with a mouth overpressure just below the threshold pressure, it is possible to determine which lip resonance will be responsible for the destabilisation of the lips if the mouth overpressure is then increased until playing occurs. As the mouth overpressure is increased the lips become more susceptible to acoustic driving forces and so the response to the signal created by the loudspeaker increases. For the specific resonance which is responsible for the destabilisation of the lips, coupling occurs between the lips and the instrument, thus increasing the response of the lips. As the mouth overpressure approaches the threshold pressure this feedback becomes stronger, and so the response grows until at threshold pressure the lips have destabilised sufficiently that the feedback from the instrument is enough to create self sustained oscillation. At this point the mechanical response becomes effectively infinite as the acoustic driving force from the loudspeaker needed to create a response becomes zero.

3.3.4 Comparison between upstream and downstream driven measurements

Due to the greater experimental simplicity, most mechanical response measurement have been done driving the lips with an acoustic signal created by a loudspeaker mounted on the mouth. It is assumed that the response of the lips to a driving acoustic pressure is independent of whether the driving pressure is in the mouth (upstream) or the mouthpiece (downstream). To test this assumption, a loudspeaker mounting was made enabling the driving speaker to be attached to the mouthpiece as shown in Figure 3.12. With this setup, comparable mechanical response measurements can be made, first with a loudspeaker mounted on the mouth providing the driving signal and then with a loudspeaker on the mouthpiece providing the driving signal. For this comparison, the measurements taken using downstream driving of the lips were done with the loudspeaker on the mouth removed and left open to the atmosphere so as to keep the pressure in the mouth constant at atmospheric pressure.

A comparison between the mechanical response obtained using the upstream and downstream driving of the lips is shown in Figure 3.13. From this figure, it can be seen that although there are some slight differences between the two measurement methods, mostly in terms of the relative amplitudes of the response peaks, the general features of the measurements are very similar both in terms of the frequency of the amplitude response peaks and the $\pm\pi/2$ crossing points.

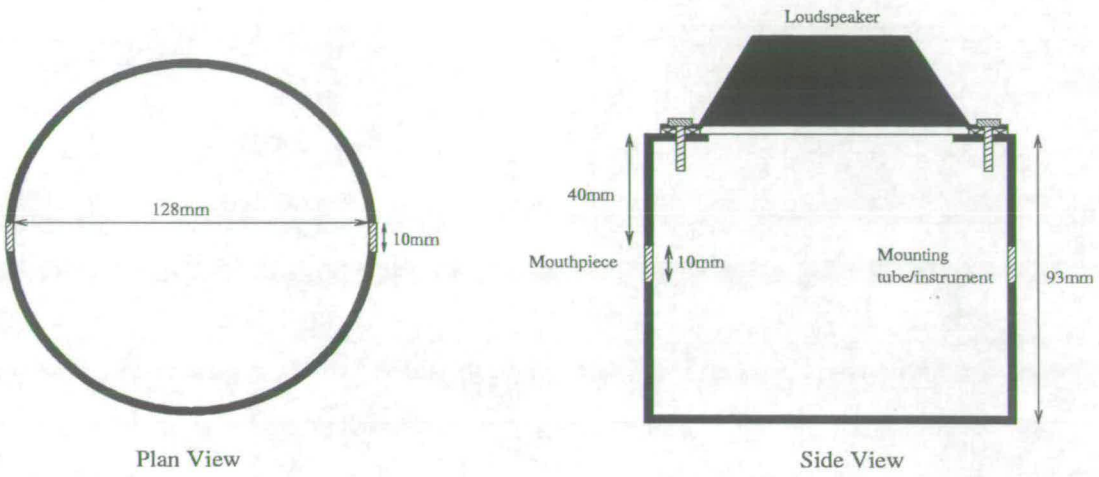

Figure 3.12: Mounting for the loudspeaker on the mouthpiece.

The larger differences in phase between the upstream and downstream driven measurements occur mostly when the amplitude response of the lips is very small. When there is a very small amplitude response of the lips, the signal from the diode can become unclear as the background noise in the measurements can reach levels comparable with the measured signal, thus leading to large errors. This is not a critical problem as the areas of interest are around the response maxima where there is a clear signal from the diode, and so the signal to noise ratio is much better leading to much smaller errors.

These results show that there is little difference between upstream and downstream driven mechanical response measurements, especially at the resonance frequencies of the lips. Differences between the two methods of measurement may occur when there is a mouth overpressure due to non-linearity of the flow between the lips, but the main features of the lip destabilisation is visible with

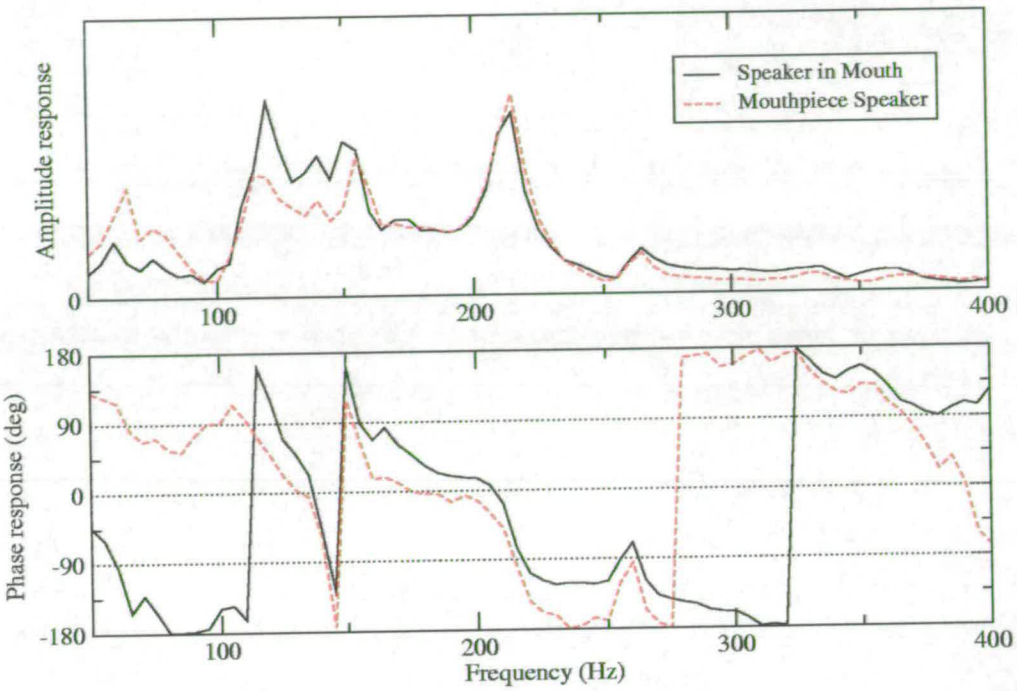

Figure 3.13: Mechanical response driven from upstream and downstream.

either method. With the downstream driving technique, the loudspeaker mounting means that the instrument cannot be directly attached to the mouthpiece but rather must be attached to the other side of the loudspeaker mounting, thus considerably changing the acoustic impedance of the resonator. Taking the above results into consideration, the two methods of mechanical response are considered interchangeable as required by the measurement being made. It should be noted that the two different measurement methods give a phase difference of 180^o which must be compensated for during the analysis.

3.3.5 Lip resonance destabilisation

From the above results and discussion of the mechanical response measuring technique it is clear that useful data on the resonance properties of the lips can be obtained by performing this type of measurement, particularly if measurements are taken both with and without a mouth overpressure.

By taking a mechanical response measurement, first with no mouth overpressure and then with a mouth overpressure which is just below the threshold pressure, the lip resonance which is responsible for the note played can be seen, as shown in Figure 3.14. In this case it is clear that there is some effect on the mechanical response caused by the resonator, as the destabilisation of any lip resonance is controlled by its proximity to and relationship with an acoustic resonance of the instrument.

In this example measurement it can be seen that there are a number of lip resonances at frequencies of 95Hz, 122Hz, 172Hz, 300Hz and 343Hz. As the mouth pressure is increased, the resonance at 172Hz grows in amplitude much faster than any of the other lip resonance frequencies. This indicates that it is this lip resonance which will destabilise and so be responsible for the auto oscillation of the lips, and so the note produced will, according to the simple one mass model, have a frequency which is around, although slightly higher than, 172Hz, due to the outward striking nature of this lip resonance.

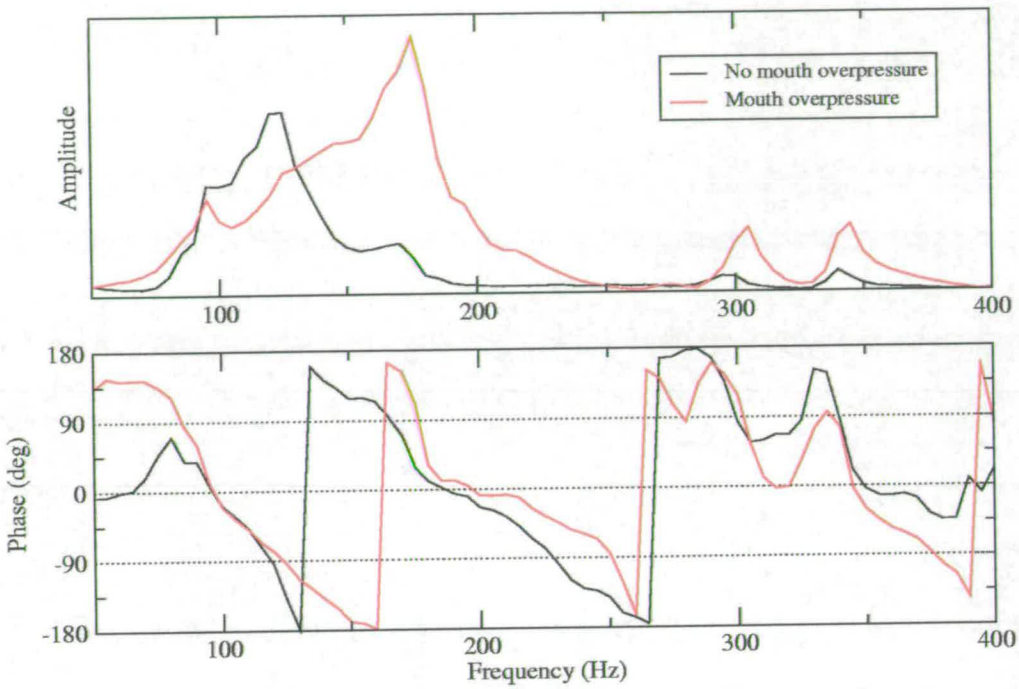

Figure 3.14: Mechanical response showing destablilising lip resonance for artificial lips with just a mouthpiece.

It is often seen in the mechanical response measurements that for the case of no mouth overpressure the amplitude response of the resonance which is eventually responsible for the destabilisation of the lips is very small. One of the factors contributing to this is that if there is an impedance maximum of the instrument resonator at the same frequency as a lip resonance, there is a reduction in the amplitude response of that resonance. This is due to the acoustic impedance maxima of the instrument effectively adding a load to the lips. A simple example of this can be found when two mechanical response measurements are taken without changing the lips but one having the mouthpiece present and the other

with the mouthpiece cup removed. In this case there is a overall reduction in the amplitude response of the lips, as the resonance of the mouthpiece has a higher frequency than most of the resonance peaks (518Hz), but there is a considerable increase in the overall acoustic impedance as seen by the lips. There is a corresponding decrease in the mechanical response, so two curves are given with similar form, but the one for the measurement with the mouthpiece cup in place has smaller amplitude response.

3.3.6 Mechanical response with varying pipe length

Previous measurements by Chen[18], Cullen[22] and Yoshikawa[52] have shown how the playing frequency of a brass instrument changes from being above the acoustic instrument resonance to below it depending on the playing situation. By performing measurements of mechanical response both with and without a mouth overpressure, and also measuring the threshold playing frequency, the reed type measured by the mechanical response can be compared with the reed type derived from the relationship between playing frequency and acoustic resonances of the instrument. The mechanical response measurement of lip destabilisation gives considerably more information than is given by just examining the difference between the playing frequency and the instrument resonance, as in addition to the reed type of a single lip resonance, information on other lip resonances approaching destabilisation can be seen.

The mechanical response measurement of the artificial lips taken with a mouthpiece attached to a short pipe length is shown in Figure 3.15. It can be seen in this figure that there are two lip resonances at frequencies of 120Hz and 153Hz with corresponding phases of $-\pi/2$ and $+\pi/2$ respectively, implying that the lower lip resonance (120Hz) has an outward striking behavior and the higher one (153Hz) has a inward striking behaviour. Also shown in this figure are the playing frequency and the acoustic resonance frequency of the instrument (pipe) as obtained from acoustic input impedance measurements [6]. In the measurement without mouth overpressure there is very little amplitude response at the higher resonance frequency (153Hz), but the presence of this resonance is shown by the phase response which crosses the $+\pi/2$ line at this point. When there is a mouth overpressure this resonance can be seen clearly both from the amplitude and phase plots, although the lower resonance still shows a larger amplitude response, the higher resonance is growing more rapidly and has a frequency which is very close to the playing frequency. If the mouth overpressure was increased closer to the threshold pressure this second resonance peak would become clearly larger than the lower one, but increasing the threshold pressure to this high a value can create problems with the measurement: when the lips are driven by the loudspeaker at a frequency close to the playing frequency there is a tendency for the lips to start self-sustained playing for a short while, thus obscuring any of the measurements round about this peak.

Figures 3.16 and 3.17 show a series of mechanical response measurements

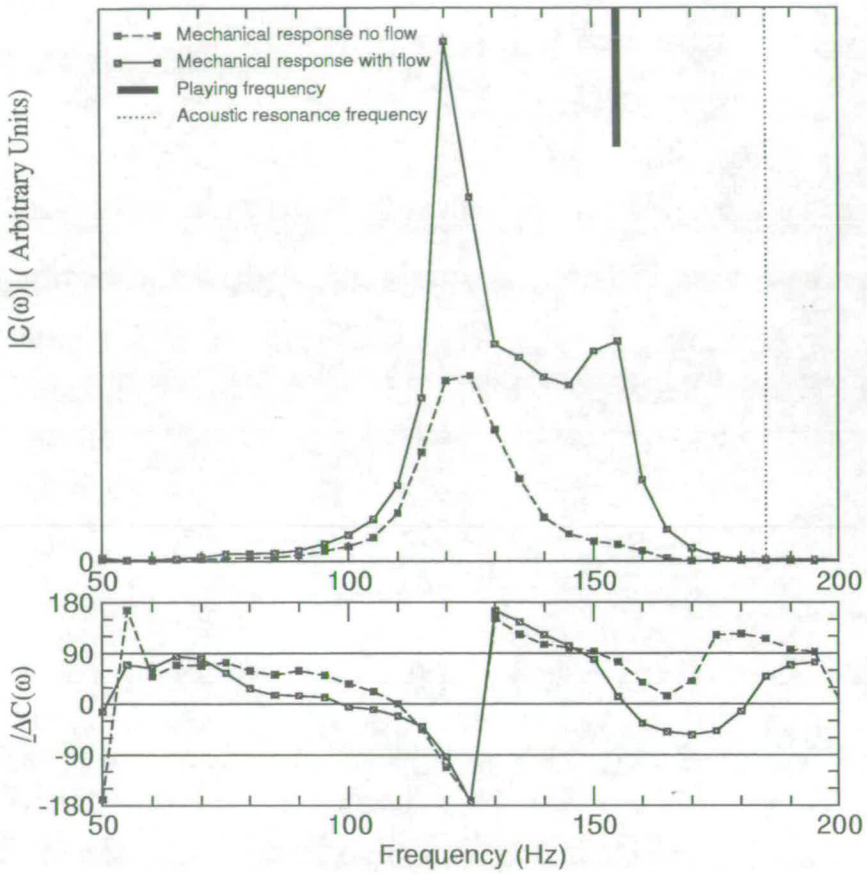

Figure 3.15: Mechanical response of lips with a short pipe.

taken with the telescopic pipe attached to the mouthpiece and extended over a range of lengths between 1.3 and 2.1 metres. For each pipe length a response measurement is shown, both for the case with no mouth overpressure (dotted line) and with a mouth overpressure just below the threshold playing frequency (solid line), as well as the threshold playing frequency and the instrument resonance in the same form as was shown in Figure 3.15. Throughout this series of measurements no adjustments were made to the lips, so the resonance properties of the lips remain constant and all changes in the mechanical responses are due

to interactions between the lips and the pipe resonances.

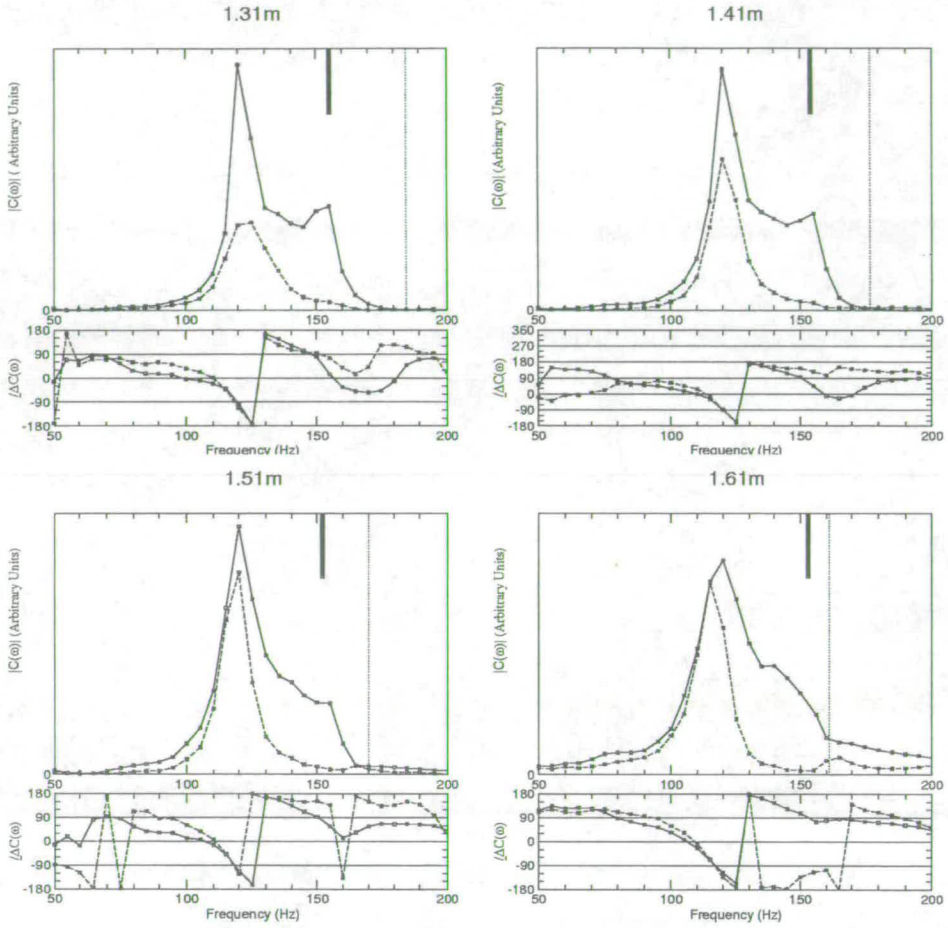

Figure 3.16: Mechanical response for different pipe lengths (1)

Looking at the first graph for the 1.31 metre pipe length (Figure 3.16) it can be seen that in the case of no mouth overpressure there is only one resonance visible in the amplitude response of the lips at 120Hz which has an outward striking behavior. When the mouth overpressure is increased another resonant peak appears at 153Hz. This resonance is also close to the playing frequency of the lips and has an inward striking behavior. Although this peak cannot be seen in the amplitude response curve for the case of no mouth overpressure, its presence

can be predicted by the phase response at this frequency which has a value of $+\pi/2$ at 153 Hz. The lack of an amplitude response at this frequency when there is no mouth overpressure can be attributed to the fact that the acoustic impedance of the pipe is much larger at 153Hz than at the 120Hz resonance which falls very close to an impedance minima of the pipe, thus reducing the response at 153Hz but not at 120Hz. This can be seen by comparing the responses with no flow for the 1.31 metre pipe and the 1.81 metre pipe (Figure 3.17) where there is no suppression of the 153Hz resonance due to impedance of the pipe, giving this lip resonance a much greater amplitude response. As the mouth pressure is increased for the 1.31 metre pipe, the resonance peak at 153Hz approaches destabilisation, so the height of the amplitude response peak grows much more dramatically than that of the 120Hz resonance. Thus this peak can be identified as the destabilising peak having an inward striking behaviour; this concurs with the fact that the playing frequency is below the acoustical resonance frequency of the instrument, as is predicted by a single mass forced oscillator of the lips as shown in chapter 2 [14].

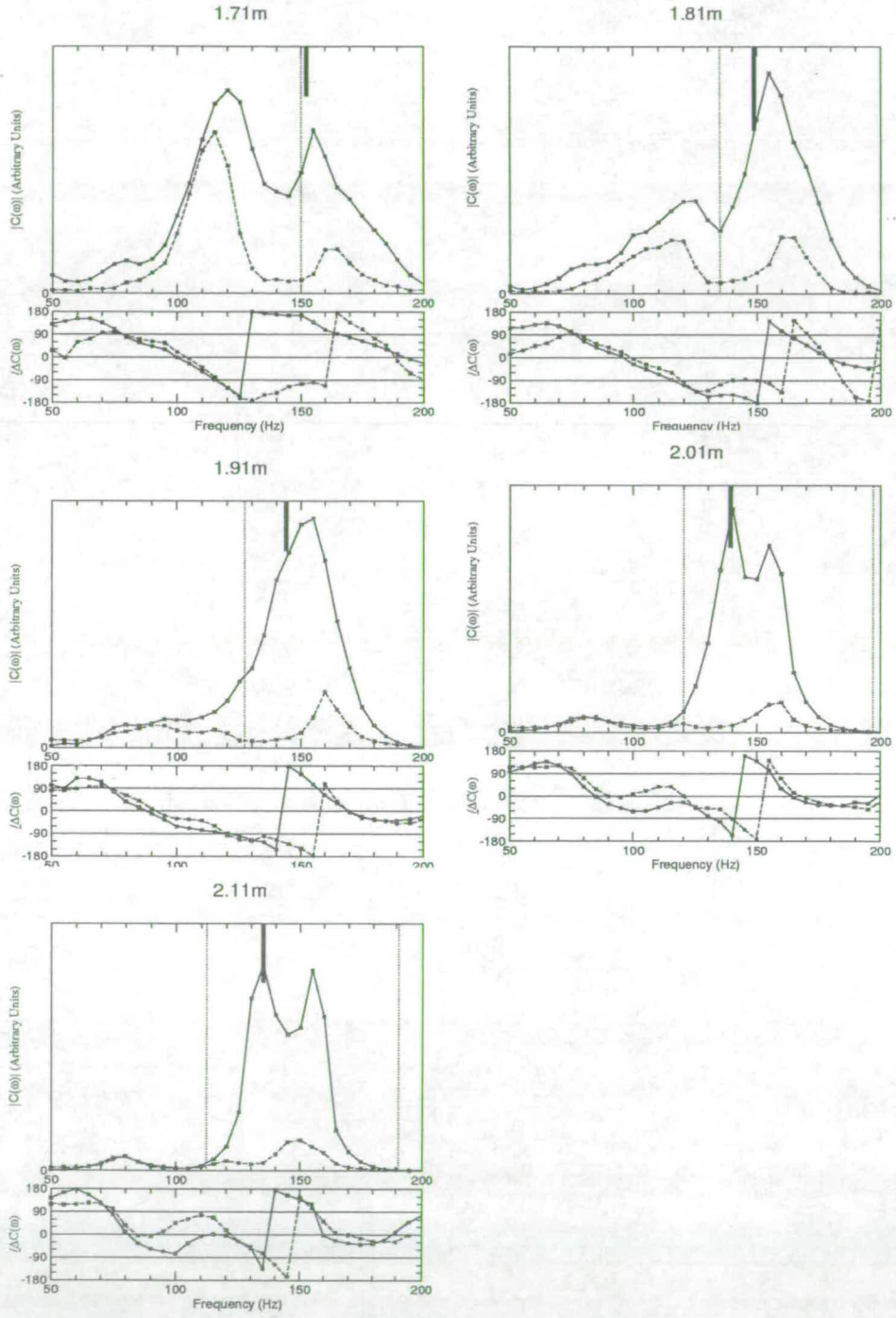

Figure 3.17: Mechanical response for different pipe lengths (2)

A contrasting case can be seen in the graph for the 2.11 metre pipe length. Here the resonance which destabilises (135Hz) has an outward striking characteristic and the playing frequency is above the acoustical resonance of the instrument, thus also agreeing with the single mass forced oscillator model. In the intervening lengths between these two cases it is much less clear whether there is an inward or outward striking behaviour. Instead there is a much more complicated interaction between the the different lip resonances with some coupling clearly happening between the different resonant modes of the lips, which cannot be accounted for by the simple one mass model which has so far been considered.

It is this intermediate region between the clear inward and outward striking lip reed behaviour where the mechanical response shows much more detail than can be obtained from just looking at the relationships between the frequencies of the played note and the instrument resonances. If the data is analysed purely from this relationship between the playing frequency and the pipe resonance frequency, then the pipe lengths from 1.31 metres up to 1.61 metres show an inward striking behaviour and the lengths from 1.71 metres up to the full extension at 2.11 metres all have outward striking behaviour. Comparing this with the phase plots from each of the graphs it is clear that although there is a tendency towards the shorter pipe lengths having an inward striking behaviour and the longer lengths having an outward striking behaviour, the phase response at the playing frequency is not always exactly $\pm\pi/2$. This can be seen more clearly in Figure 3.18 which plots the phase of the mechanical response measured just below threshold against playing

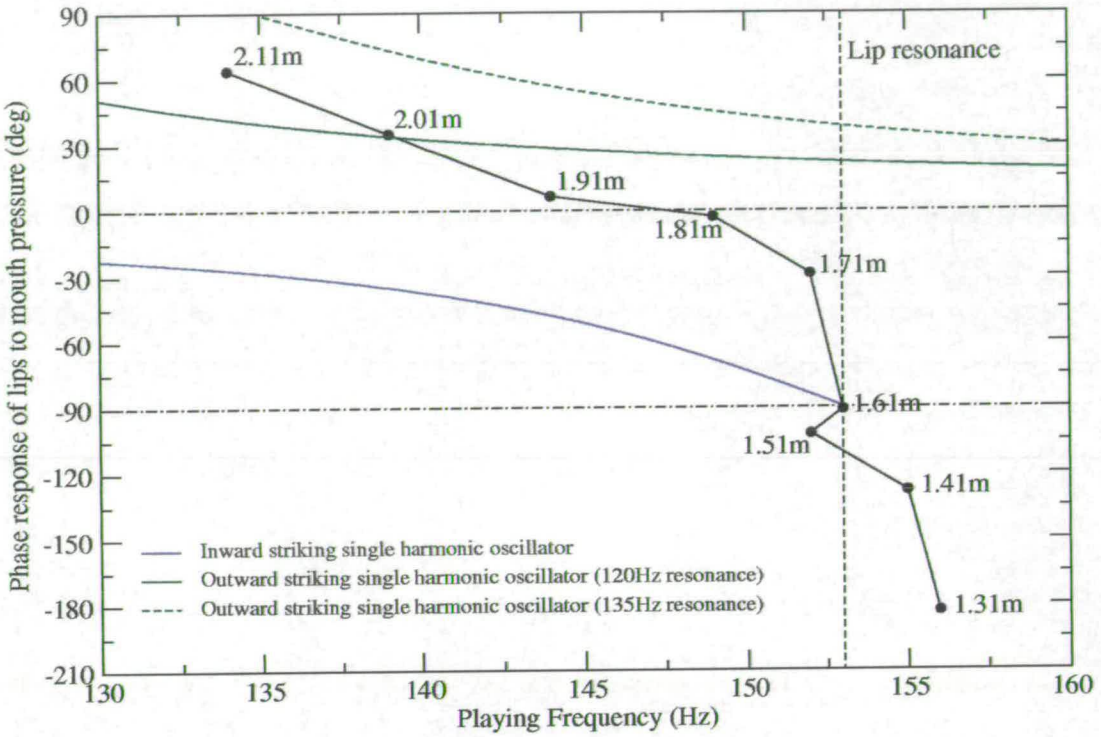

Figure 3.18: Phase response at playing frequency for mechanical response measurements with mouth overpressure.

frequency for a range of pipe lengths. For all pipe lengths from 1.31 metres up to 1.71 metres there is a negative phase response at the playing frequency, and for pipe lengths greater than 1.81 meters there is a positive phase response at the playing frequency, with the value at pipe of length 1.81 meters having a response very close to zero.

Examining the measurements with mouth overpressure in Figures 3.16 and 3.17, it can be seen that both of the resonance peaks always have a phase response of $-\pi/2$ for the lower resonance and $+\pi/2$ for the upper resonance and this is

not affected by any changes in tube length. However it can be seen that the lower resonance shifts in frequency at the longer pipe lengths; this is clearly seen in the measurement for the 2.11 meter pipe, where this resonance has a frequency of 135Hz as opposed to the normal measured frequency of this resonance of 120Hz. The effect of the acoustic resonance of the pipe on the mechanical response measurements can be seen by looking at the phase response for the case with no mouth overpressure. The phase response for both mouth overpressure and no mouth overpressure show good similarity over most of the frequency range, except at the frequency where the pipe resonance falls. At this frequency, the two measurements diverge with the phase response for the case with no mouth overpressure having a phase which is between 60^o and 180^o greater than for the case with mouth overpressure. This is what would be expected if the lips are considered as a simple harmonic oscillator, with the pipe resonance adding an extra mass to the resonator.

In Chapter 2 it was shown that for a single harmonic oscillator model of the lips, an inward striking reed must play at a frequency which is below the reed resonace and an outward striking reed must play above its resonance. Looking again at the graph of the phase response of the lips at the playing frequency (Figure 3.18), it can be seen that all the notes played have a frequency which is higher than the lower lip resonance and lower or just above the higher lip resonance. It should be noted that the mechanical response measurements were taken with a resolution of 5Hz and therefore the lip resonance frequency is accu-

rate to ±2.5Hz. The two resonances of the lips can be considered independently as damped single harmonic oscillators, the first one have a resonance frequency (f_{o1}) of 120Hz and a quality factor (Q_1) of 5 and the second resonance having a resonance frequency (f_{o2}) of 153Hz and a quality factor (Q_2) of 7.4, as obtained from the response without a resonator. In this case the phase response of these two harmonic oscillators can be calculated using equation 3.3.

$$\angle C(\omega) = tan^{-1} \frac{\gamma\omega}{\omega_o^2 - \omega^2} \tag{3.3}$$

The plots for the inward and outward striking simple harmonic oscillator phases calculated using this equation are shown in the Figure 3.18. It can be seen that over most of the frequency range the phase response at the playing frequency falls somewhere between the two single mass model phase response curves. At the longest pipe length the phase response at the playing frequency has a higher value that which is given by the simple harmonic model, which would put it outside the possible playing values; as noted above, however, for the 2.11 metre pipe length the frequency of the first lip resonance has moved to a higher value at 135Hz, which as shown on the graph puts the phase at the playing frequency below the phase obtained from equation 3.3.

For the shorter pipe lengths the phase at the playing frequency falls below the $-\pi/2$ value which would mean, according to the simple model, that there should

not be energy input to the system. It should be noted for these pipe lengths that the playing frequency is higher than that of the second lip resonance which has a clear phase of $-\pi/2$. It should also be noticed that the frequency change for each shortening of the pipe becomes very small, suggesting that there may be another lip resonance at a higher frequency which is enabling the lips to play above the second lip resonance frequency, but the effect of the second lip resonance is very strong and so the frequency does not increase much above its value of 153Hz.

From the above data it is clear that the lips do not act as a clearly inward or outward striking reed or as a single harmonic oscillator; it can be seen from figure 3.18 that the played note is a result of interaction between the two lip resonances.

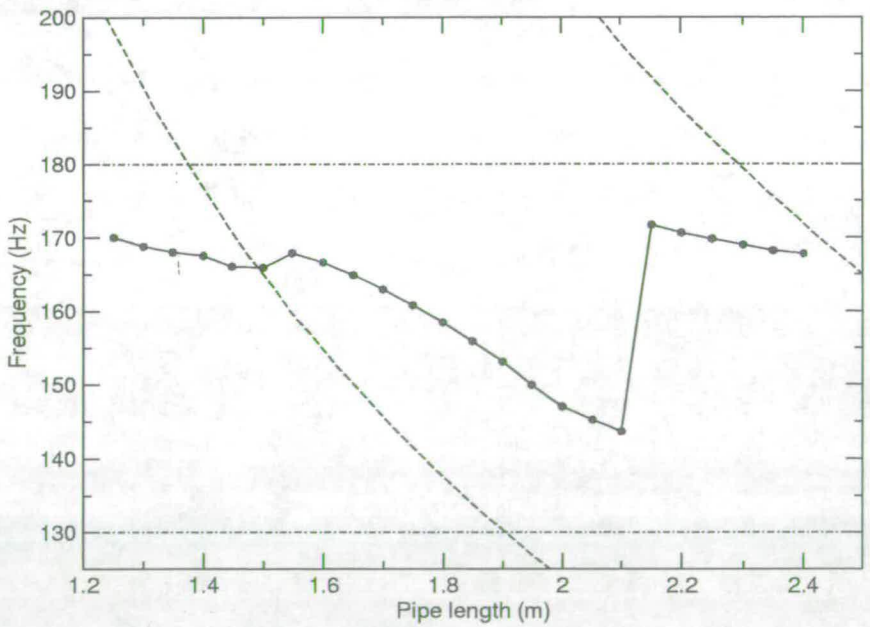

Figure 3.19: Playing frequency against pipe length.

Despite the change in the dominant lip resonance there is a smooth change in playing frequency as the pipe is extended (Figure 3.19). Although the change in frequency remains smooth, some interesting features of the coupling between lip resonances can be found in the region between clear dominance of one lip resonance or the other. It can be seen in Figure 3.19 that as the pipe is extended, the playing frequency does not show a continual drop in frequency, but rather there is a small region where the pitch of the note rises as the playing frequency crosses the acoustical resonance frequency of the instrument. This fluctuation in the playing frequency seems to be a feature which is often present in the note produced by the artificial lips using both the telescopic pipe and a trombone. Studies of this effect and other effects which occur during playing both of the artificial mouth and by real players are presented in Chapter 4.

3.4 Conclusions

The artificial lips provide a method by which experiments can be performed on the playing characteristics of brass instruments which are not possible or very difficult to perform on real players. Mechanical response measurements provide a way of analysing the resonance properties of the lips, giving detailed insight into the lip resonance frequencies and the reed type of these resonances. These measurements can also be used to see how the resonance properties change depending on the presence of acoustic resonators (instruments). By performing mechanical

response measurements with no resonator or mouth overpressure present, the resonance properties of just the lips themselves is given. If there is a resonator and mouth overpressure of a value just below the threshold playing pressure, coupling between the lip resonances and the acoustic impedance of the resonator leads to an increase in one of the lip resonances, thus identifying the destabilising resonance and its reed type behaviour. Measurements show that the lip resonance which destabilises as the mouth pressure reaches threshold changes depending on the acoustic resonance frequency of the instrument which is attached to the mouthpiece. These measurements have shown that the lips can change between acting as an inward striking reed at one extreme to an outward striking reed at the other. This change of lip characteristic happens in a smooth manner, with a region between the two extremes where the lips do not act clearly in either of the oscillation regimes, but rather as a superposition of the two.

Chapter 4

Lip reed under playing conditions

4.1 Introduction

In the previous chapter measurements of the mechanical response of the lips were presented for the artificial lips with a telescopic pipe resonator attached to the mouthpiece and extended over a range of different lengths. In this chapter, these results taken with the mouth overpressure (P_m) less than the threshold pressure are extended in their application to the situation where the mouth overpressure is sufficient to destabilise the lips. Most of these measurements are performed at or around the threshold pressure, where the lips can be considered to act as a linear oscillator due to the small amplitudes of the lip motion and acoustic pressures, although some measurements are extended to higher pressures. Measurements are also presented giving some insight into the effects of the mouth cavity on the

playing of a brass instruments as well as some validation of experiments on the artificial lips by comparison between the playing of artificial lips and that of real players.

4.2 Threshold playing effects of pipe extension

In Chapter 3 an example graph of the playing frequency against pipe extension was shown (Figure 3.19). A more detailed graph of this type including showing the threshold pressure measurements is given in Figure 4.1. It was noted previously that there is often a slight rise in frequency as the telescopic pipe or trombone slide is extended such that the playing frequency changes from being below the acoustic resonance to above. This rise coincides with the point at which the dominant lip resonance changes from being inward striking to outward striking, and can best be understood by looking at the single mass model behaviour. Just before the transition there is a dominant inward striking behaviour, and so as previously shown using the single mass model, the playing frequency must be below the acoustical resonance frequency of the instrument. As the slide is extended the outward striking behaviour becomes dominant, and so the playing frequency must be above the acoustical resonance frequency of the instrument. If this transition happens over a short range of pipe expansion, and as there is only a small decrease in the acoustical resonance frequency of the instrument across this small extension, then one would expect there to be little lowering or possibly

even a slight rise in the playing frequency at this transition point. This rise in frequency as the pipe is extended is an effect which although not always present in the measurements is often seen, being dependent on the spacing, strength and Q values of the lip resonances. This rise in frequency which can be seen in some of the measurements is probably too subtle to be noticed if the instrument is being played by a real player, as the lips need to remain unchanged while the slide is extended; using the artificial lips in some configurations a clear rise in frequency can be heard when extending the slide, both using the telescopic tube and using a real trombone.

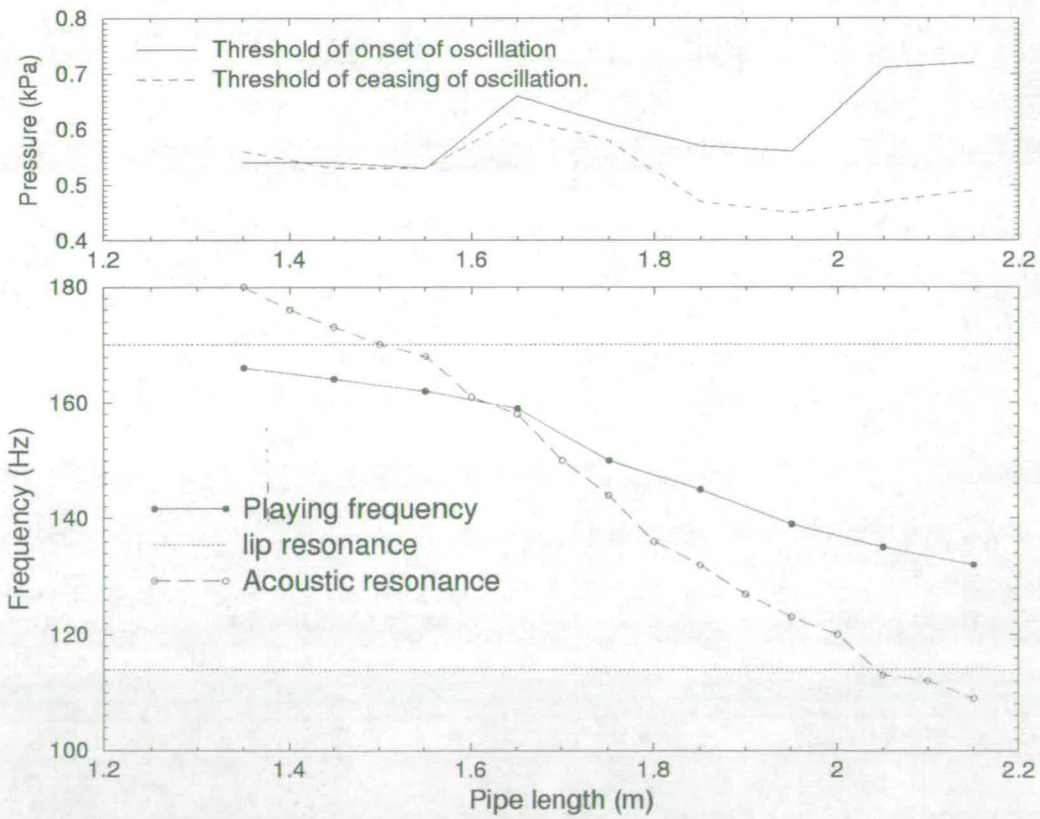

Figure 4.1: Playing frequency against pipe length for telescopic tube.

In Figure 4.3 a graph similar to that in Figure 3.19 is shown but using a trombone in place of the telescopic tube. This enables a much larger change of length, thus allowing the artificial lips to play more than one of the instrument resonances without adjustment of the lip parameters. It can be seen from this graph that there is a similar descent of the playing frequency with pipe extension as there was when using the telescopic tube, although details at the transition points are not as clear due to the larger scale. Due to the extra length of the trombone compared with that of the telescopic tube, the artificial lips usually play higher modes of the instrument; in the case shown in Figure 4.3 the third and fourth modes of the trombone are sounded, whereas on the telescopic pipe the second mode is predominantly played. The third and fourth mode impedance peaks of the trombone have a much higher Q value than those of the second mode of the telescopic pipe, as can be seen by comparing the acoustic impedance of the trombone (Figure 2.3) with that of the telescopic pipe (Figure 4.2). In addition extension of the slide of the trombone by 50mm has the effect of lengthening the resonator by double this (100mm), so that a much wider range of lengths is available when using a trombone given the limitations of space for the experiments. As a consequence, measurements can be taken using the trombone where there is a jump between two or more different modes of the instrument in a single extension of the slide, whereas with the telescopic tube there is a much smaller range which can be obtained and so it is not possible within the experimental limitations to have both the crossing of the playing frequency from below to above the acoustic

resonance and a jump to the next mode for one lip setting.

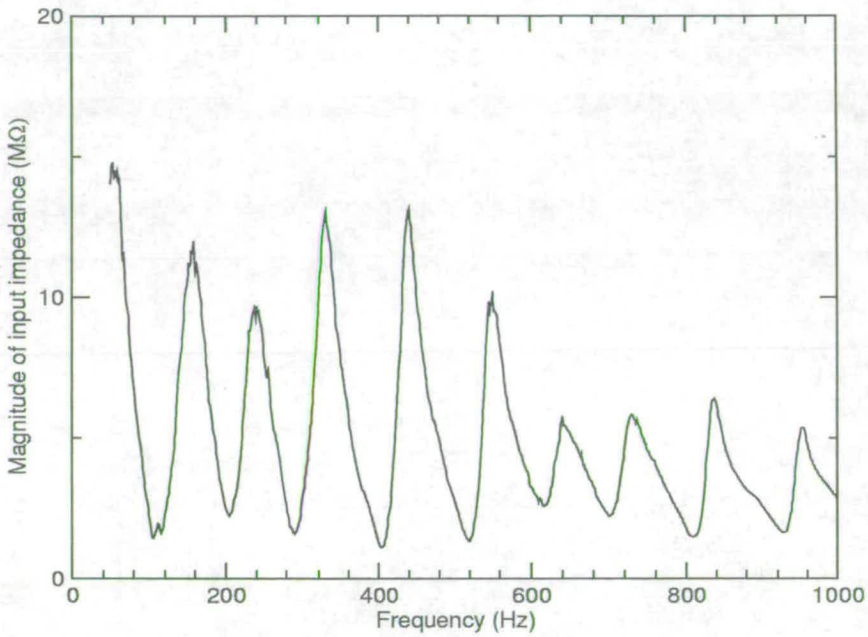

Figure 4.2: Acoustic input impedance of the telescopic pipe.

Another effect of the change in resonator length can be seen in the pressure graph in Figure 4.1. Here there are two lines shown for the threshold pressure: one for the pressure needed to start playing and the other for the pressure at which playing ceases. It can be seen that for the short pipe length these pressure coincide with each other, suggesting a direct bifurcation. For the longer pipe lengths the pressure needed to start the lips playing is higher than that for the ceasing of playing. This suggests that in this case there is an inverse bifurcation [43].

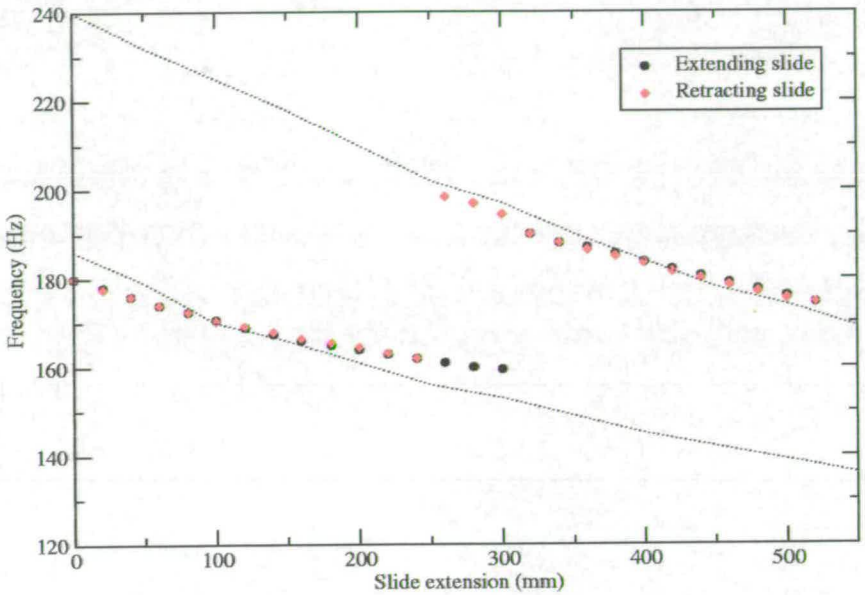

Figure 4.3: Playing frequency against pipe length for trombone.

4.3 Effects of mouth cavity

The effects of the mouth cavity of the player have been discussed in previous literature although most of this work has involved just theoretical analysis [29], [46], rather than experimental measurements. Cullen [21] performed some simple measurements of the effects of the mouth volume on mechanical response using an artificial mouth. From these measurements it was concluded that there was little if any effect caused by a change in the mouth volume. A more sensitive measurement on the effect of the mouth volume on the mechanical response can be obtained by driving the lips from the mouthpiece side.

It has been suggested that the impedance of the mouth and respiratory system

creates the acoustic feedback which enables a person to buzz their lips without any instrument present [29]. This would imply that there can be significant coupling between the lips and the acoustic impedance of the mouth cavity. In normal playing the impedance of an instrument is much larger than that of the mouth, and therefore any effects on the played note due to changes in the mouth impedance are expected to be much smaller than effects created by changes in the instrument. In addition to this, the acoustic pressure level in the mouth is usually considerably lower than in the instrument; measurements taken using the artificial lips playing at just above threshold give sound pressure levels of around 85dB in the mouthpiece while the level in the mouth is around 60dB. These factors must be considered alongside the fact that the player can very easily change the shape and size of the mouth cavity. Furthermore, even if there is little change in the sound produced by the instrument, the acoustic pressure in the mouth will be directly affected by any change in the mouth impedance and thus the sensation of the note as perceived by the player will change. For example, if the note played corresponds exactly to a resonance frequency in the mouth, sound pressure levels in the mouth would be expected to be considerably higher than if the playing frequency was away from any of the mouth resonances.

4.3.1 Effect of mouth volume on mechanical response

To measure the effect of the mouth cavity, mechanical response measurements were taken using the loudspeaker mounted on the mouthpiece, driving the lips from the downstream side. The volume of the mouth cavity was changed by pouring a known volume of water into the bottom of the artificial mouth, thus reducing the overall volume. The mouth cavity has a volume of either 1330ml with the loudspeaker mounting on top of the mouth attached, or 1090ml when it is removed. This volume can be reduced by an amount of up to 300ml by pouring water into the bottom of the mouth before the level of the water becomes such that it touches the bottom lip. Mechanical response measurement were taken with a 1Hz accuracy over the frequency range of 50 - 250Hz.

The results from two of the series of measurements taken with different lip settings and different mouth volumes are shown in Figures 4.4 and 4.5. In these graphs a change in the mechanical response of the lips depending on the mouth volume can clearly be seen. This is most easily observed in Figure 4.4 where the peak at 103Hz shows a steady decline in amplitude as the volume of the mouth is reduced. This effect is analogous to that seen in Chapter 3 when performing mechanical response measurement from the mouth side, when the amplitude response of a lip resonance is reduced due to the presence of an impedance maximum of the instrument at the same frequency as one of the lip resonances, as seen in the response without flow in Figure 3.15. This suggests that there is an

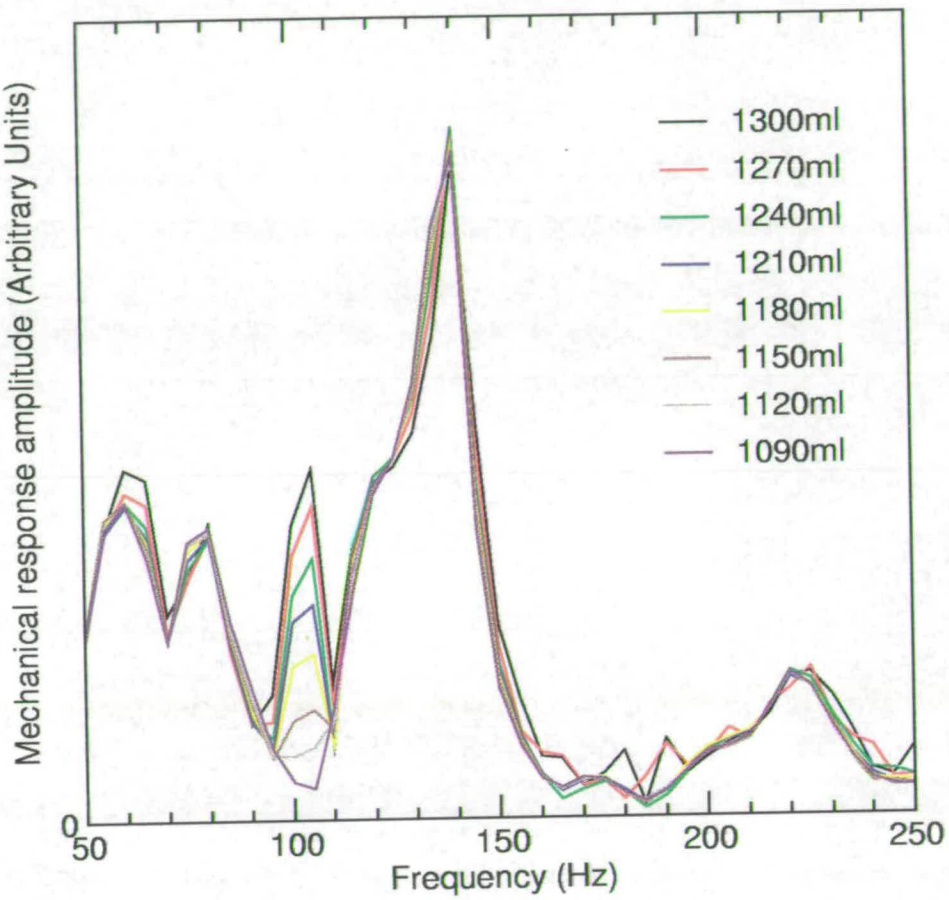

Figure 4.4: Mechanical response of lips with varying mouth volume.

impedance maximum of the mouth in the region of 100-200Hz. As the dimensions of the artificial mouth are such that any resonances due to standing waves in the mouth must have frequencies of greater than 1kHz, this impedance maximum must be equivalent to a Helmholtz resonance of the mouth. A rough estimate of the Helmholtz resonance frequency of the mouth can be gained by considering the mouth to be a Helmholtz resonator with volume $V = 1.08 \times 10^{-3}\text{m}^3$ and an opening through the lips with effective length $L = 0.006\text{m}$ and area

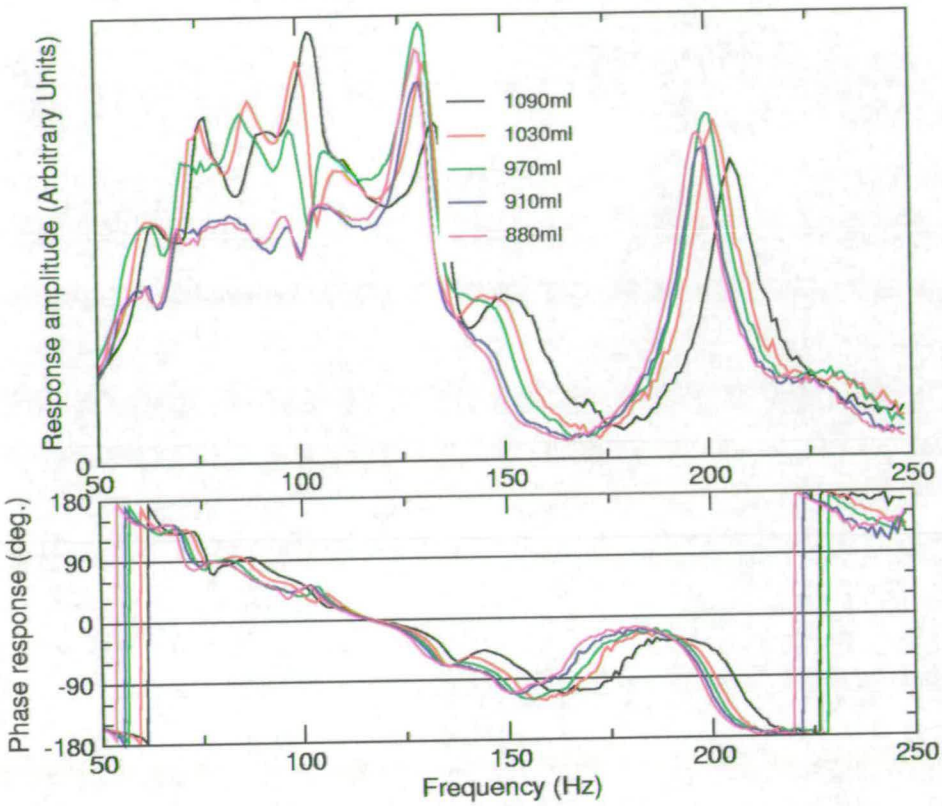

Figure 4.5: Mechanical response of lips with varying mouth volume.

$S = 4 \times 10^{-6}\text{m}^2$: calculating the Helmholtz resonance using equation 4.1 gives a resonance of $f_0 = 41\text{Hz}$, and a change in this resonance to around 49Hz (a change of 17%) if the volume of the mouth cavity is reduced by 300ml.

$$f_0 = \frac{c}{2\pi}\sqrt{\frac{S}{LV}} \tag{4.1}$$

These calculated values have a considerably higher frequency than that at which changes are seen in the experiments (Figure 4.4), which show a change in the mechanical response at 100Hz, which can be attributed to the Helmholtz

resonance of the mouth. This deviation between the calculated and measured values can be understood, as the calculated values are based only on estimated values of the effective lip channel size. Also the mouth does not conform to an ideal Helmholtz resonator as is assumed in equation 4.1, due to the non-symmetrical shape and the oscillating size of the opening between the lips. It does show that the Helmholtz resonance of the artificial mouth is likely to be around the frequency of commonly played notes on the trombone. Considering this for Figure 4.4 it can be seen that the resonance frequency of the mouth at 1300ml must be around 90Hz rising to around 103Hz for the 1090ml mouth volume. The change in resonance frequency is around 14% for a volume change of 210ml, which is similar to the change which would be expected for a reduction in volume as calculated using equation 4.1.

The volume of the artificial mouth is somewhat larger than that of a real player, where the volume of the mouth cavity and upper vocal tract is around 200-500ml. Using equation 4.1 with the same size lip opening as in the above calculations gives a Helmholtz resonance of between 270Hz and 426Hz. This frequency range is in the same frequency region in which many of the normal notes played on a trombone or other brass instrument occur. This would suggest that the mouth resonances may have a noticeable effect on the playing of brass instruments.

4.3.2 Mouth volume and playing tone

In order to further determine whether the effects of the mouth cavity shown in the previous section have any effect on the note produced when playing a trombone, measurements were taken of the radiated sound from a trombone played by the artificial lips while changing the volume in the mouth. Figure 4.6 shows the frequency spectrum of the signal from a trombone measured on axis at a distance of 5cm from the bell using a B&K type 4192 $\frac{1}{2}$" reference microphone. Data is shown for the same note produced with two different mouth cavity volumes played at the same mouth overpressure.

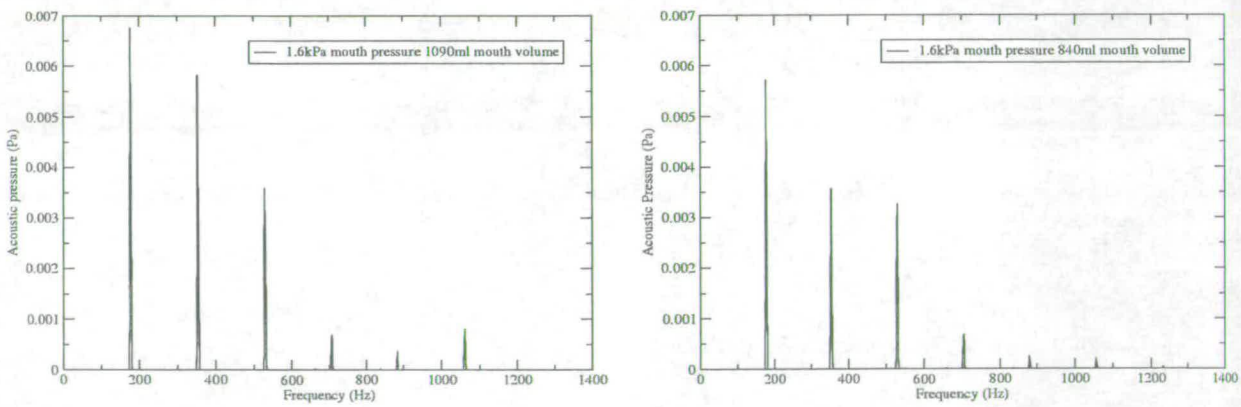

Figure 4.6: Frequency response of trombone played with different mouth volumes

This graph shows a noticeable difference in harmonic content between the two different measurements, although the frequencies are identical for both measurements. In order to give a clearer picture of these changes, a series of measurements were taken with the artificial mouth playing constantly while small changes to the mouth volume were made, starting with the maximum possible volume of water

in the mouth and reducing this volume by a small amount for each measurement. Figure 4.7 shows the amplitude of the first four harmonics of the note produced by the trombone as a function of mouth volume. It can be seen from this figure that there is a steady progression in the amplitude of some of the harmonics as the volume changes. This is especially visible in the case of the 3rd harmonic which shows a fairly steady decline in amplitude as the mouth volume increases.

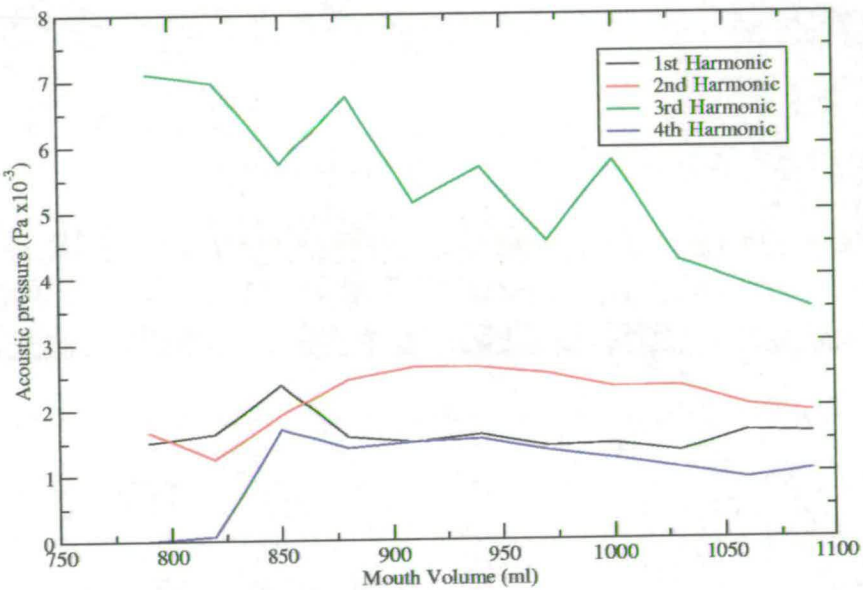

Figure 4.7: Dependence of the harmonic amplitude of the note produced by a trombone as a function of mouth volume.

These results show that there are some noticeable effects both on the mechanical response and more importantly on the played note due to the changes in the mouth volume. The mouth cavity does not have any effects on the actual frequency of the notes produced by the instrument; this is to be expected as the acoustic impedance of the mouth is much smaller than that of an instrument and

therefore the playing frequencies are much more strongly controlled by the instrument than the mouth impedance. The volume of the artificial mouth is around two to three times larger than the effective volume of a real player's mouth and upper vocal tract. This means that the resonances of a real player's mouth will be higher in frequency than those of the artificial mouth. Despite these differences the lowest resonance of the mouth both for the artificial mouth and, as can be implied from the calculations, for a real player, fall in a region which is well within the important frequencies produced by brass instruments.

4.4 Comparisons between real players and artificial lips

One of the important questions when performing experiments using the artificial mouth is that of their applicability to the case of a real player. It has so far been assumed that, due to many of the realistic effects which can be obtained from instruments played using the artificial mouth such as the tone, pitch and threshold pressure, that the artificial lips perform in a similar way to a real player. To gain further insight into the similarity between the artificial mouth and a real player a series of measurements were done following the method suggested by Ayres [4].

For these experiments a mouthpiece is used with a 6mm hole bored into the

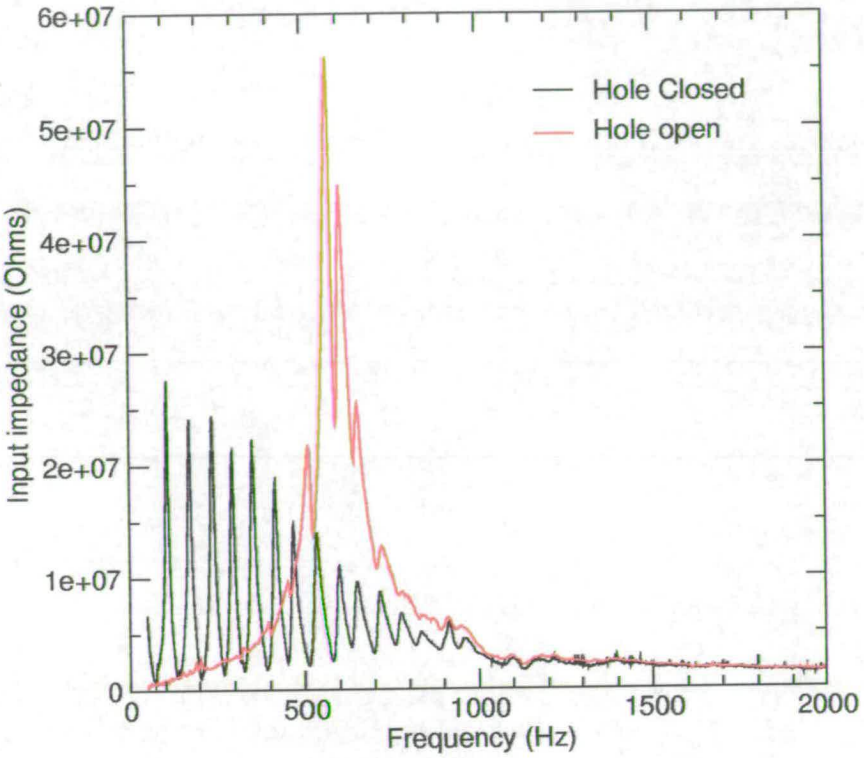

Figure 4.8: Input impedance for trombone with mouthpiece hole open and closed.

side of the mouthpiece shank which can be covered with a finger. This hole when open has the effect of substantially decoupling the mouthpiece from the instrument, as can be seen in impedance measurements of a trombone using this mouthpiece with and without the hole closed (Figure 4.8). If the lips are buzzed into the mouthpiece with the hole open, the lips will oscillate at a frequency close to one of their natural resonance frequencies as there are no strong instrument impedances for the lips to couple to. In the following work this frequency is referred to as the "lip frequency". By then closing the hole in the mouthpiece the oscillation frequency of the lips couples to one of the instrument resonances and so

is altered, producing a note which is the result of coupling between the lips and an instrument resonance (the playing frequency). By repeating this measurement, keeping the trombone slide at the same position but varying the lip resonance frequencies, a plot can be obtained which shows the relationship between the lip resonance frequencies and the note which is produced on an instrument.

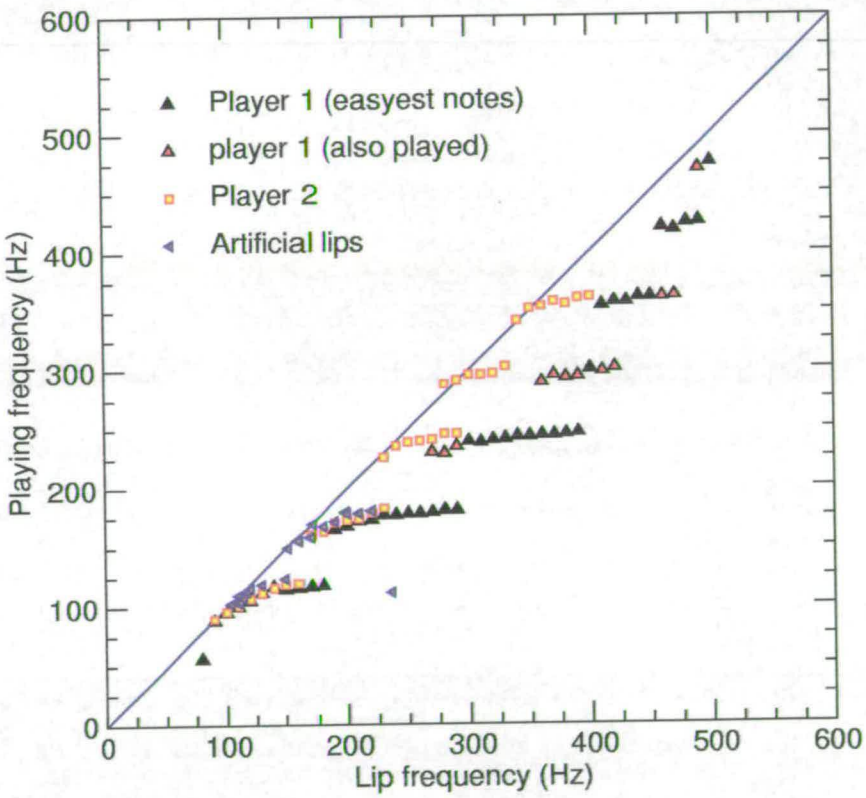

Figure 4.9: Lip frequency and playing frequency for two human players and the artificial lips.

A set of these measurements for two human players and the artificial lips is shown in figure 4.9. It can be seen from this figure that for both the human

players and the artificial lips, that this type of measurement gives a lip frequency which is almost always higher than the playing frequency. The lip frequency is below the acoustic resonance of the trombone for most measurements, rising to just above the acoustic resonance before the jump up to the next mode of the instrument. Both the artificial lips and the real players show very similar results, although the artificial lips are only able to play the second and third modes of the instrument whereas the real players are able to play to the sixth mode and beyond.

Applying these results to the question of inward or outward striking reed mechanism suggests that the lips are, for the most part, acting as an inward striking reed and, as an outward striking reed both in the case of the real players and the artificial lips only for the higher notes just before the jump up the the next mode. In order to compare this method for measuring the lip resonance frequency with the mechanical response method, a series of measurements were taken in which the lip resonance was measured both by having the lips buzzing into the mouthpiece and by taking a mechanical response measurement. Figure 4.10 shows the lip and playing frequencies obtained by using these two methods for the artificial lips playing a straight tube. This shows good consistency between the mechanical response measurements and the lip buzzing measurements. Comparing this measurement to that shown at the end of chapter 3 (Figure 3.19), it can be seen that the lips are in both cases able to play a note which is either below or above the acoustic resonance of the instrument.

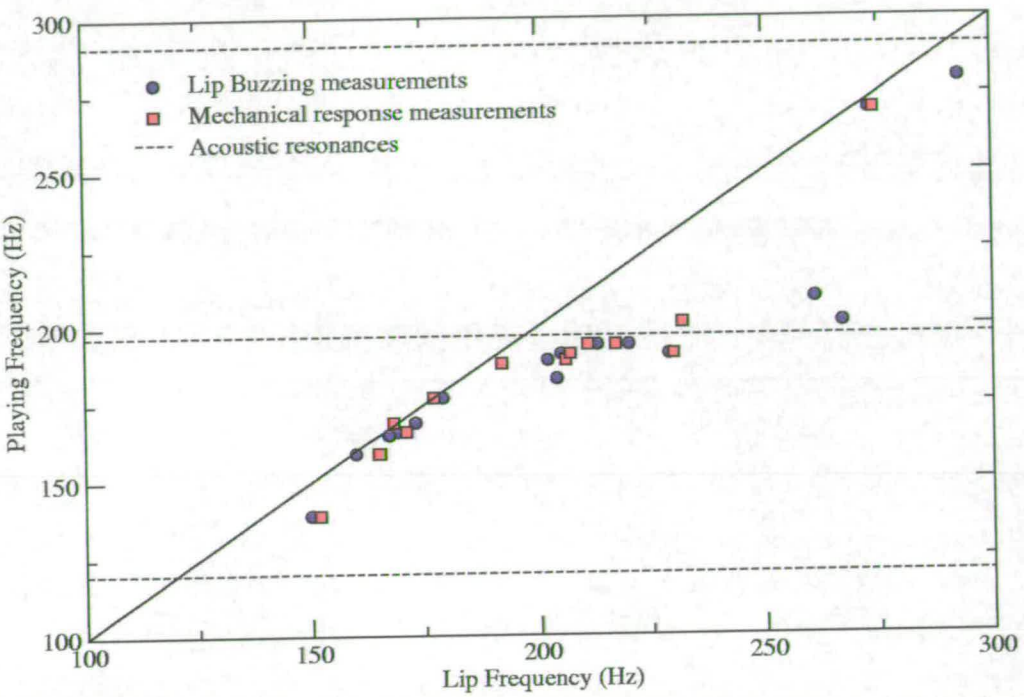

Figure 4.10: Mechanical response and lip buzzing measurement for artificial lips.

This method of measuring the lip resonance frequency gives good agreement with measurements of lip frequency taken from the mechanical response of the lips in the case of the artificial lips. There are still some difficulties with performing these measurements with a real player as there is a tendency for the player to "correct" the note after the hole in the mouthpiece has been closed. These problems can be overcome to some extent by taking the measurement of the playing frequency in a very short time period after the hole has been closed and before the player has had time to make any "corrections" to the note. Throughout these experiments the data obtained from both the real players and the artificial lips show a strong similarity, although the real players are able to play much higher

modes on the instrument, as well as obtaining a larger range of playable notes from any one mode of the instrument. In this way the artificial lips seem to show close similarity to a novice brass player, giving reasonable notes for the first few modes of the instrument, but unable to get the greater control of tone and pitch which an experienced player can obtain.

4.5 Conclusions

In addition to mechanical response measurements taken with the mouth overpressure below the threshold pressure, various experiments have be performed with the artificial lips playing instruments. A detailed look at the playing frequency as a function of slide extension, both for a trombone and for the telescopic tube, shows that there is not usually a steady decrease in playing frequency with slide extension, but rather a fluctuation as the playing frequency changes from below the acoustic resonance of the instrument to above it and sometimes even a rise in playing frequency as the slide is extended across this transition point. This change also coincides with a maximum in the threshold pressure.

Experiments were then performed looking at the effect which changes in the mouth cavity volume have on the playing of a brass instrument. Distinct changes were seen in the mechanical response of the artificial lips when driven from the downstream side, and through basic calculations it was shown that the frequencies

at which these changes occur correspond to a Helmholtz like resonance of the mouth. Measurements were then made of the signal produced at the bell of a trombone as the mouth volume was changed. These measurements show that there is a distinct change in the relative strength of the different harmonics in the note as the mouth volume changes.

In an attempt to further validate the applicability of the artificial lips to the situation of the real player, experiments were performed using a mouthpiece with a hole bored in the side enabling the lips to be decoupled from the instrument without removing them from contact with the mouthpiece. These experiments show that the artificial lips are consistent with real players, and any variations between the artificial lips and a real player are less that the variations between one player and another, although the artificial lips are not able to play the higher notes which a skilled player can obtain. This suggests that the artificial mouth shows consistency with real players, in many ways resembling the playing ability of a novice brass player.

Chapter 5

Theory of Lattice Boltzmann Method

5.1 Introduction

The Lattice Boltzmann Method (LBM) is a numerical simulation technique for viscous fluids capable of simulating both incompressible and slightly compressible flows. It is a method based on kinetic theory and developed from the Lattice Gas Model (LGM) [48]. This technique has been used for a wide variety of fluid simulations including acoustic and multiphase wave propagation [12], [11], high Reynolds number turbulent flow [39], multiphase flow [34], magnetohydrodynamics [16] and chemically reacting flows [24]. The method utilises a computational grid where, at each node of the grid a distribution function is defined in the direc-

tion of all the nearest neighbouring nodes. At each computational time step, the particle distribution functions are streamed along the vertex to the next node, and the collisions between the arriving distributions are calculated utilising the Boltzmann equilibrium function. Chen et. al. [17] have shown that the equations governing the LBM can, by performing a Taylor expansion in space and time and a Chapman Enshog expansion, recover the correct form of the Navier-Stokes equation. The Lattice Boltzmann Method provides an alternative to many of the more common computational fluid dynamics methods which involve numerically solving the Navier-Stokes equation. The Lattice Boltzmann Method has the advantage of allowing easy handling of complicated boundary conditions with no extra computational power and is particularly suitable for parallelisation.

5.2 Formulation of the LBM

In two dimensions the Lattice Boltzmann Method can be implemented using either a hexagonal model, where each node is connected to six nearest neighbours or a square model with diagonals, where each node is connected to eight nearest neighbours. It can also be extended to three dimensions [39]. All of the results presented here are generated using an implementation of the two dimensional hexagonal model. For the hexagonal model the simulation area is divided up into a hexagonal grid with each node of the grid connected up to its six nearest neighbours (Figure 5.1).

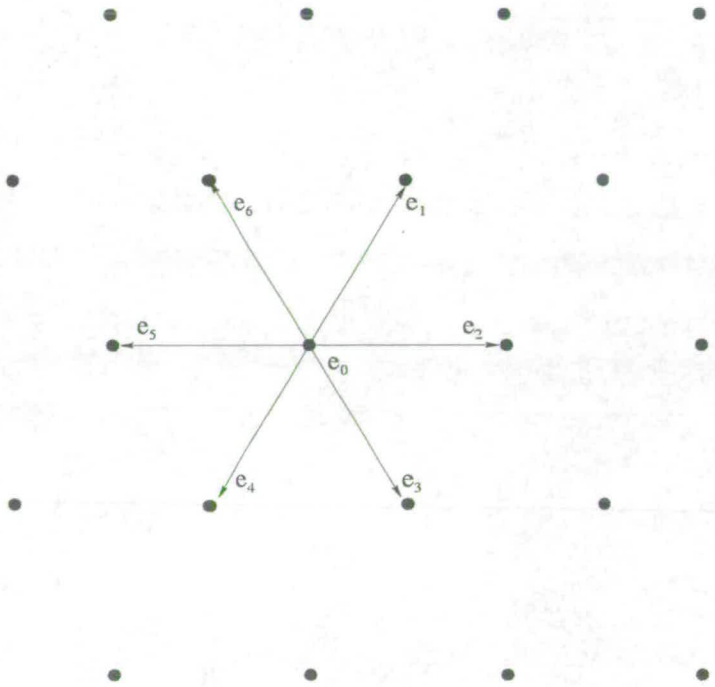

Figure 5.1: The LBM hexagonal simulation grid

At each node of the grid, at any time step a population distribution function (f_i) is defined for each of the six streaming directions $i = 1, ..., 6$ directed along each of the vectors $\mathbf{e}_i$ and one rest distribution function f_0. The primary variables of velocity and density can be found from these particle distribution functions using

$$\rho \mathbf{u}_i = \sum f_i \mathbf{e}_i \tag{5.1}$$

and

$$\rho = \sum f_i \tag{5.2}$$

All the variables f_i are initialised at the start of the simulation from a predetermined ρ and $\mathbf{u}$ from which the flow evolves. At each time step, the populations are

streamed along the vertices of the grid and new distributions are calculated from the collisions between the different arriving populations according to a Boltzmann collision function. Thus $f_i(\mathbf{x}+\mathbf{e}_i, t+1)$ is given by:

$$f_i(\mathbf{x}+\mathbf{e}_i, t+1) = f_i(\mathbf{x}, t) + \Omega_i \left[f(\mathbf{x}, t)\right]. \tag{5.3}$$

The term Ω_i is the collision operator and is given by:

$$\Omega_i = -(1/\tau)(f_i - f_i^{eq}) \tag{5.4}$$

where τ is the relaxation time. The form of the equilibrium distribution function, f_i^{eq} is chosen such that there is conservation of mass, momentum and any other required parameters. The following formulation as devised by Chen et. al. [17] satisfies these requirements:

$$f_i^{eq} = \rho\left[\frac{1-d_0}{6} + \frac{1}{3}\mathbf{e}_i\cdot\mathbf{u} + \frac{2}{3}(\mathbf{e}_i\cdot\mathbf{u})^2 - \frac{\mathbf{u}^2}{6}\right], \textbf{for}: i = 1, 2, ..., 6 \tag{5.5}$$

and

$$f_i^{eq} = \rho(d_0 - \mathbf{u}^2), \textbf{for}: i = 0 \tag{5.6}$$

where d_0 is a constant.

Using the above formulations, each time step in the Lattice Boltzmann simu-

lation can be broken down into two stages. Firstly there is a collision operation where the particle distributions are relaxed towards equilibrium. Secondly, the particle distributions are streamed along the vertices between the nodes of the grid.

5.2.1 Coordinate transformations

Transformations between LBM simulation space and real space is done through non-dimensional scaling using the Reynolds number. The Reynolds number in simulation space is give by:

$$Re = \frac{ul}{\nu} \tag{5.7}$$

where u is the simulation flow velocity (grid units per timestep), l is the channel width (grid units) and the viscosity ν is give by:

$$\nu = \frac{2\tau - 1}{8}. \tag{5.8}$$

By comparing this with the Reynolds number in real space which is given by:

$$Re = \frac{UL}{\eta} \tag{5.9}$$

where U is the flow velocity (ms^{-1}), L is the channel width (m), and η is the viscosity of the fluid ($\mathrm{kgm}^{-1}\mathrm{s}^{-1}$), transformations between simulation flow velocity

and real space flow velocity can be made. Using this transformation it is then possible to equate all simulation parameters to real space parameters.

5.3 Boundary conditions

There are three different types of boundaries in the Lattice Boltzmann simulation. These are the wall boundaries where a no slip condition must be applied, the inflow point where the required flow velocity and flow profile can be input to the simulation, and the outflow point which ideally must allow the flow to pass without any reflections or restraining of the flow so as to give the same flow profile as would occur if the simulation grid was extended indefinitely.

5.3.1 Wall boundary conditions

The typical method for modelling the boundary condition for the wall in LBM simulations is to use the bounce-back method. The technique is similar to that used in the Lattice Gas Model and provides a first order approximation to a no slip wall. Although this is less accurate than the LBM simulation is capable of, it has been shown [45] that the bounce-back boundary condition shows a good approximation to analytical results as long at the relaxation parameter τ is kept small ($\tau < 1$), but can cause considerable inaccuracies for larger values of τ.

The bounce-back boundary condition is implemented by having particles which

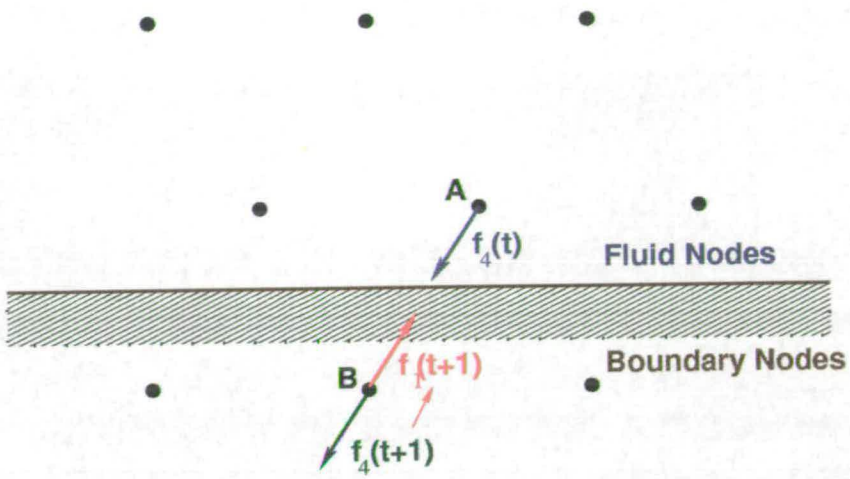

Figure 5.2: The wall boundary for the LBM simulation

stream into the wall and bounce back, returning in the direction from which they came. For example, in Figure 5.2 a particle distribution which is streamed along the $\mathbf{e}_4$ direction from the fluid node A to the boundary node B will be flipped back, such that on the next time step node B will have a value for f_1 which is equal to the previous f_4 value. It should be noted that the actual boundary lies half way between nodes A and B.

The bounce-back boundary condition is simple to code and compute, giving minimal extra computational time as well as being able to handle complicated boundary conditions with no extra computational difficulty, unlike some of the other more accurate wall boundary methods. This enables a graphical grid defining program to be used as no extra programming is needed when the walls in the simulation are moved between simulations. For these reasons the bounce-back boundary conditions were used in all the following work.

5.3.2 Inflow boundary condition

The inflow boundary condition used in the current simulations is a straight forward forcing of the flow with pre-defined values for the velocity ($\mathbf{u}$) and the density (ρ). The inflow is defined at any of the grid nodes at the left side of the grid which are not marked as a wall node. At these nodes the pre-defined values of $\mathbf{u}$ and ρ are inserted into equations (5.5) and (5.6). If required the values for $\mathbf{u}$ and ρ can be varied throughout the simulation to give a variable inflow. Although this method takes no account of what is happening downstream of the flow, and thus may cause problems if there are turbulent eddies or density waves in the area of the inflow, for the situations currently under examination there is little happening of interest in the vicinity of the inflow, and so this method is considered suitable.

5.3.3 Outflow boundary condition

The outflow boundary condition is considerably more complex than the inflow boundary, especially in many of the following simulations where flow reaching the end of the simulation grid may have considerable velocity and density variations. In this work various different outflow conditions were tried before the final solution was chosen. These vary between the simplest fixed boundary condition to those which take account of the velocity and density gradients at the approach to the end boundary.

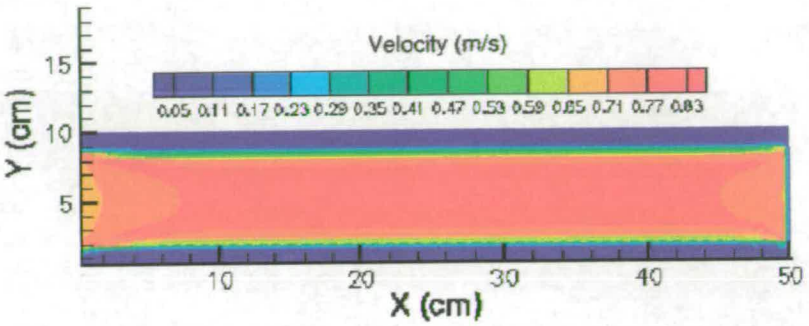

Figure 5.3: Flow in a straight pipe with fixed flow velocity end conditions

5.3.4 Fixed end boundary condition

The simplest outflow boundary condition is constructed by matching the outflow condition with the inflow condition, thus giving a fixed velocity and density at the outflow which is of the same form as that at the inflow. This keeps the total mass and momentum in the simulation area constant. This is equivalent to driving the flow in the simulation area at both the inflow and outflow point. For very simple flow geometries, such as flow through a straight pipe, this end condition can be sufficient although it tends to lead to the creation of unrealistic artifacts in the section of the simulation close to the outflow boundary. An example of this can be seen in Figure 5.3 which shows flow in a pipe with the velocity contours displaying the flow developing from the inlet point which has a flat velocity profile into a poiseuille flow. As the end point is approached, there is what looks like an inversion of the developing pattern, with the flow changing from a fully developed profile back into a flat velocity profile.

Although this type of simulation artifact can be overcome for cases like those

seen in Figure 5.3, by changing the end conditions in such a way that the outflow has a fixed profile in the same shape as the fully developed flow, there are other more serious problems with this type of end boundary which cannot be solved. These occur with flow profiles where the flow through the end condition is not constant over time, either due to a change in overall flow velocity caused by a time-dependent input condition, or due to the creation of turbulent or unsteady flow by obstructions in the simulation area. The fixed output condition effectively reflects any velocity or density variation back into the simulation area, as shown in Figure 5.4, where step changes in the inflow and outflow conditions have set up a density wave which travels through the flow until it reaches the outflow boundary where it is reflected. These reflected waves have created large density and velocity variations throughout the simulation obscuring most other features. It is clear from this reflection effect which the fixed outflow boundary exhibits that this type of outflow boundary is not sufficient for any unsteady or time varying flows.

5.3.5 Constant velocity end condition

The next development of the outflow boundary condition was to calculate the outflow point such that $\frac{\partial v}{\partial x} = 0$ and $\frac{\partial \rho}{\partial x} = 0$. This method, which has been used for outflow conditions in some literature [39], gives a considerable improvement over the fixed boundary condition, and can be used for many unstable and turbulent

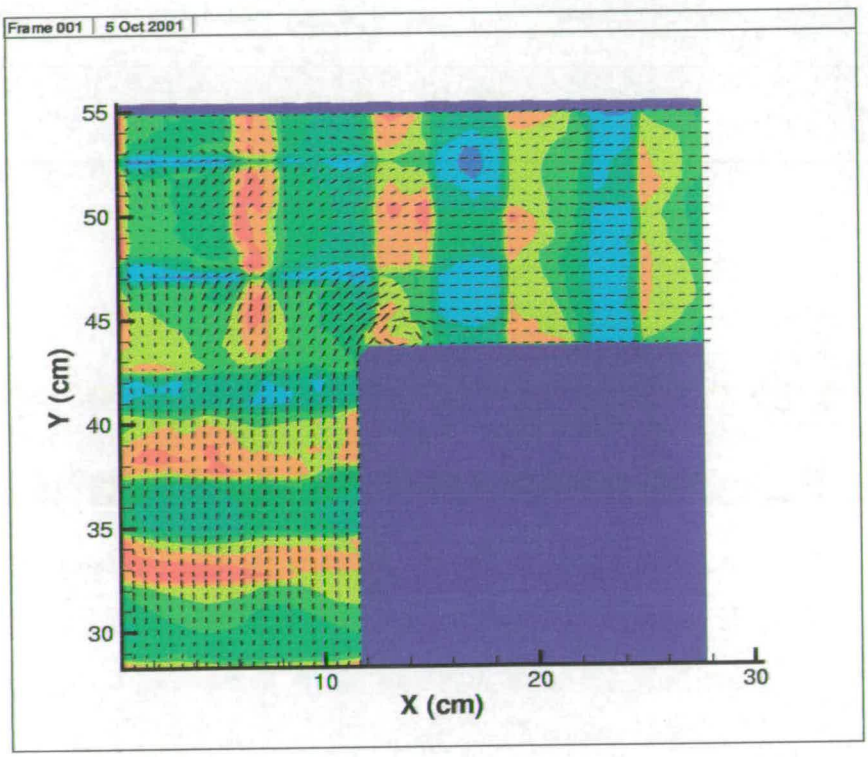

Figure 5.4: Reflections caused by fixed input and output boundary conditions.

flows. It is also very simple to implement, as it can be done by simply setting the velocity and density variables at the outflow grid points equal to those at the previous grid point at each time step as shown by equation (5.10).

$$f_i(n,t) = f_i(n-1,t) \tag{5.10}$$

where n: grid size in $\perp$ direction.

This method, although a considerable improvement over the fixed outflow boundary condition, still has some effect on the flow approaching the outflow boundary, as there is some damping of the velocity gradient and a small amount of reflection of velocity and density variations. These simulation artifacts are minimal and only cause problems in immediate proximity to the outflow. More importantly, this outflow condition breaks down completely if there is any flow reversal at the outflow point, as might happen in the case of strong eddy formation in a flow with a low overall velocity flux. In this case the outflow condition creates a sustained inflow at the point of flow reversal and causes complete breakdown of the simulation. Due to the nature of many of the flow geometries used in the current work, this boundary condition proved unsuitable.

5.3.6 Damped velocity gradient end condition

The final outflow boundary condition which was used in thesis work involved calculating the velocity gradient over the last grid nodes before the outflow boundary, and creating the final boundary point so that it gives a smoothly damped velocity curve at the outflow. This is done as shown in equation (5.11):

$$f_i(n,t) = f_i(n-1,t) - [f_i(n-2,t) - f_i(n-1,t)] \tag{5.11}$$

$$= 2f_i(n-1,t) - f_i(n-2,t) \tag{5.12}$$

After this calculation of the new value for $f_i(n,t)$ a test must be run to check that there is not a change in the sign between $f_i(n,t)$ and $f_i(n-1,t)$, i.e.:

$$\textbf{if}(f_i(n-1,t) \times f_i(n,t) < 0)$$

$$\textbf{then} f_i(n,t) = 0. \tag{5.13}$$

This end condition, like the previously discussed methods, causes some effects close to the boundary, but like the constant velocity method these effects are restrained to the simulation points close the the outflow, and so problems caused by the end condition can be minimised by allowing a short outflow buffer region at the end of the simulation. It can be seen from the series of vorticity and ve-

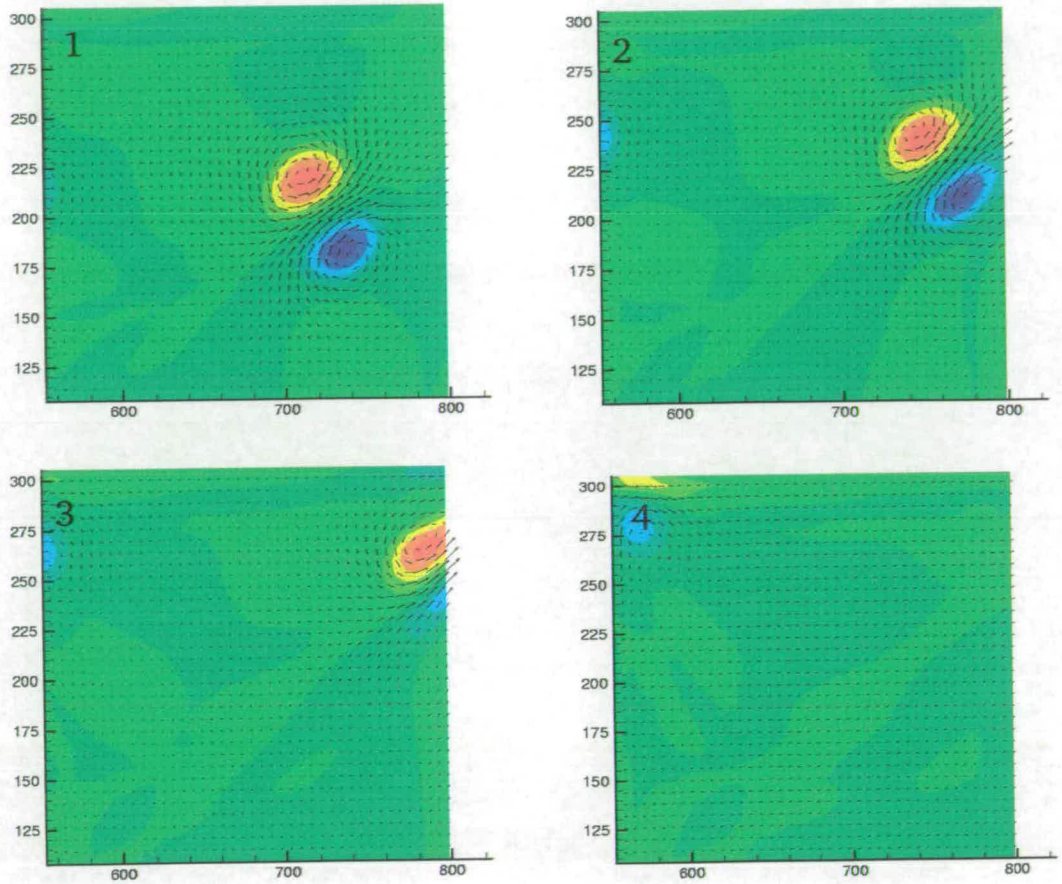

Figure 5.5: Large eddy passing through the damped velocity gradient boundary condition at x=800.

locity maps in Figure 5.5, which show a large eddy passing through the outflow boundary at $x = 800$, that the damped velocity gradient outflow boundary condition allows large fluctuations in the flow to pass out of the simulation area with minimal side effects.

5.4 Graphical interfacing for LBM

To run the Lattice Boltzmann simulation a computational grid must be set up where each point on the grid is either defined as a fluid node or a wall node. This configuration can either be done as part of the simulation code or alternatively can be read to the simulation in the from of a separate file containing the grid specification, the initial state of the simulation and the inflow parameters. This method was chosen as it makes changes to the computational grid as quick and simple as possible. To further aid the setting up of the grid and simulation parameters, a graphical front end called *picsim* was developed.

This program was initially developed so that the simulation grid was presented on the screen as a grid of coloured squares, which could be clicked using the mouse pointer to change the colour of the squares. When the boundaries of the simulation had been fully defined this way, the grid was written to file with the lighter coloured squares representing the fluid nodes and the darker colour representing the wall nodes. This program was called *latsim*. As the grid size of the simulation increased to enable greater accuracy and higher Reynolds number flows to be simulated, this method for interfacing became impractical so the graphical interface was changed. In this second stage the form of the boundaries used in the simulation was defined by drawing a black and white picture of the simulation area using any graphics or technical drawing software package. Once drawn, this picture saved as a bitmap format graphic can be loaded into the picsim

program which, after allowing changes to the initial state and inflow parameters, converts the bitmap picture into a data file which can then be read in by the Lattice Boltzmann simulation program. The conversion of the bitmap to a data file is done by allowing the user to specify the size of the simulation grid to be used. The picsim program then steps across the bitmap in the required number of steps, defining the dark areas as boundary nodes and light areas as fluid nodes. This method for performing the grid creation has the advantage over the latsim method of being able to grid pictures taken from other sources, as well as the facility to set up simulations of the same boundary configuration using various different grid sizes.

Figure 5.6 is a flow diagram of the picsim program showing the basic operation of the program. Full details and code of the program can be found in appendix B. Figure 5.7 shows a screen shot of the picsim program with the main image viewing window on the left, the simulation parameter editing window on the lower right and the grid size window on the upper right side of the figure.

The picsim program is written in the C++ programing language utilising QT graphical interfacing libraries from Trol Tech [49], [23] which is a set of C++ class libraries designed primarily for graphical user interface (GUI) programming. The program has three main sections, the main program from which all the function are called, the menu section which enables the simulation parameters to be changed and the grid creation section. These different sections of the program

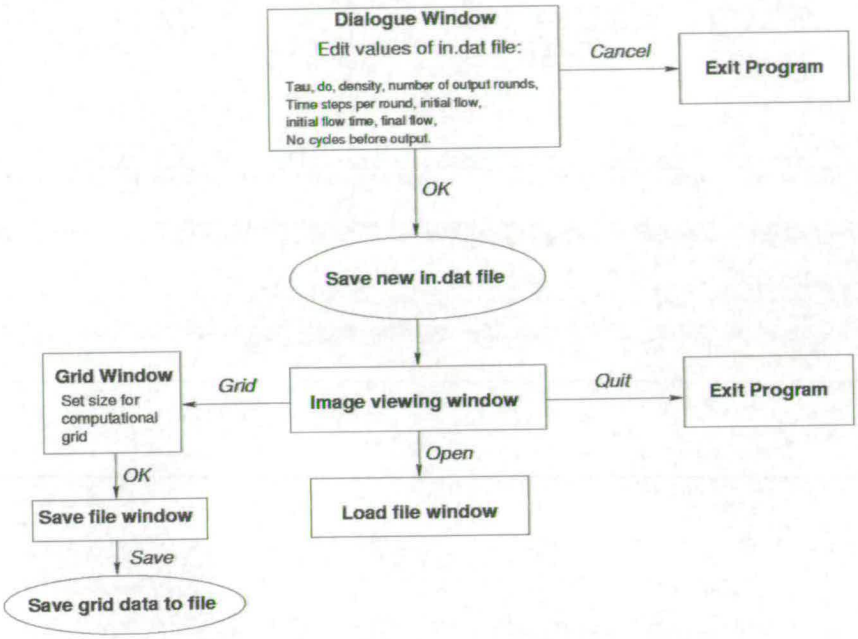

Figure 5.6: Flow diagram of operation of the picsim program.

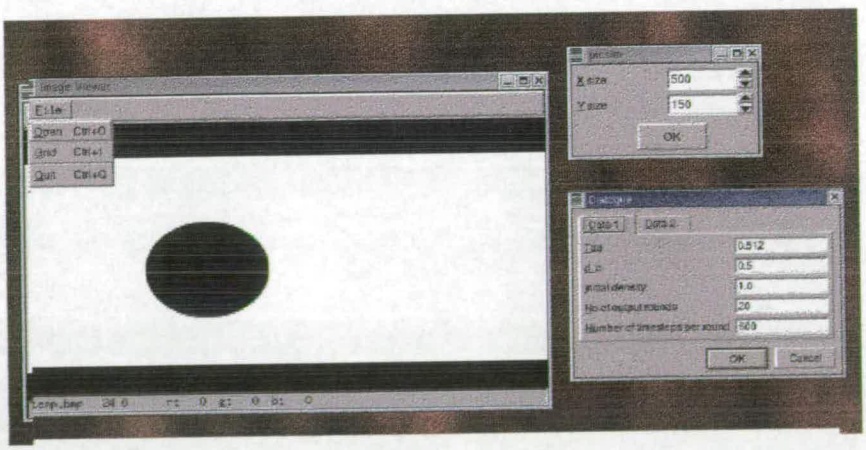

Figure 5.7: Screen shot from the picsim program.

have their own pop up windows. The menu section presents a window containing two sheets of five editing boxes which can be changed by the user, and the grid creation section presents a graphic window showing the bitmap from which the grid is created along with a menu, from which other windows allowing file load, save and grid size windows are called up. The output from the picsim program is in the form of two text data files, one called 'in.dat' which contains the simulation parameters from the menu section of the program, and the other called 'grid.dat' which contains the grid size and boundary specification.

5.5 Processing requirements

The LBM program takes a considerable amount of processing power to run, with some simulations taking over a week of processing time running on a 1GHz single PC processor in order to obtain simulations of suitable duration. The LBM code has been written so as to enable easy parallelisation, although this possibility has not been used in the current work. The simulations were initially run on a farm of Sun workstations at Edinburgh University collectively know as "Waverley." As more powerful computers became available this was changed to running the simulations on one of a collection of dual 1 GHz processor PCs, which gave a significant improvement in the time taken to complete each simulation.

As the LBM method only takes into account interactions between nearest

neighbouring nodes the computational time taken for the simulation scales roughly linearly with the number of nodes on the grid and with the number of time steps computed. The size of the grid and time steps are in turn controlled by the Reynolds number (Re) of the flow which is required. The Reynolds number through a pipe with a diameter of l grid points in simulation space is given by equation 5.14.

$$Re = \frac{ul}{\nu} \tag{5.14}$$

where the kinematic viscosity in simulation space is given by:

$$\nu = \frac{2\tau - 1}{8}. \tag{5.15}$$

The variables for the relaxation time τ and the flow velocity u have limits beyond which numerical instability occurs leading to complete breakdown of the simulation. These limits mean that in order to get to larger Reynolds numbers above this point where numerical instability occurs the simulation grid must be enlarged and thus the computational time increased.

Running on a single 1GHz processor PC a simulation attaining a Reynolds number in a pipe of around 8000 and simulating a real life time interval of around 10ms, the simulation takes about 20 hours of computation. Using two dual processor PCs, a set of computational data consisting of 7 simulations as used in the current experiments thus takes between three and four days.

5.6 Code validation

The Lattice Boltzmann method has been used in many areas where fluid simulations are required, and it can be shown using expansions on the Lattice Boltzmann equations that the correct form of the Navier-Stokes equation can be obtained [32]. The current simulation code was validated by comparison against two flows for which numerical solutions exit. These two test arrangements simulate low Reynolds number flow through a straight pipe and the expansion of a free jet.

5.6.1 Flow through a pipe

The flow in a two dimensional pipe can be calculated from first principles [50], and it can be shown that the velocity profile is that of a parabola known as Poiseuille flow. In addition, flow with a flat velocity profile entering a pipe has an entry length which is dependent on the Reynolds number as given by equation (5.16), with X defined as the distance downstream at which u_{max} is within 5% of its Poiseuille value. These known facts can be used to test the validity of the LBM simulation code.

$$\frac{X}{d} \approx \frac{Re}{30} \tag{5.16}$$

The development of the velocity profile in a simulation of pipe flow with a Reynolds number of 150 is shown in figure 5.8. It can be seen in this figure that the parabolic flow profile is reached between 4 and 5 pipe diameters downstream

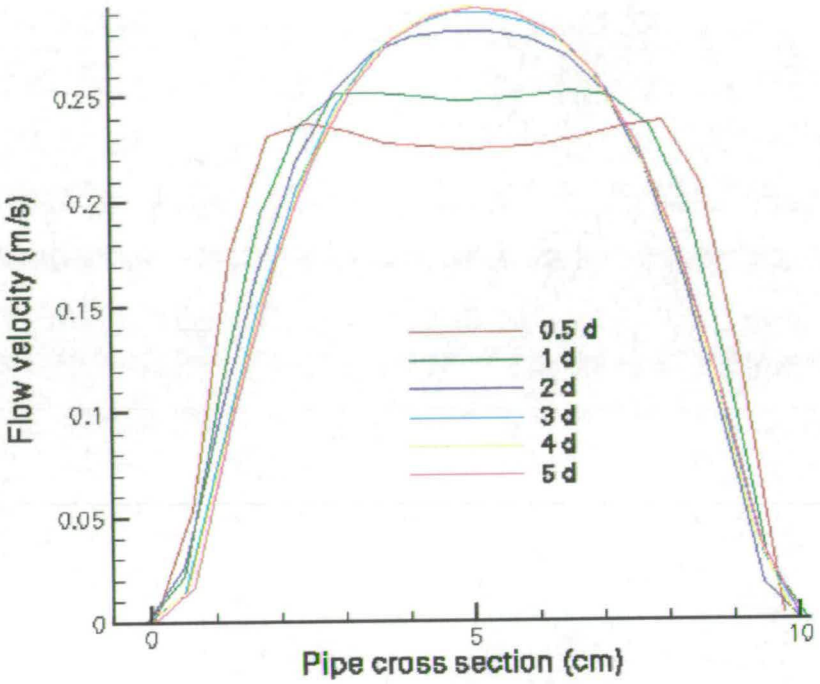

Figure 5.8: Developing flow in a pipe Re=150.

of the pipe entry point as would be expected from equation (5.16).

5.6.2 Expansion of a free jet

The second method of validation of the LBM simulation model was to simulate a free jet, by having a very large step change in the diameter of a channel. The width δ of a two dimensional free jet emerging from an opening of width A is given by equation (5.17) [50].

$$\delta \propto x^{\frac{2}{3}} + A. \tag{5.17}$$

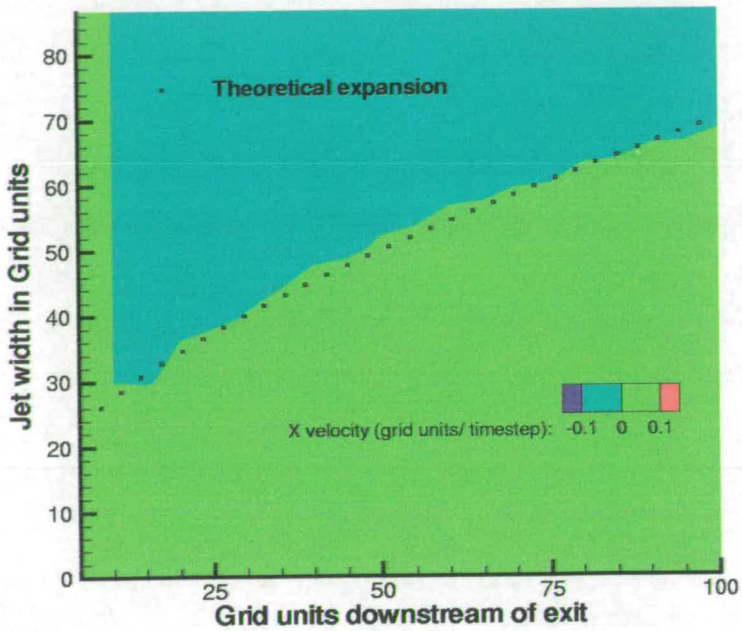

Figure 5.9: Expansion width of a simulated free jet.

Figure 5.9 shows a comparison between the calculated and simulated widths of a free jet, the colour map showing the simulated x direction velocity contours and the points representing the equation:

$$\delta = 2.5 \times x^{\frac{2}{3}} + 15. \tag{5.18}$$

It can be seen from this figure that the LBM simulation again gives very good agreement with theoretical fluid motion for these test cases.

Chapter 6

Flow simulations using LBM

6.1 Introduction

In this chapter the results from simulations using the Lattice Boltzmann Method are shown for a number of different boundary profiles in a rectangular grid with an inflow at one side of the grid and an outflow at the opposite side. These simulations are all based on static boundary models, starting with simulations of a channel with a rapid expansion, simulated both with sharp corners at the expansion and two different rounded edge profiles (Section 6.2). Simulation results are then shown for a constant size channel with lip shaped apertures placed part way along it (Section 6.3.1). These lip model simulations are then extended to simulate the same lip models and inflow parameters but with a boundary in the shape of a trombone mouthpiece backbore after the lips (Section 6.3.2). Discussion and

analysis of these results along with some applications to brass instruments and their playing is then given in Section 6.4.

6.2 Flow out of a channel expansion

The first series of simulations was done for a step expansion in a channel with a diameter ratio between the smaller and the larger cross-sections of around 1:9.3. The Lattice Boltzmann Simulation code used in this work is two dimensional and so the results can only be applied to two dimensional flows. The main body of this work is concerned with the flow between slit type expansions such as the lips of a brass player which form an aperture which is much wider than it is high. Flow through this type of aperture can be considered as two dimensional other than at the edges of the aperture. For this reason two dimensional Lattice Boltzmann simulations were considered sufficient. Further discussion of the ramifications of this can be found in Section 6.4.

There have been various studies of step channel expansions such as these, both experimentally [28], [26] and using numerical simulation methods [3], although many of these studies focus on lower Reynolds number flows and smaller expansion ratios. Hofmans [38] performed a number of experimental and numerical simulations on both step expansions and various static models of vocal folds at higher Reynolds numbers. Much of the following work is based around simi-

lar models to those used by Hofmans as there are many similarities between lip modelling and vocal fold modelling.

For the simulations of a step channel expansion, a series of three similar expansion profiles was studied. These three expansion profiles had different corner radii (r) at the step expansion. The first of these simulations has a sharp 90^o corner at the exit from the smaller channel ($r = 0$) with the other two having rounded exit profiles. The first of the rounded corner simulations has a corner radius equal to half of the smaller channel height (i.e. $r = \frac{h}{2}$), and the second simulation has a round corner profile similar to the first but with a corner radius equal to the smaller channel height (i.e. $r = h$). These three exit profiles for are shown in Figure 6.1.

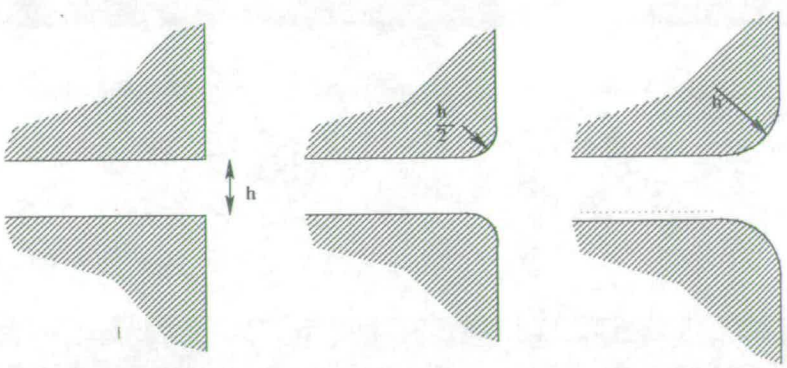

Figure 6.1: Exit profiles for pipe expansion.

The Reynolds number for the sustained flow in the narrower channel before the expansion was around 820, and the simulations were run for 30000 time steps giving a real time equivalent of around 0.4 seconds for a channel with an initial

diameter of 2mm. The grid size used for the simulations was 1400 x 560 grid points with an initial channel length of 420 grid units and an initial channel width of 60 grid units as shown in Figure 6.2. In all three cases the simulation

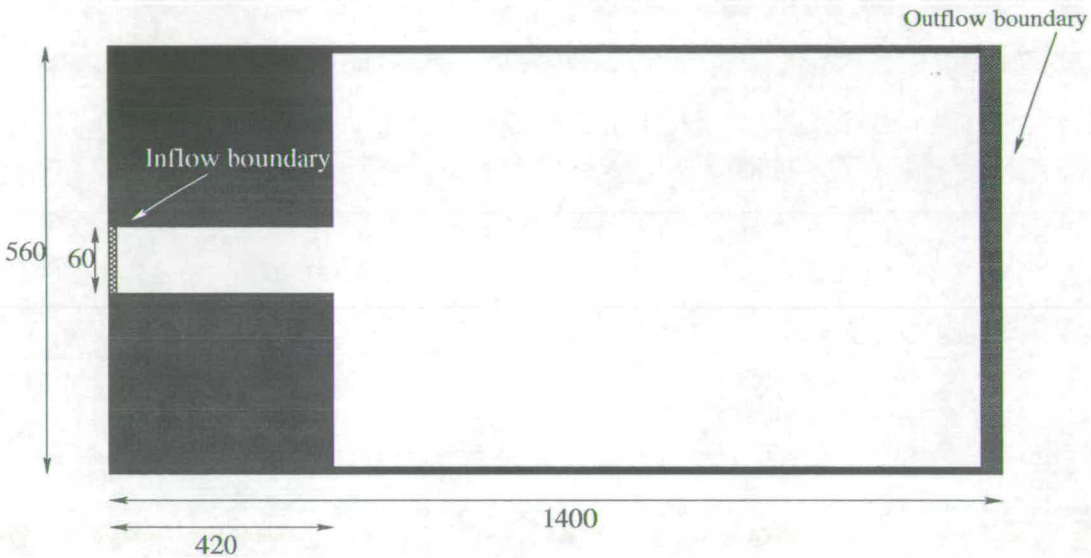

Figure 6.2: Computational grid used for simulations.

was started with initial conditions such that there was no flow at the fluid nodes of the simulation grid other than along the inflow boundary. This inflow was sustained at a constant value throughout the simulation period so as to create a starting flow traveling across the simulation. This starting flow can be seen in Figure 6.3 which shows the centre-line velocity as a function of time at a point in the smaller diameter channel 4mm before the expansion. The length of the initial channel section is around 7 channel heights (14mm), which is long enough for the flow to reach a fairly developed profile before the expansion, as is confirmed by measurements of the flow profile just before the expansion (Figure 6.4).

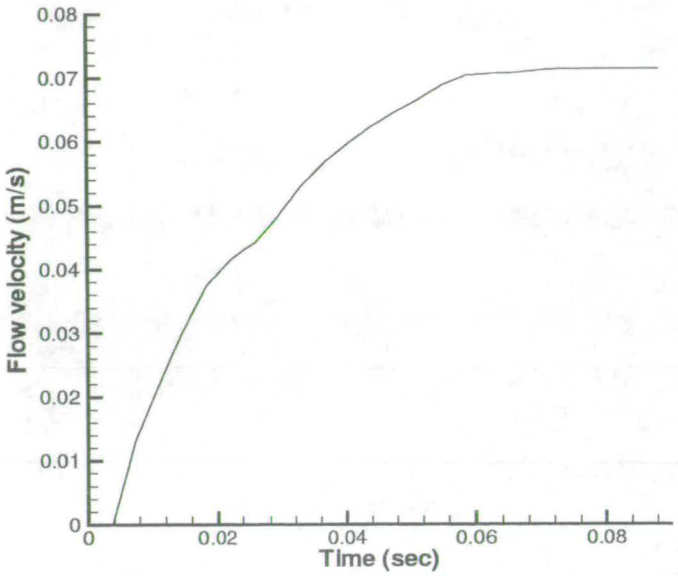

Figure 6.3: Centre-line flow velocity 4mm upstream of expansion.

The simulated time period of 0.4 seconds is sufficient that the initial starting flow has time to travel most of the length of the simulation grid. A longer simulation was also run with 75000 time steps giving an equivalent simulation time of 1 second in order to check for any significant change in the flow patterns beyond 0.4 seconds, for which it was assumed that a steady state flow had been achieved. This simulation confirmed this assumption that the there are no significant changes in the flow patterns beyond 0.4 seconds.

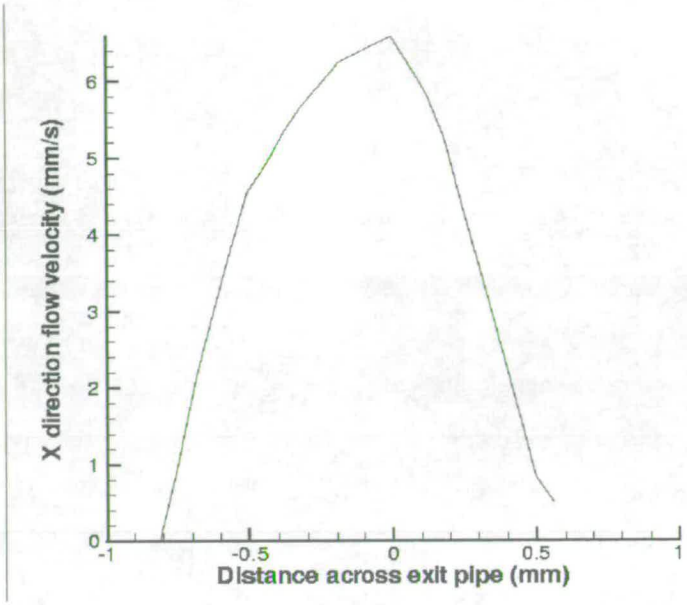

Figure 6.4: Flow profile just before expansion.

6.2.1 Sharp edge pipe expansion

The first simulation is of the rapid pipe expansion with sharp corners at the exit of the initial pipe. The results of these simulations are shown using colour maps representing the vorticity magnitude ($|\omega|$) of the flow calculated using equation (6.1). The vorticity maps give a clear picture of the formation of jets and turbulence in the flow.

$$\omega = \frac{\partial v}{\partial x} - \frac{\partial u}{\partial y} \tag{6.1}$$

where v is the velocity component in the y direction and u is velocity component in the x direction.

A series of maps showing the vorticity magnitude can be seen in Figure 6.5

for various time intervals throughout the simulation. Areas of strong vorticity are shown by red colours and areas of low vorticity are shown by blue colours. The boundaries of the flow can be seen by the dark blue shaded area. The dimensions on the x and y axis are measured in millimetres from the centre point of the expansion. In addition to these vorticity maps, Figure 6.6 shows the velocity profile of the jet formed at the pipe expansion for different distances downstream of the expansion at the time step 366msec after the start of the simulation.

It can be seen from the vorticity maps (Figure 6.5) that there is the formation of a jet at the rapid expansion. The formation of this jet starts with two symmetrical vortices created as the starting flow passes the expansion. This vortex pair is carried downstream by the flow and a smooth jet is formed as the flow approaches a steady state. As the jet travels further from the expansion, instabilities in the flow begin to appear. These instabilities can be seen first by the slight asymmetry of the vortex pair starting to appear in the last time step (366 msec) of Figure 6.5. This instability occurs about 15mm downstream of the expansion and up to this point the jet stays smooth with little change in velocity or width. Simulations using a greater number of time steps have shown that the jet profile seen at the 366 msec time step demonstrates the same general characteristics as are seen at any later time as long as a constant inflow is applied, remaining cohesive until around 15mm downstream of the expansion and then breaking up into turbulence. The consistency of the jet up to this point can be seen by looking at the jet profiles for different distances downstream of the expansion (Figure 6.6)

336msec after the start of the simulation. It can be seen from this figure that the profile of the jet remains almost constant as it travels downstream with the width 10mm downstream of the expansion being only around 0.1mm wider than at the exit (0mm).

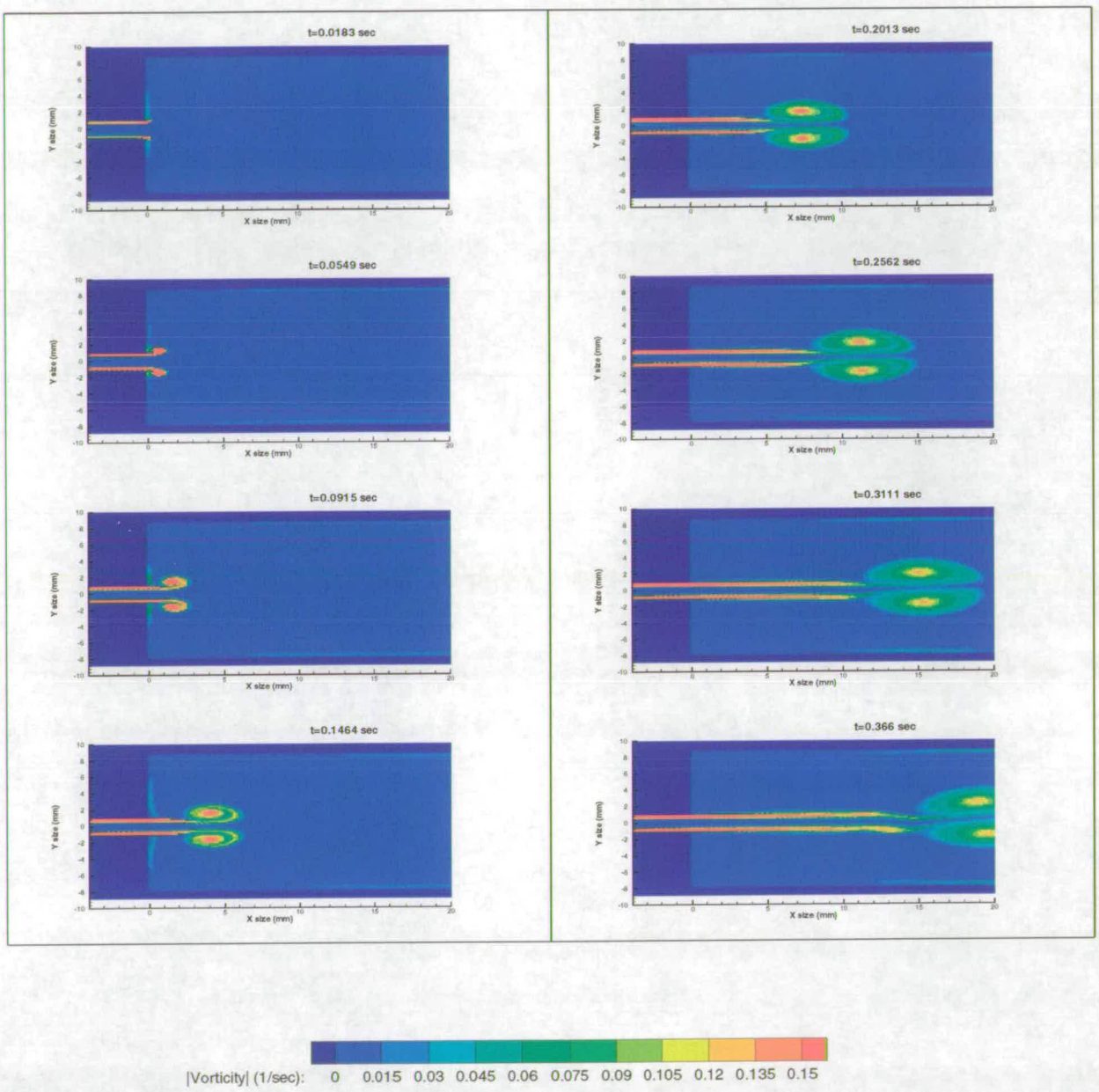

Figure 6.5: Flow vorticity magnitude maps for r=0 exit profile

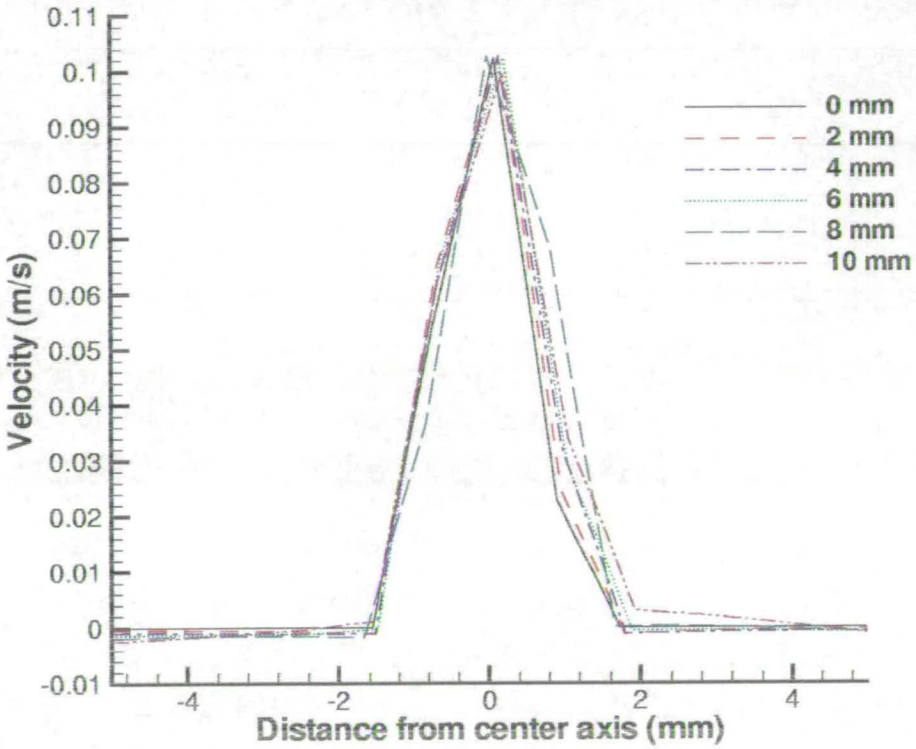

Figure 6.6: Flow profiles of jet 366 msec after start of simulation at different distances downstream of the expansion.

6.2.2 Rounded edge pipe expansions

The second and third sets of simulations were of flow through the same expansions but with rounded corners at the expansion. These simulations were run with the same inflow and initialisation parameters as those used for the sharp edged expansion. Maps of the vorticity magnitude are shown for the same time steps as in the case of the sharp edged expansion, Figure 6.7 showing the results from the expansion with a $r = \frac{h}{2}$ rounded edge and Figure 6.8 showing the results from the rounded edge with a corner radius of $r = h$. Velocity profiles are also shown for various different distances downstream from the expansion, Figure 6.9 showing the results for the $r = \frac{h}{2}$ rounded corner and Figure 6.10 showing the results from the $r = h$ rounded corner. In all the simulations the boundary points on the simulation grid can be seen by the dark shaded area.

It can be seen from the vorticity maps that there is a clean separation of the jet at the expansion in both of the two rounded edge profiles. This separation happens in a similar way to the case of the sharp edged expansion and there are few distinctions between the two round edge expansions. In the case of the $r = \frac{h}{2}$ corner the vortices formed by the starting flow have a slightly more symmetrical form and it takes longer for the breakup of the vortex pairs to occur than it does in the case of the $r = h$ corner, where the instabilities in the jet can be seen beginning to appear 256 msec into the simulation and around 5mm downstream of the expansion. This suggests that in the case of the $r = \frac{h}{2}$ corner the flow has a

cleaner separation from the wall than in the case of the larger radius. This can be understood by considering the Reynolds number of the flow over the curved exit. Clearly for the smaller radius of curvature there will be a lower Reynolds number than for the larger curvature corner and so one would expect a smoother flow to be obtained from the case of the small radius exit. Comparing this with the jet profiles shown in Figures 6.9 and 6.10, it can be seen that the larger rounded corner exit leads to a slightly wider jet profile as well as stronger vorticity around the edge of the jet, shown by the greater variations in flow velocity for the larger rounded edge expansion.

Comparing the above simulations results with those given in previous work, particularly the experimental flow visualisation performed by Hofmans [38], shows good agreement. Experimental observation shows that in the same way as is seen in the Lattice Boltzmann simulations there is a formation of a vortex pair as the starting flow passes the expansion point, followed by a jet which at some distance downstream of the expansion breaks up into turbulence.

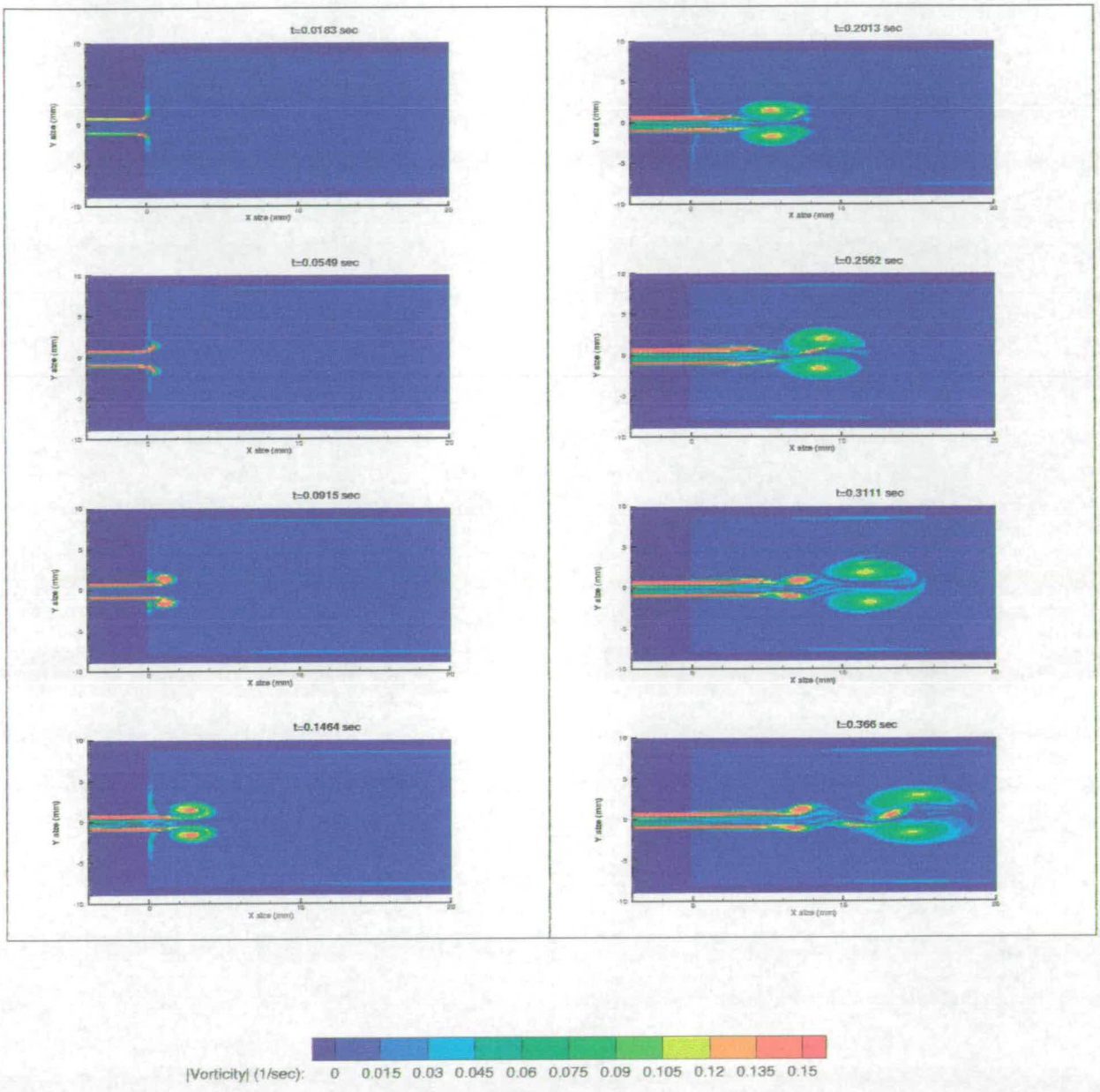

Figure 6.7: Flow vorticity maps for r=h/2 exit profile

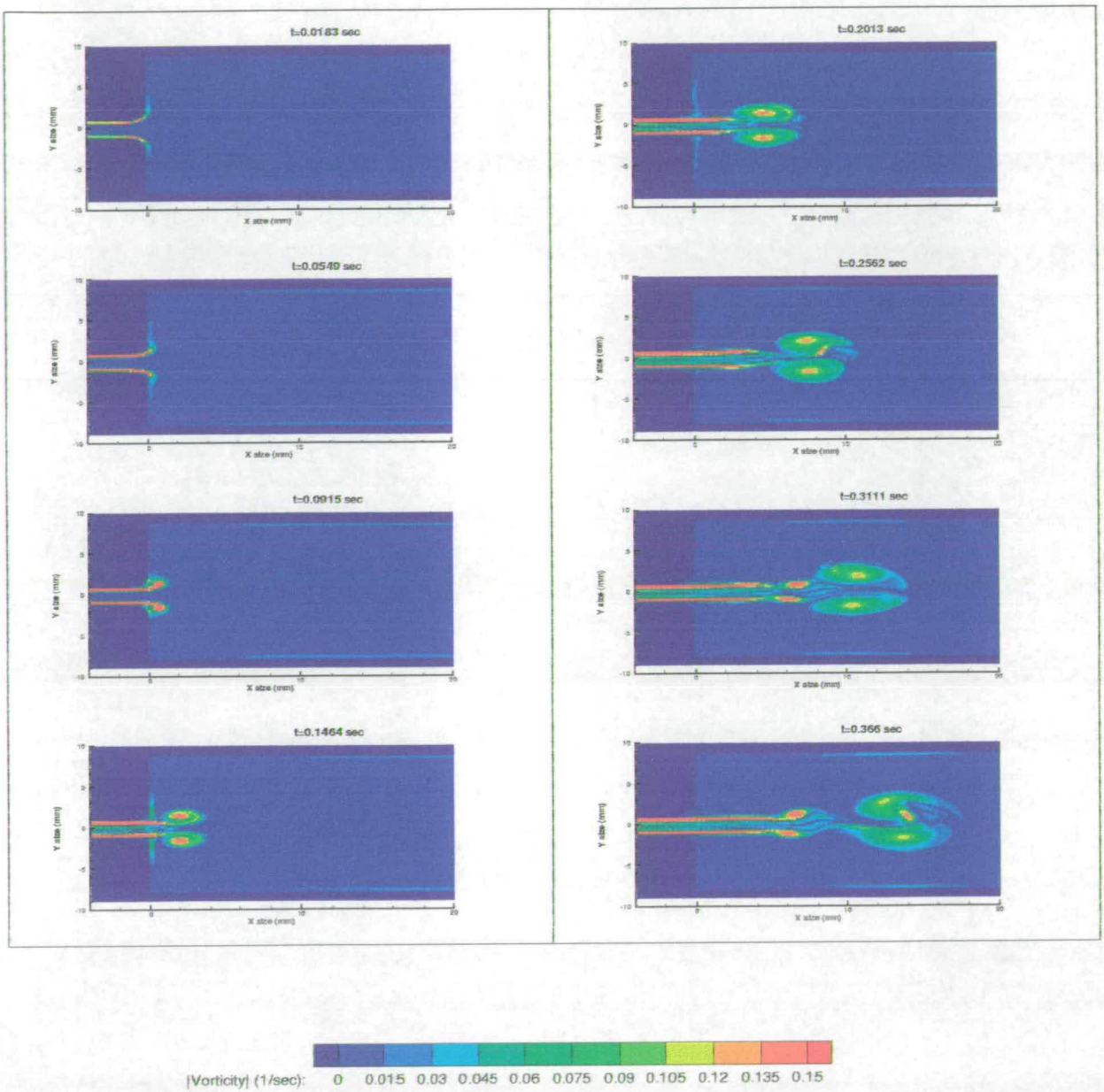

Figure 6.8: Flow vorticity maps for r=h exit profile

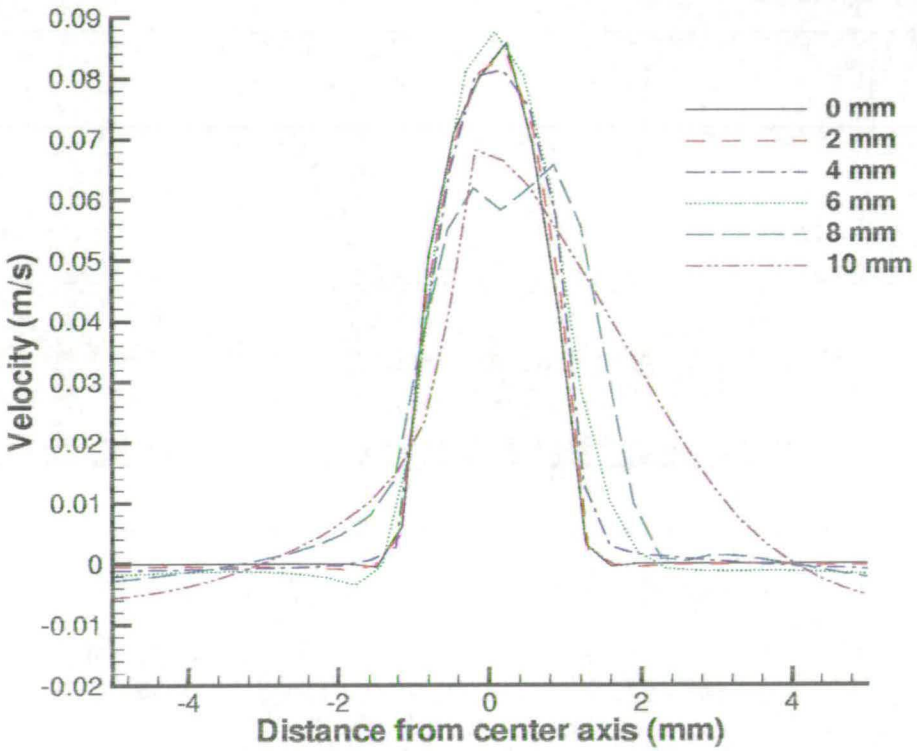

Figure 6.9: Flow profiles of jet 366 msec after start of simulation for r=h/2 corners.

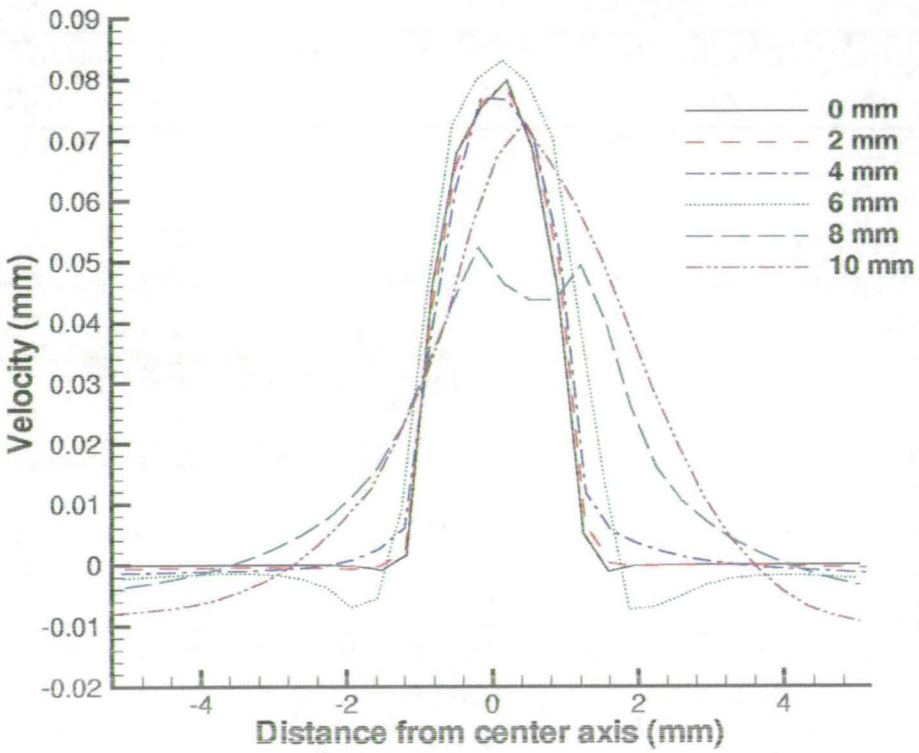

Figure 6.10: Flow profiles of jet 366 msec after start of simulation for r=h corners.

6.3 Flow through static lip models

Following the simulations of the rapid expansion of a channel, a set of simulations were performed using a similar grid but studying the flow through apertures with a form based on static models of the lips. This was done using a series of seven different constriction profiles based on models used for both experimental and numerical simulation by Hofmans [38]. These lip models consisted of two symmetrical constrictions (lips) with various different profiles at the coincident sides of the two lips. The first of these models had semicircular profiles while all the other models had profiles consisting of two rounded corners connected by a straight edge, the round corners having a radius of $\frac{1}{4}$ of the total lip width. Simulations were run for both converging and diverging lip angles (α) with a set of three different angles between the straight edges of 10^o, 20^o and 30^o for both inward and outward α. A schematic of these lip models is shown in Figure 6.11.

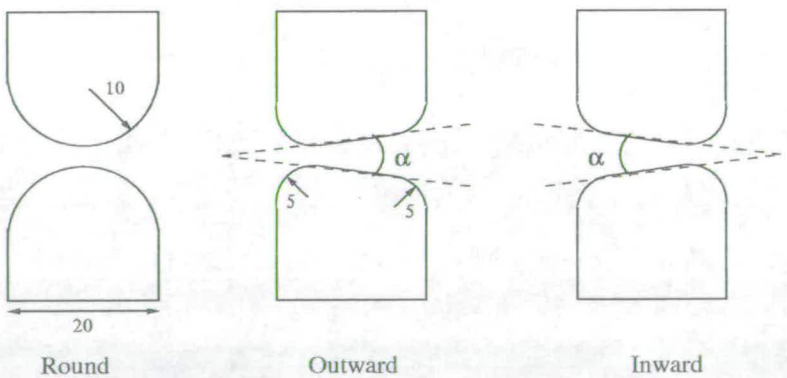

Figure 6.11: Lip models used for simulations

Two different simulations were run for each of the seven different lips models.

In the first set of simulations the lip models were situated $\frac{1}{5}$ of the way along a straight channel with no following constriction; in the second set of simulations the same lip models were used in the same position in the channel, but this time followed by a constriction with a profile similar to the backbore of a brass instrument mouthpiece. All of these simulations were run on a grid size of 1400 x 560 grid points with a Reynolds number (Re) for the flow between the lips of around 600. Simulations were run over 30000 time steps giving an equivalent real life simulation time of around 60 msec for a lip gap of 1mm and a flow velocity between the lips of 11 ms^{-1}.

6.3.1 Static lip model in pipe

As in the case of the pipe expansion, a series of vorticity maps from different time steps throughout the simulations are shown, starting from when the flow is just reaching the lips through to when the steady state flow pattern has been achieved. As previously, high vorticity magnitude is shown by red colours and low vorticity by the blue colours, with the boundaries of the flow visible as the dark shaded area.

The first set of graphs (Figure 6.12) shows the flow through the round lip model. It can be seen in this figure that in a similar way to the rapid expansion there are two symmetrical vortices formed by the starting flow passing the lips. These vortices are carried downstream by the flow which forms a jet, leaving the

lips as the steady state regime is approached. As the jet travels downstream of the lips it eventually becomes unstable and breaks up into turbulence at a distance of about 20mm downstream of the lips. This pattern of jet formation and subsequent breakdown into turbulence can be seen for all the different models (Figures 6.12 to 6.18), with the different lip shape models leading to variations in the distance downstream of the lips at which the instabilities appear and the level to which this turbulent breakdown occurs. An example of these differences can be seen by comparing the 10^o inward angled model (Figure 6.13) with the 20^o inward model (Figure 6.14). Here it can be seen that the jet formed by the 20^o inward angled lip has greater instability than that formed by the 10^o inward angled lip model. In the case of the 10^o inward angled lip, the jet remains mostly stable untill about 15mm downstream of the lip gap with the initial vortex pair traveling remaining symmetrical untill after the 0.244 sec timestep. For the case of the 20^o inward angled lip, greater variations in the vorticity can be seen further upstream in the jet and the vortex pair become noticably aysmmetrical after the 0.0153 sec timestep with the small vorticity instabilities in the jet leading to rapid breakdown into turbulence around 15mm downstream of the lips. Looking at the flow patterns for the 30^o inward angled lip model it can be seen that although there are still vorticity variation in the jet, the overall profile returns to a more symmetrical pattern, with the flow remaining in a well defined jet until around 20mm downstream of the constriction in a similar way to the case for the round lip model. This can be attributed to the lip angle α being large enough so that

only the last round section of the lips has much effect on the flow, thus becoming similar to having a single semicircular constriction with a radius of $\frac{1}{4}$ of the lip width.

A progression of the flow patterns can be seen for the outward angled lip models. For the 10^o outward model (figure 6.16) the flow pattern is similar to that of the 10^o inward model (figure 6.13) except that the jet has a slightly larger width. When the lip angle is increased to 20^o there is a marked change in the flow pattern with a large increase in the instability of the jet. In addition to this, it can be seen that the flow attaches itself to one side of the lip after the initial edge. This asymmetric flow pattern is caused by boundary layer effects and is known as the Coanda effect. Very similar flow patterns can be seen in experimental observations of air flow in similar expansions [38] [40]. As the lip angle is increased to 30^o this flow again returns to a more symmetrical pattern (figure 6.18). In this case it can clearly be seen that the flow separates from the upstream rounded edge of the lip with the angled part of the lip and the downstream corner having little or no effect on the flow. This leads to a similar flow to that given by the 30^o inward angled lip model.

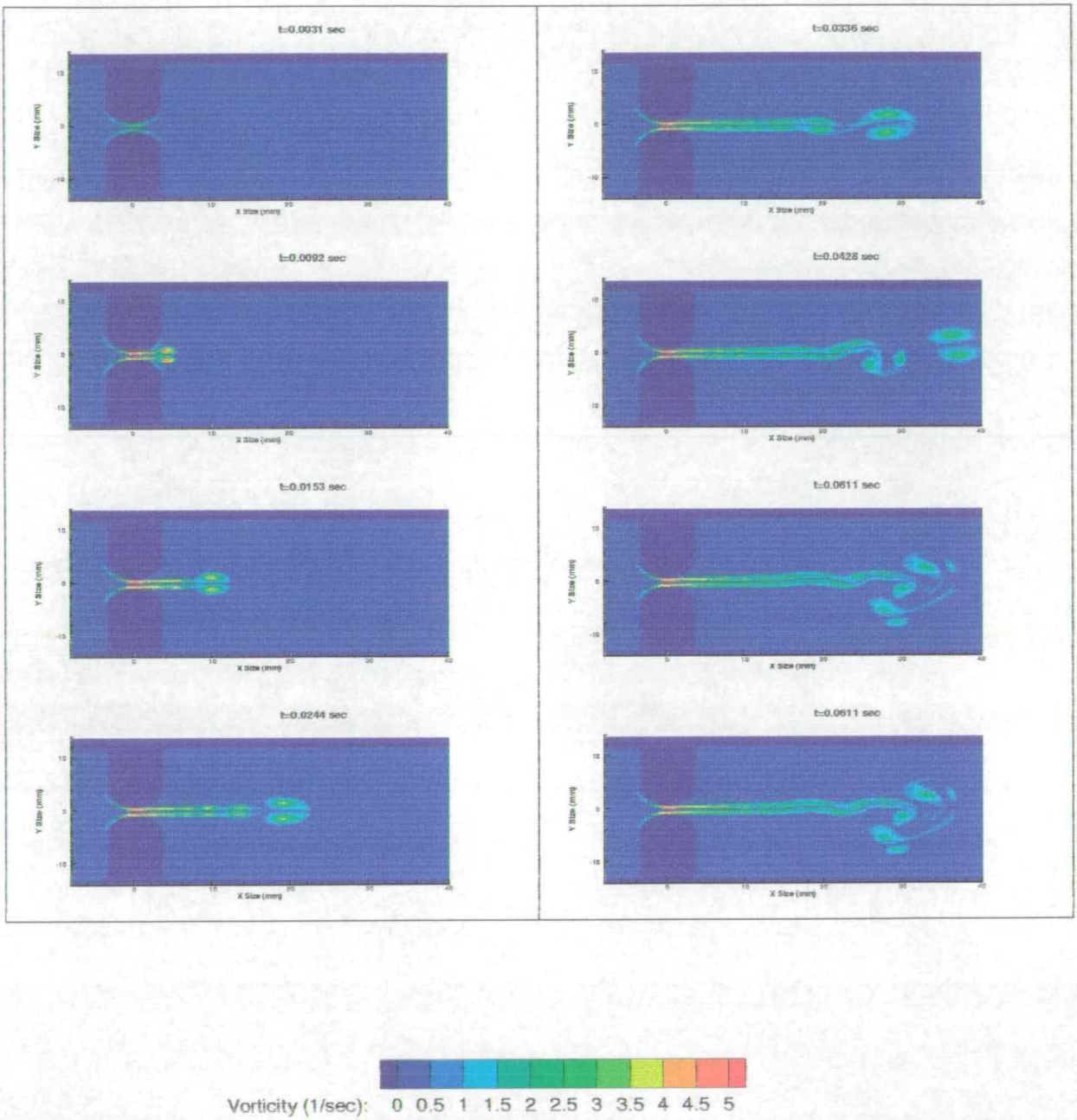

Figure 6.12: Flow vorticity maps for round lip model

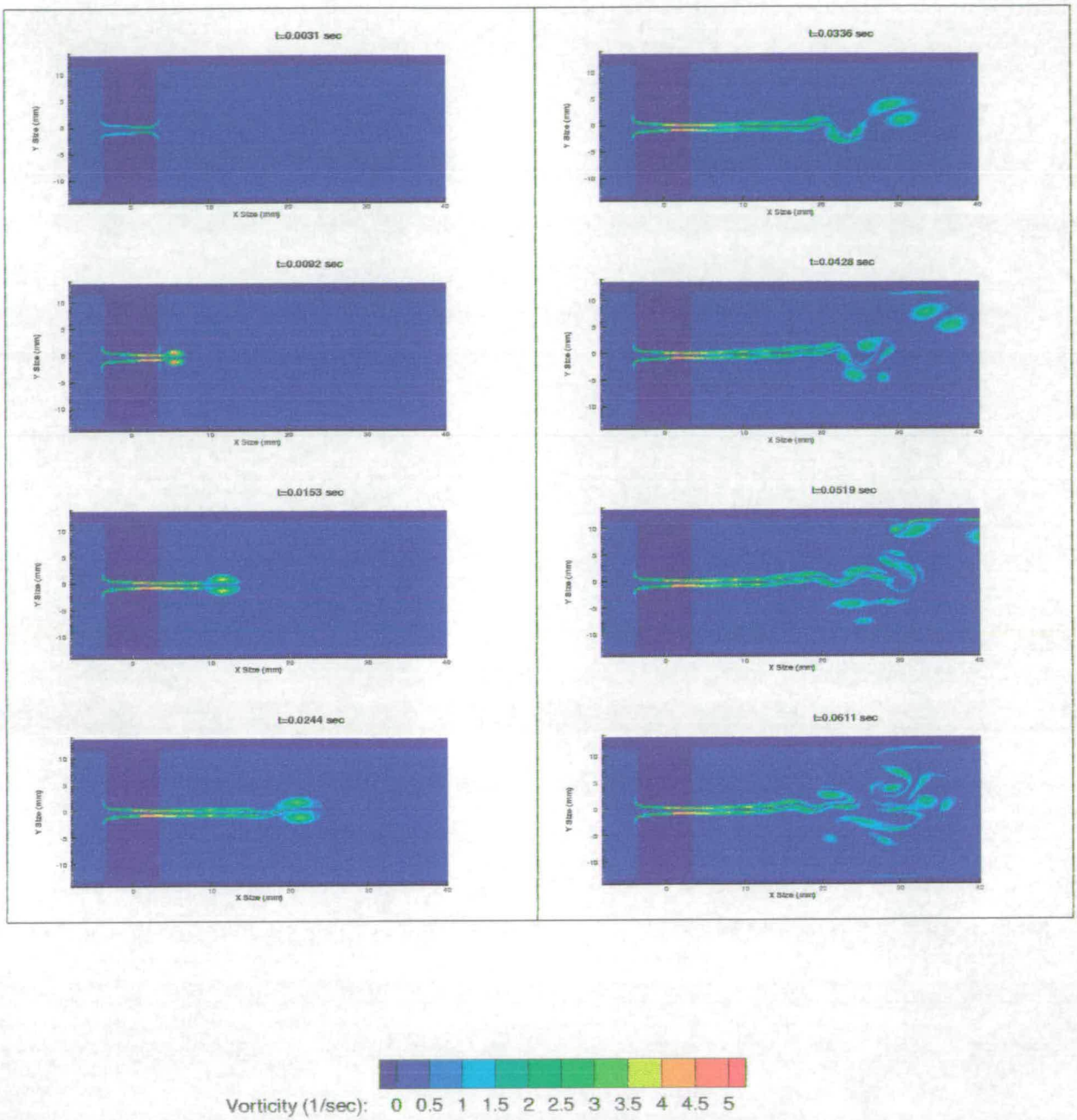

Figure 6.13: Flow vorticity maps for 10^0 inward lip model

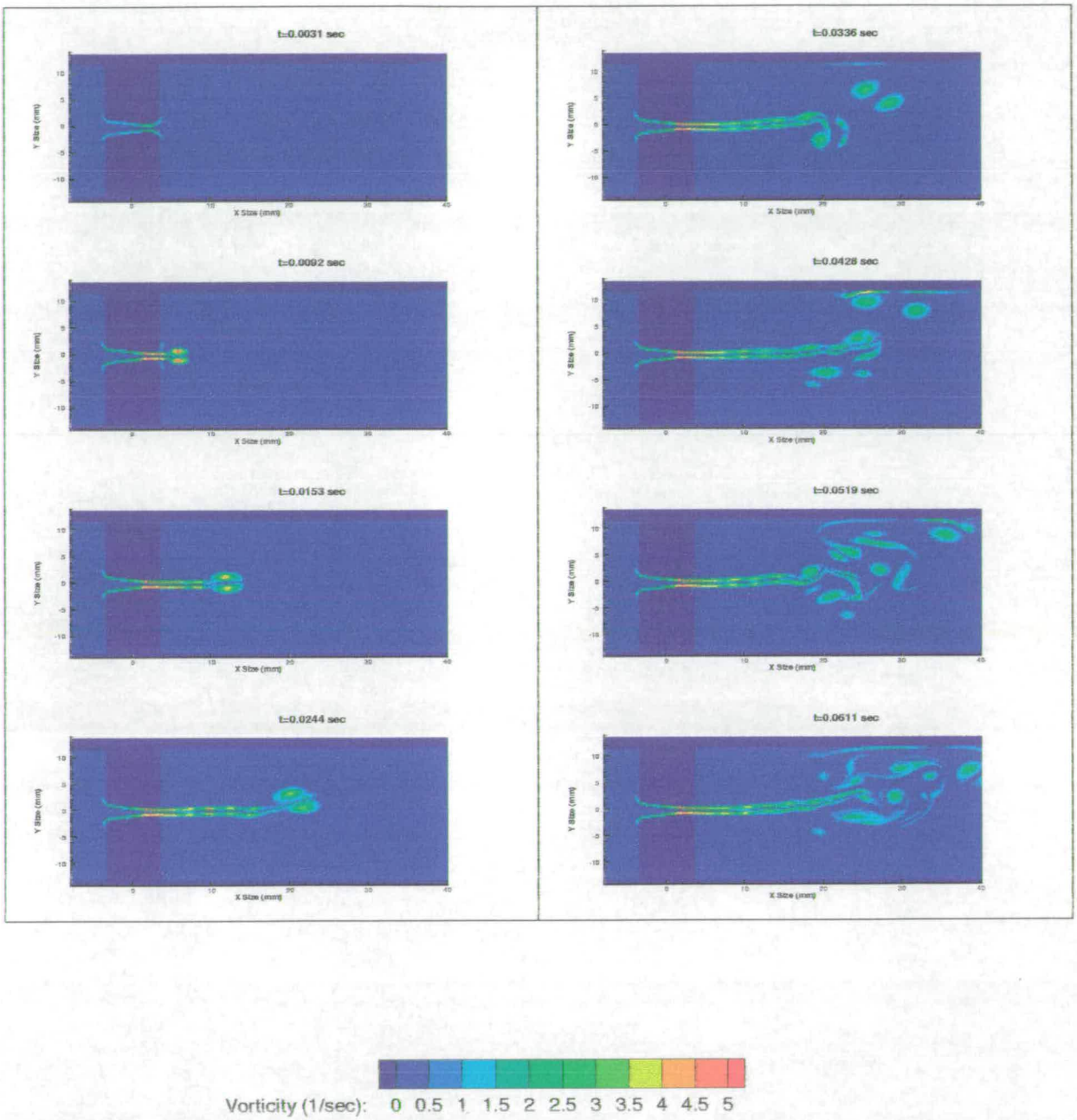

Figure 6.14: Flow vorticity maps for 20^0 inward angle lip model

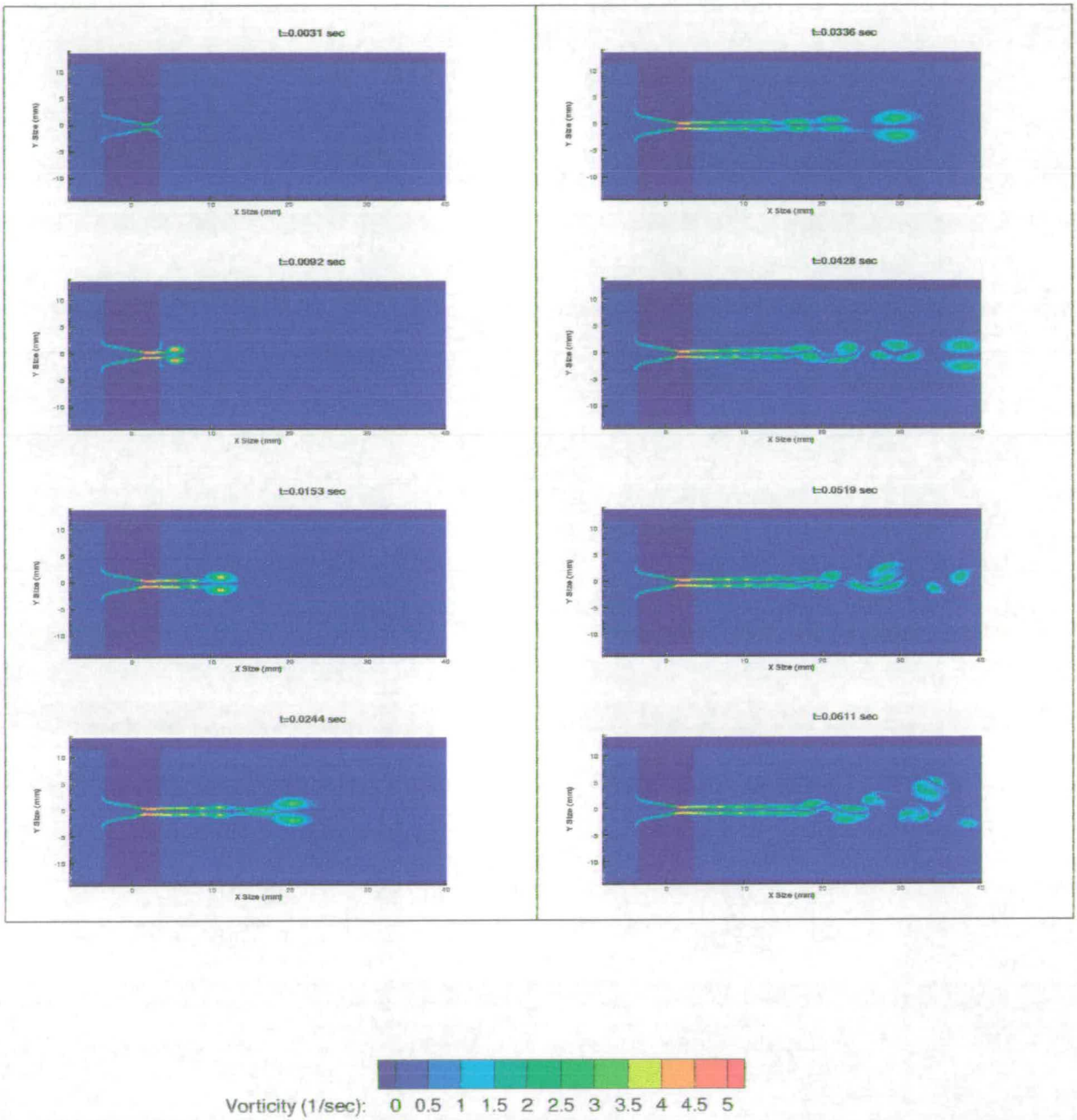

Figure 6.15: Flow vorticity maps for 30^0 inward angle lip model

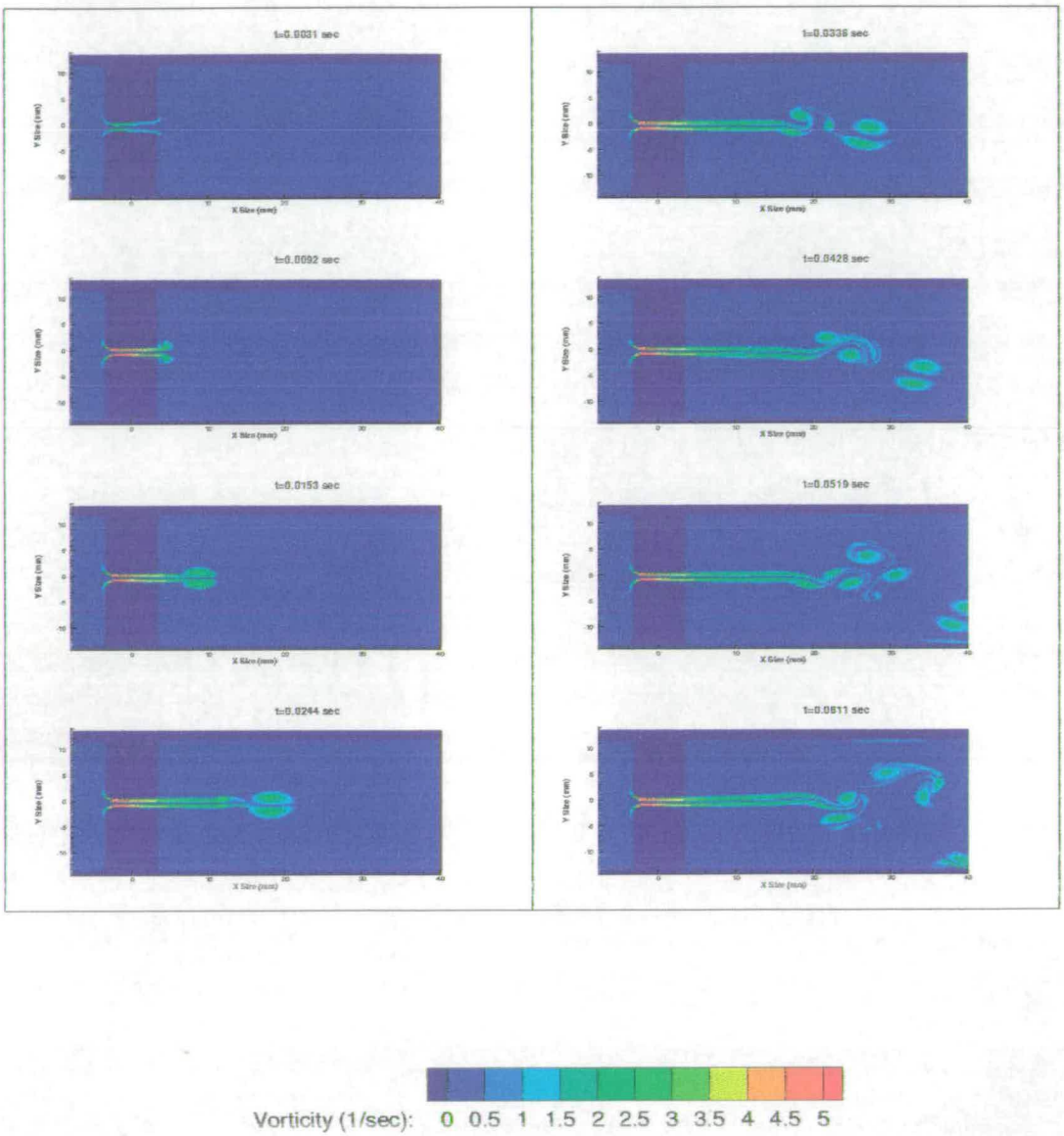

Figure 6.16: Flow vorticity maps for 10^0 outward angle lip model

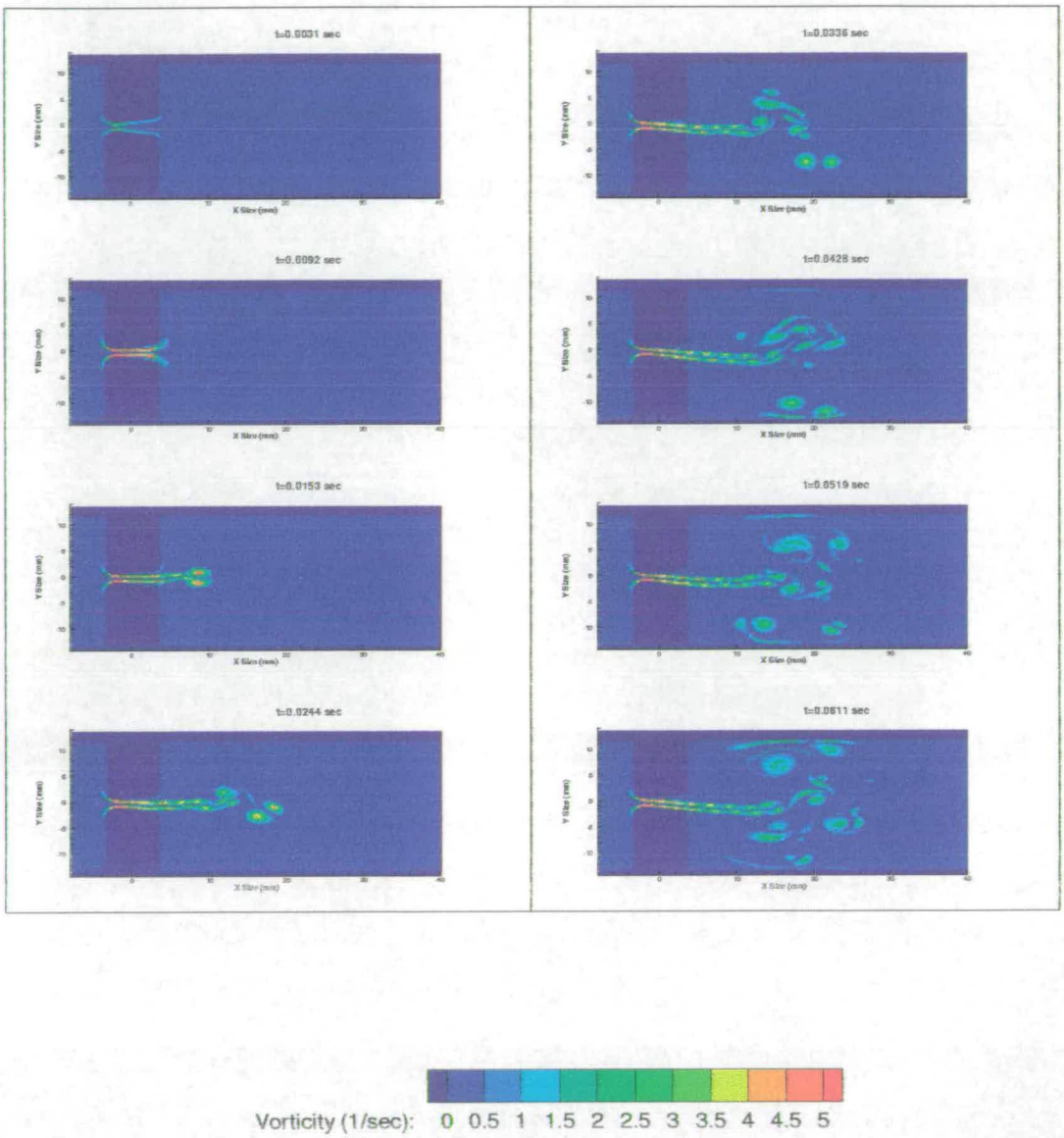

Figure 6.17: Flow vorticity maps for 20^0 outward angle lip model

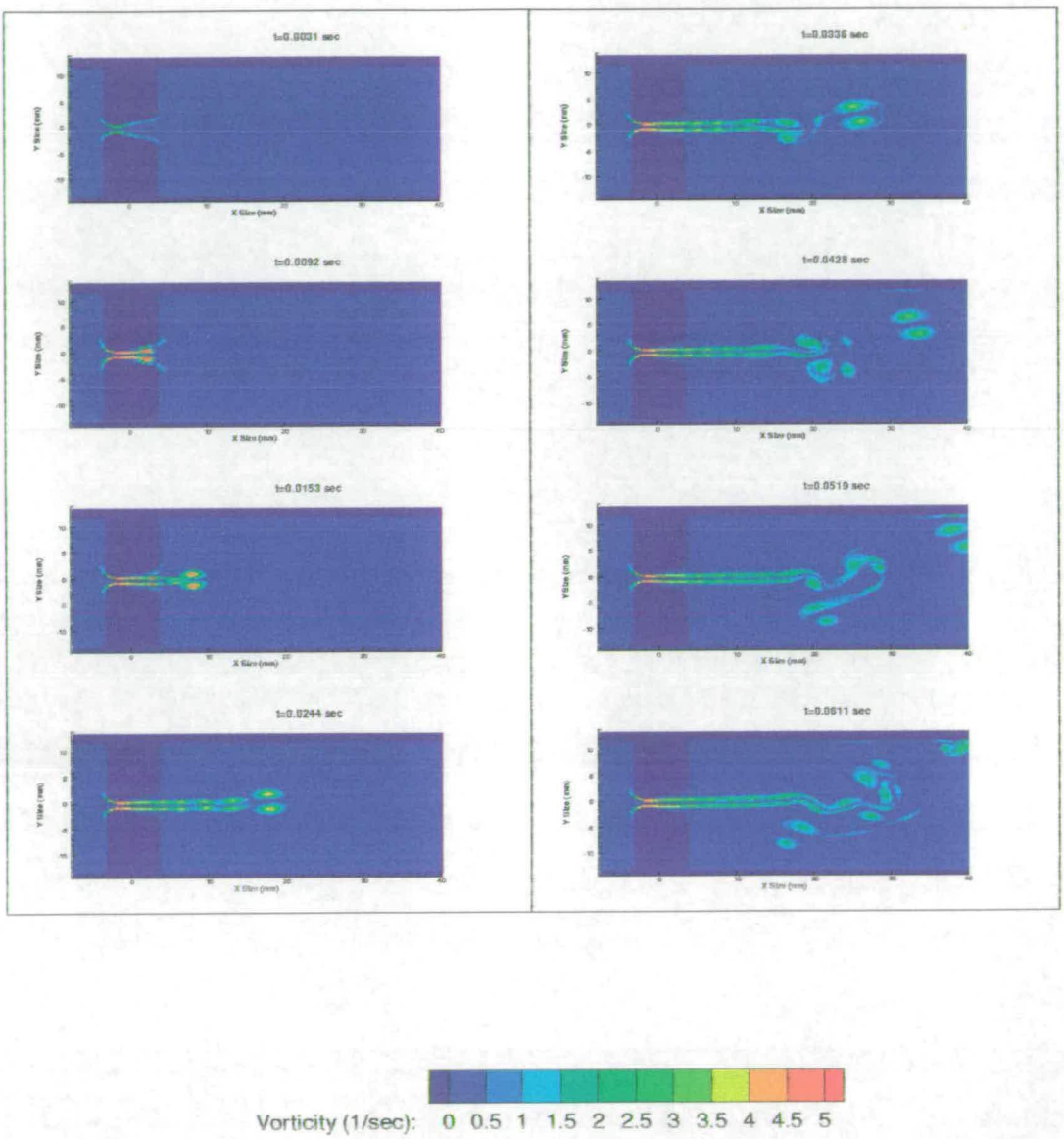

Figure 6.18: Flow vorticity maps for 30^0 outward angle lip model

6.3.2 Static lip model with mouthpiece

Following on from the lip model simulations in section 6.3.1 a further set of simulations was performed using the same lip model but with a constriction in the shape of a mouthpiece backbore placed after the lip model, rather than the continuation of the straight pipe. The shape of the mouthpiece backbore used in the simulations is similar to that of the mouthpiece used for the experimental mechanical response measurements in chapter 3. The narrowest part of the throat of the mouthpiece in these simulations occurs 20mm downstream of the centre point of the lips. It can be seen from looking at the previous simulations of the lip models without the mouthpiece that this is around the same distance at which turbulent breakup of the jet occurred in many of the simulations, with the jet for some of the more stable profiles staying coherent until around 25mm downstream of the lips (Figure 6.12) and the less stable configurations breaking up only 10-15mm downstream of the lips (Figure 6.17). This suggests that for the more stable lip configurations there should be little change between the different profiles, as the jet will still have a laminar profile when it reaches the mouthpiece throat, whereas if the jet becomes unstable before it reaches the mouthpiece throat a considerable variation in the flow profile would be expected.

The vorticity maps for the simulations with the mouthpiece backbore following the lips can be seen in Figures 6.19 to 6.25. These figures show that, as expected, for most of the different lip models there is a clean jet formed at the lips which

becomes unstable to a greater or lesser extent at the throat of the mouthpiece. It is unclear whether this instability is caused by the turbulent breakup of the jet due to amplification of instabilities occurring at the lips or due to the proximity of the flow to the mouthpiece throat, and in some cases it seems that the shape of the backbore of the mouthpiece causes the turbulent flow to be directed through the throat of the mouthpiece causing the flow from most of the lip models to look similar. The one exception to this is the case of the 20^o outward lip model where, as in the simulations without the mouthpiece, the jet is attracted to one side of the lips due to the Coanda effect and therefore does not pass directly into the mouthpiece throat, but rather is directed towards the wall of the mouthpiece and thus creates considerable turbulence in the mouthpiece cup.

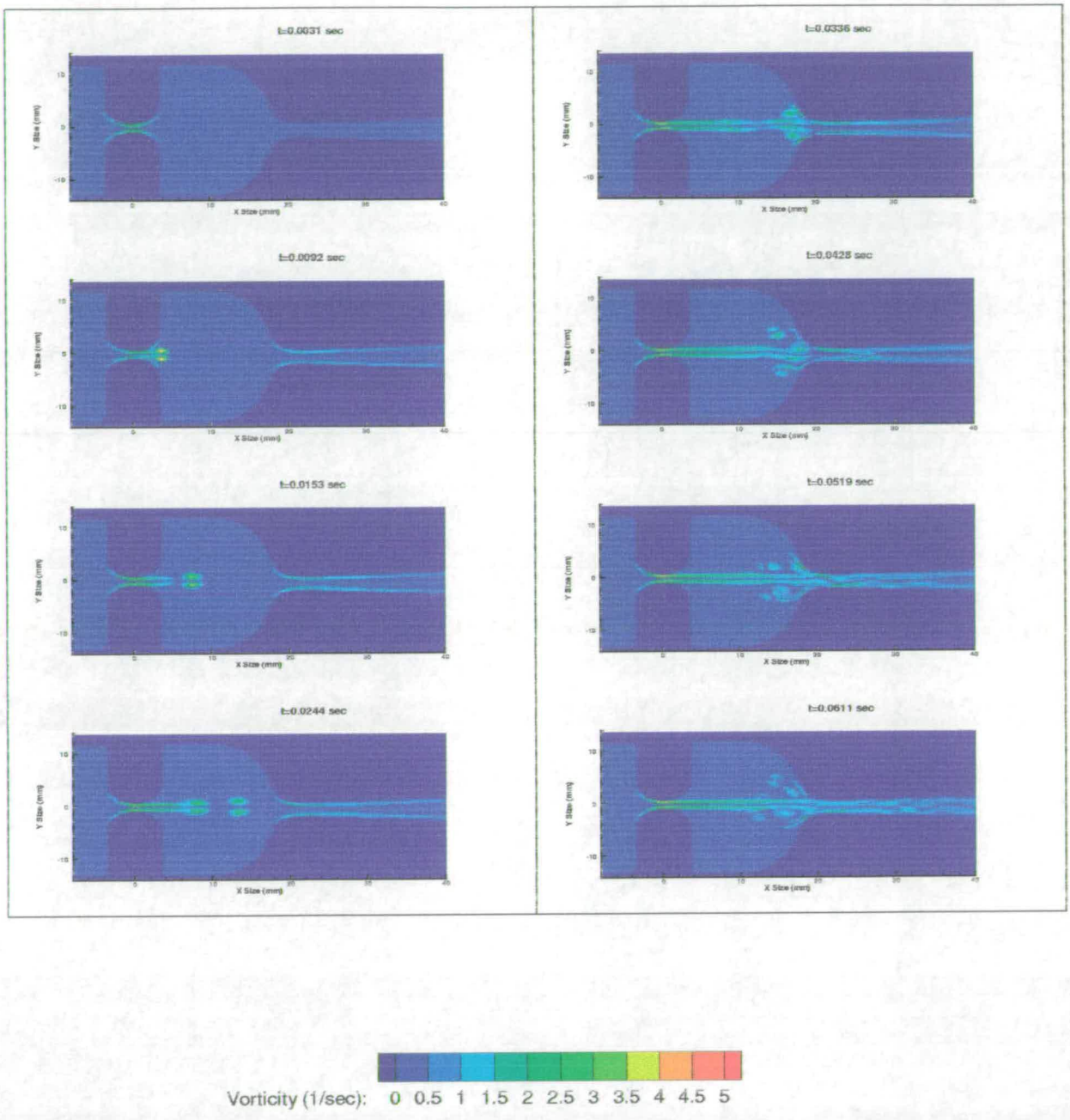

Figure 6.19: Flow vorticity maps for round lip model with mouthpiece

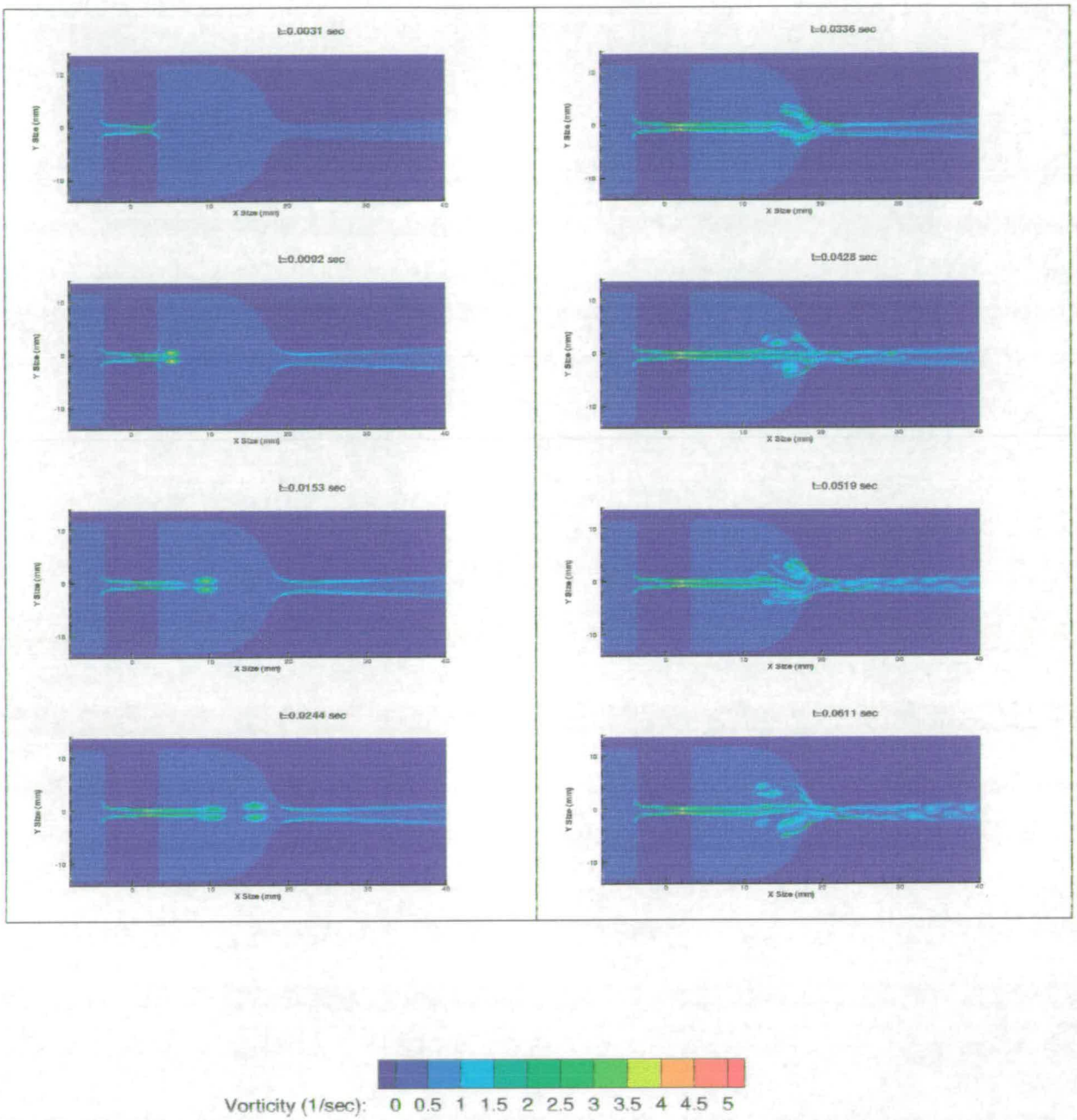

Figure 6.20: Flow vorticity maps for 10^0 inward angle lip model with mouthpiece

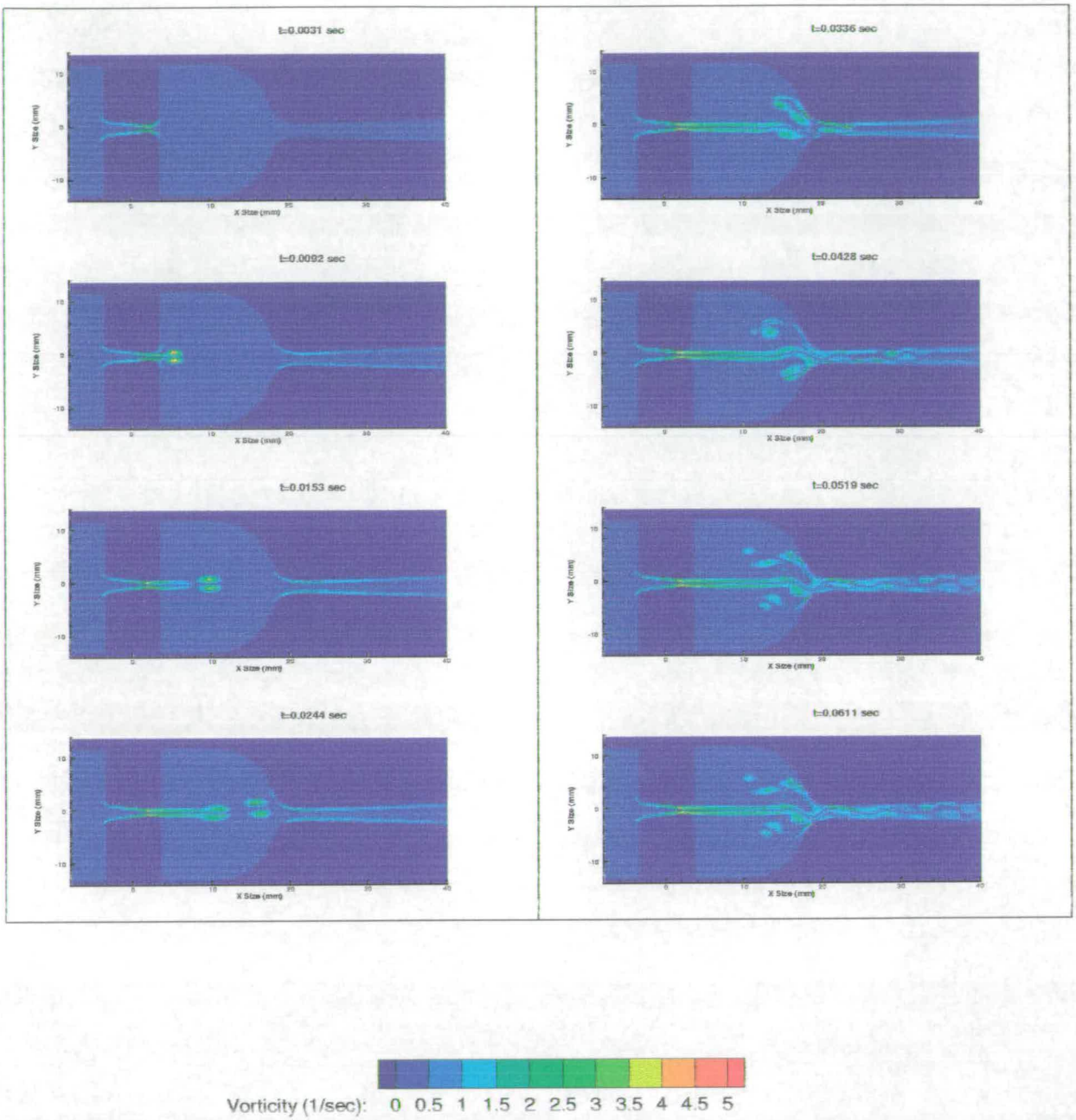

Figure 6.21: Flow vorticity maps for 20^0 inward angle lip model with mouthpiece

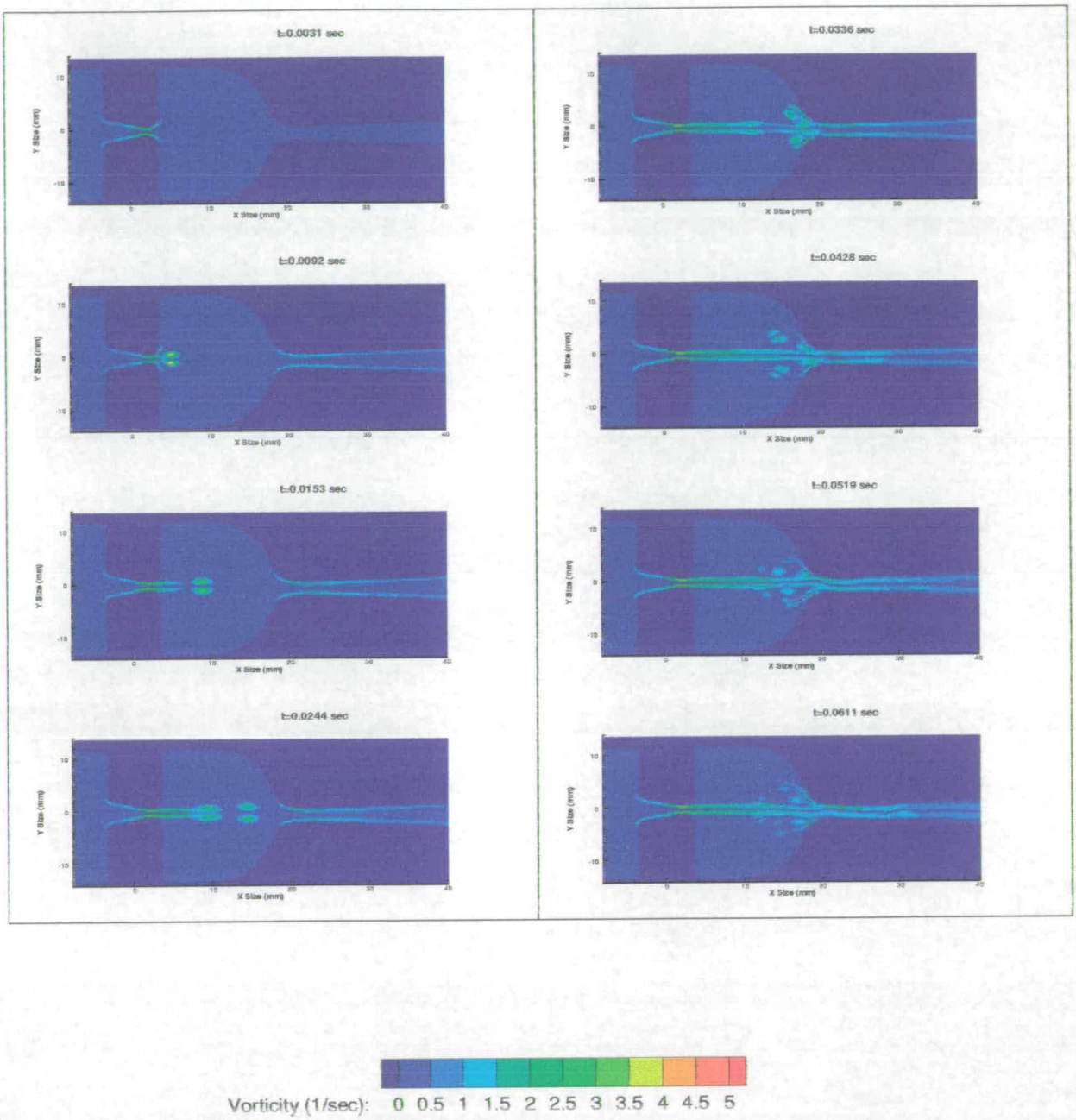

Figure 6.22: Flow vorticity maps for 30^0 inward angle lip model with mouthpiece

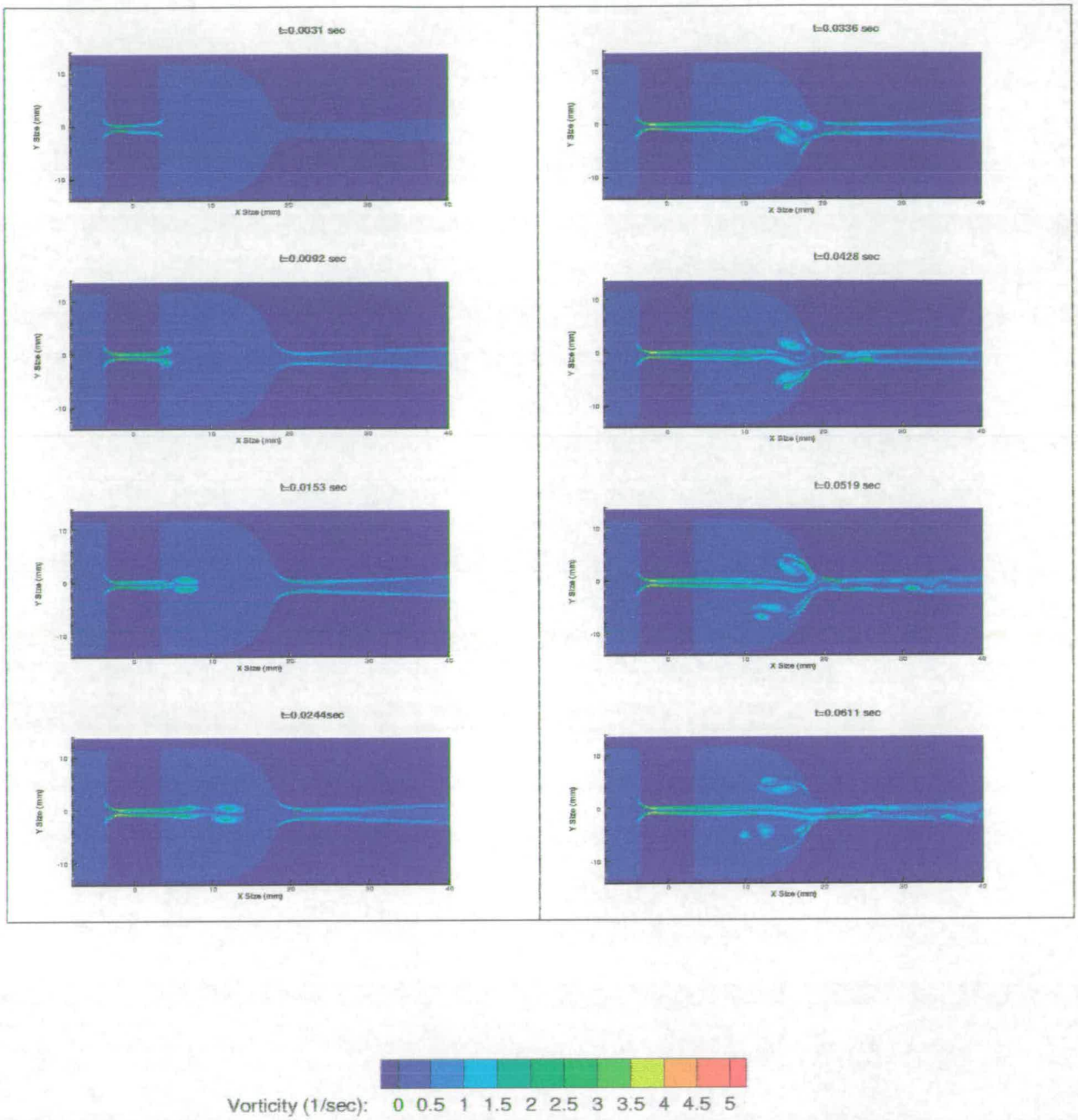

Figure 6.23: Flow vorticity maps for 10^0 outward angle lip model with mouthpiece

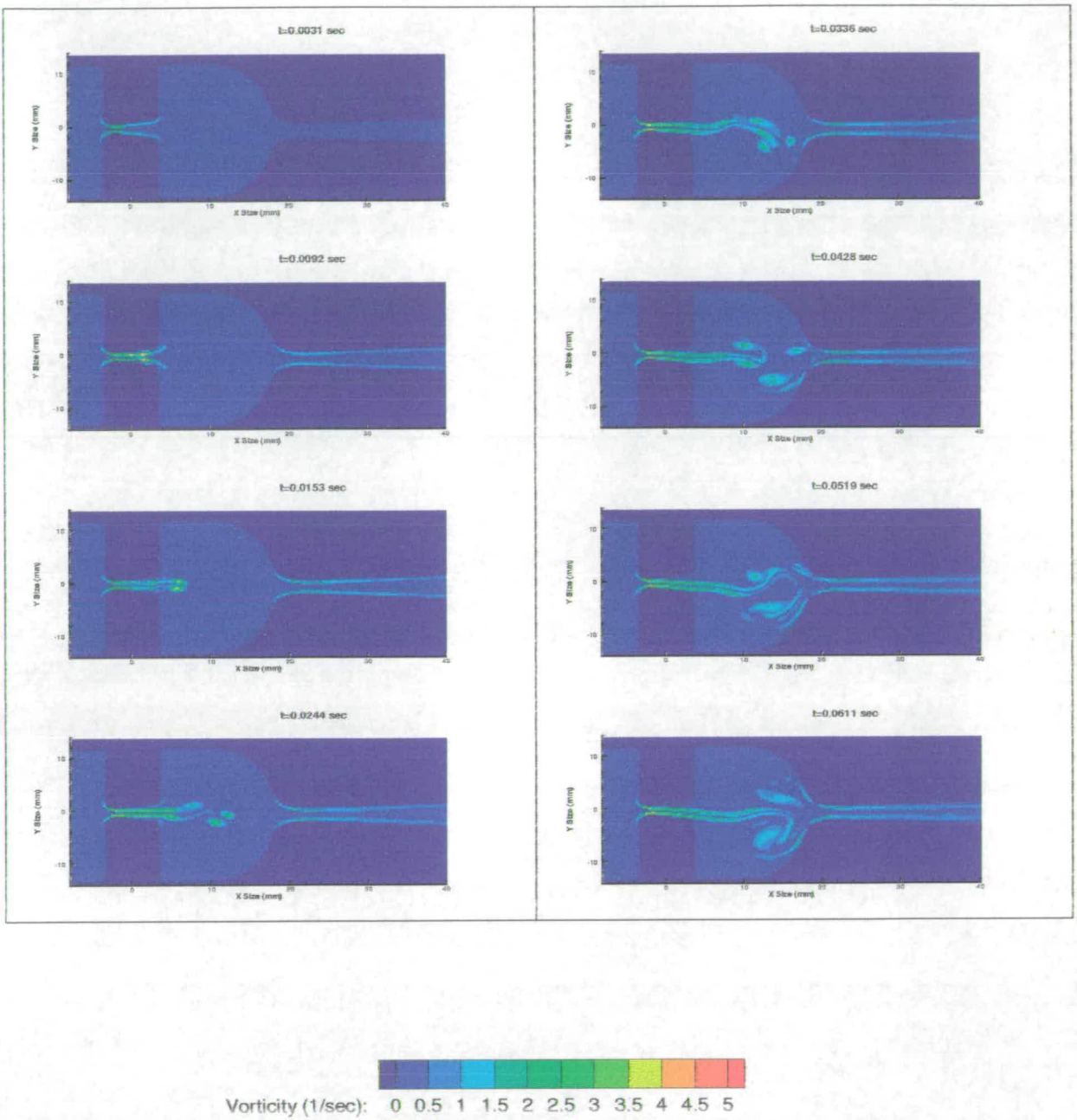

Figure 6.24: Flow vorticity maps for 20^0 outward angle lip model with mouthpiece

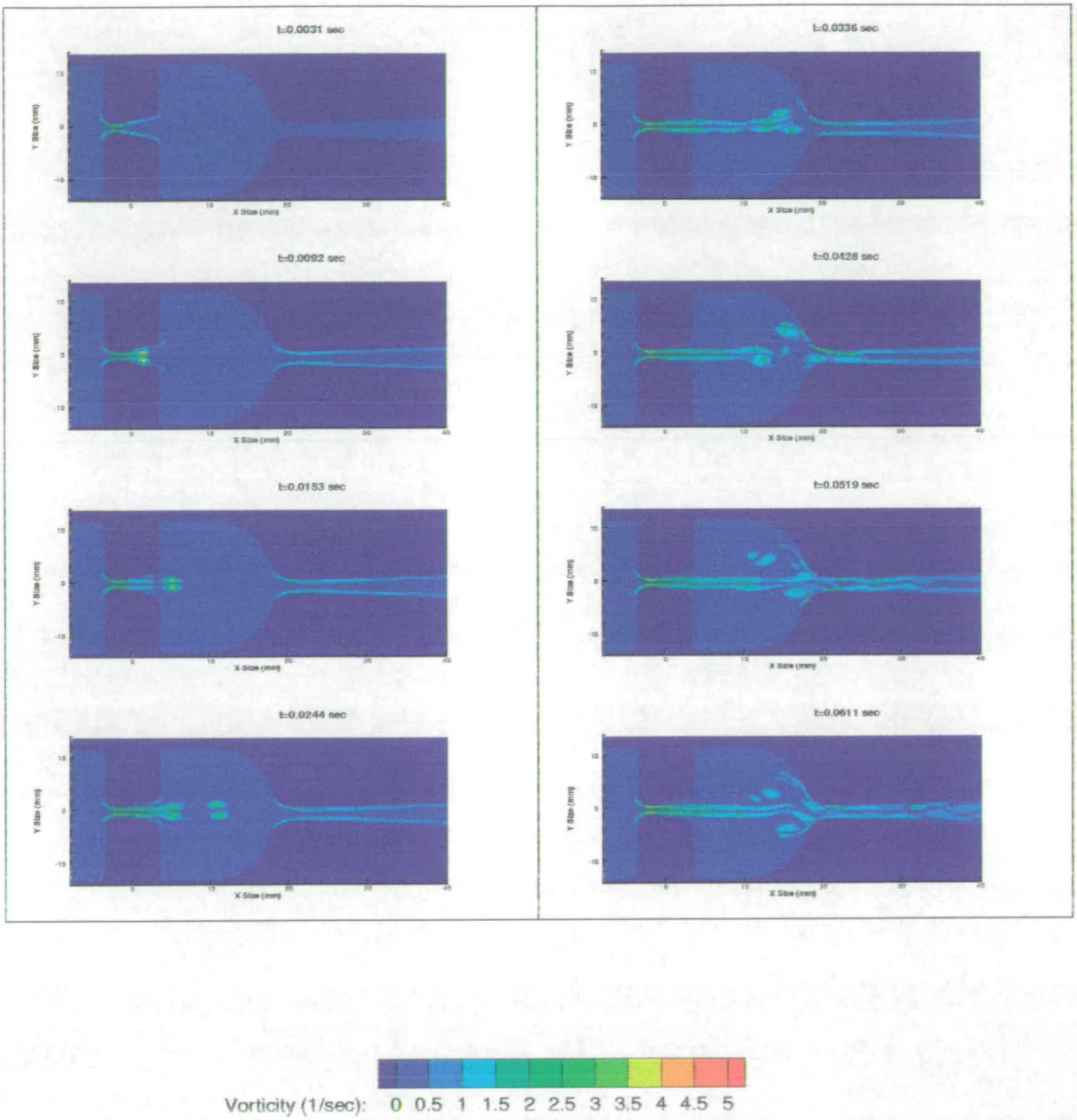

Figure 6.25: Flow vorticity maps for 30^0 outward angle lip model with mouthpiece

6.4 Application of LBM simulations to brass instruments

The application of the above results to the playing of brass instruments is in many ways limited due to the static nature of the lip models, and to a lesser extent by the two dimensional nature of the simulations. The first of these limitations means that the flow profiles shown in the simulations cannot be applied directly to the usual playing situation of brass instruments where the lips are in no way static, but rather are oscillating around a continuous path and even closing completely for part of the cycle when playing much above threshold. It must be assumed that the motion of the lips and the oscillating pressure on the mouthpiece side of the lips will have considerable effect on the profile of the jet produced by flow between the lips during playing compared to the static lip measurements as even at the lowest notes played on the trombone the period of oscillation of the lips is around 20 msec. This must be taken into consideration when analysing these simulations in terms of what would be expected of the flow during playing. Despite this, the simulations can still be useful for studying the initial fluid dynamical forces on the lips which are responsible for the destabilisation of the lips occurring at the onset of playing a note on a brass instrument. The second limitation of these simulations is that they are limited to modelling only two dimensional flow. This does not create much of a problem in term of the flow pattern between the lips, as the channel between the lips on a real player is much wider than it is long

and therefore the flow patterns through the lips in a plane at the centre will have a mostly two dimensional form, only diverging from this at the edges of the lip channel. A more subtle problem with the two dimensional simulations is that there cannot be true turbulent dissipation in a two dimensional simulation, as the main processes through which the transition to turbulence occurs is vortex twisting and stretching which cannot occur in two dimensions [41]. This means that the jet does not break up into a true turbulent flow but rather forms larger vortices which are convected downstream, as is seen in the vorticity maps of the current simulations.

By looking at the form of the jet as it leaves the lip gap, it is possible to get some idea of the strength of the forces acting on the lips which are responsible for the destabilisation occurring at the onset of playing a note. Bernoulli forces acting on the lips can be an important factor in this destabilisation. Looking at the velocity along the centre line between the lips for the lip model with a round lip profile and no mouthpiece present at the 0.0611 second time step (Figure 6.26), it can be seen that there is a large increase in velocity as the flow travels from the region before the lips into the lip channel, but after the lips there is little change in the flow velocity until the turbulent breakup of the jet occurs. If this is considered in terms of the Bernoulli equation (2.4) it can be seen that there must be no pressure recovery on the downstream side of the lips as there is no drop in the flow velocity q. On the upstream side of the lip however, the flow velocity changes from around 0.1 ms^{-1} before the lips to a value of around

2.1 ms^{-1} in the lip channel. Using the Bernoulli equation the mouth pressure P_m can be related to the lip channel pressure P_l by:

$$\frac{1}{2}\rho_m q_m^2 + P_m = \frac{1}{2}\rho_l q_l^2 + P_l \tag{6.2}$$

where q_m and q_l are the flow velocities in the mouth and lip channel and ρ_m and ρ_l are the densities in the mouth and lip channel.

Assuming that the air density remains constant through the constriction ($\rho_m = \rho_l$) this can be re-arranged to give the pressure drop between the mouth and lip gap $P_d = P_m - P_l$ as:

$$P_d = \frac{1}{2}\rho(q_l^2 - q_m^2). \tag{6.3}$$

For the above measurements this gives a pressure drop between the lips of 2.7 Pa for a standard air density of 1.225 kg m^{-3}. If the height of the gap between the lips varies between 0.5mm and 1.5mm during playing at threshold and it is assumed that the mouth pressure remains constant, then by using laminar flow theory for a two dimensional channel [50] the centre-line flow velocity in the lip channel q_l can be calculated using:

$$q_l = \frac{G}{2\mu}(a^2) \tag{6.4}$$

where:

$$G = \frac{P_m - P_l}{b} \tag{6.5}$$

and: μ is the air viscosity, $2a$ is the width of the channel and b is the channel length.

Using the flow velocities from the simulations with these equations it can be calculated that for the 0.5mm lip gap there is a pressure drop of 0.17Pa, whereas for the 1.5mm lip gap there is a pressure drop of 13.6Pa. This gives a pressure variation over the cycle of the lips of 13.4Pa.

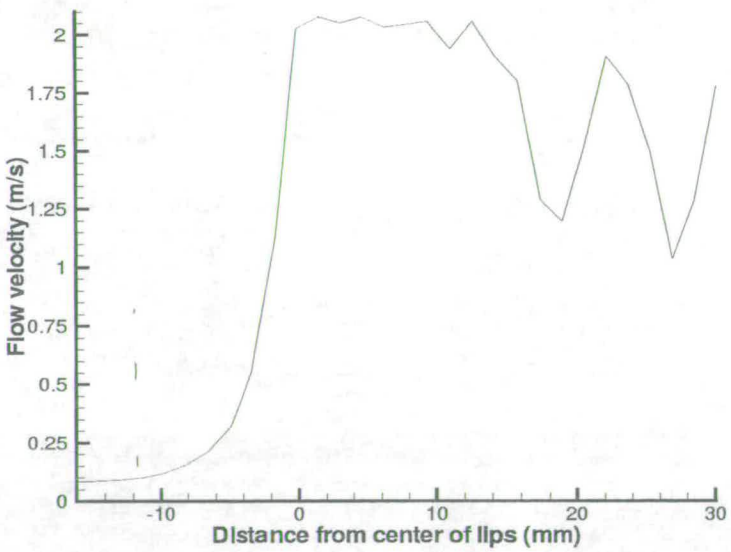

Figure 6.26: Centre line velocity of the flow between the lips of the round lip model with no mouthpiece at 0.0611 sec.

Measurements of the acoustic pressure in the mouthpiece of a brass instrument played by the artificial lips given in Chapter 4 show that there is a sound pressure

level of around 85dB in the mouthpiece when just above threshold. This is an acoustic pressure variation of around 0.35Pa. The outer surface of the lips over which this acoustic pressure variation acts is larger than the area between the lips over which the Bernoulli force is applied, as the lips are around 3-8mm thick whereas there can be up to 15mm of lip height inside the mouthpiece. Considering these values in terms of the simple model of the lips it can be seen that the Bernoulli force, which leads to an inward striking behaviour acting on the lips, should have a comparable if not greater value than the force created by the mouthpiece pressure acting on the outer surface of the lips, assuming that the flow velocity between the lips remains similar to the simulated value under playing conditions. In the case when the lips are not in motion and there is no acoustic pressure in the mouthpiece, the main force leading to destabilisation of the lips due to a steady increase in the mouth overpressure is the Bernoulli force. This is because the outward striking force acting on the inner surface of the lips will cause the lips to open further, but given a constant mouth overpressure this does not create any change in the force acting on the lips. Only in the case of an acoustic pressure variation on the mouthpiece side of the lips can this situation lead to destabilisation. On the other hand, the Bernoulli force causes the lips to be drawn together which, as seen from the above analysis causes a decrease in the flow velocity through the lips and therefore a reduction in the pressure drop between the mouth and lip channel, reducing the Bernoulli force acting on the lips. This effect is reversed as the lips open wider, where the Bernoulli force on

the lips increases, thus acting to close the lips.

6.5 Conclusions

The Lattice Boltzmann simulations provide a way to model fluid flow between static models of the lips and give good agreement with flow visualisation of similar experimental models. The simulations show that there is a clean separation of the jet in almost all the models; the main exception is the model with the 20^o outward angle in which the flow adheres to one side of the lips due to the Coanda effect, leading to an asymmetrical jet downstream of the lips. The various other lip models create a symmetrical jet which then breaks up into turbulent flow at various distances downstream of the lips, depending on the lip shape. As all of the different models produce a jet of about the same width and velocity immediately downstream of the lips, it can be assumed that the pressure drop between the lips is the same for all the models. This means that any effect of the lip shape on the Bernoulli force must be due to a change in the effective surface area rather than a change in the pressure difference in the lip channel. The presence of the mouthpiece does not make any significant difference to the flow between or immediately after the lips and so does not change the lip forces leading to destabilising of the lips. Although these small changes in lip shape do not have much effect on the pressure drop between the mouth and the lip gap, it has been suggested [37] that under some situations the small changes in

separation point of the jet may be critical for effects such as the buzzing of the lips when no instrument or mouthpiece is present.

The static nature of these simulations limits the usefulness in studying the nature of the lip reed under playing conditions, although some assumptions can be made about the threshold playing. It should be possible to extend the scope of this type of simulation by creating non-static models of the lips and a boundary condition at the outflow of the simulation which would emulate one or more resonant modes of an instrument. The main limitation of this type of simulation is the computational time needed perform a simulation of suitable duration, but this is rapidly becoming less of a problem as available computer power increases. This can be seen from the fact that computational time needed for the simulations in this chapter dropped from over a week to less than twelve hours over the three year period in which these simulations were developed and run.

Chapter 7

Summary and Conclusions

The objectives of this work were set out in Chapter 1. This chapter addresses these objectives, giving a summary of how they were achieved and the main results given.

7.1 Mechanical response measurements of artificial lips

The mechanical response measurement on the artificial lips followed a similar method and experimental setup to that used by Cullen [21]. The artificial mouth used in this work was also the same model as used by Cullen. Changes were made to both the experimental techniques and the analysis software to allow further

extensions to the work done by Cullen. The addition of a straight telescopic pipe along with suitable optics enabled measurements of the lip motion to be performed in the presence of an acoustic impedance on the downstream side of the lips. A suitable mounting was also designed and built to allow the creation of a known acoustic field on the mouthpiece side of the lips, thus enabling measurements of the mechanical response to be performed driving from the downstream side of the lips, as is the case during normal playing of a brass instrument. Improvements were also made in the quality of the loudspeakers and driving signals used to perform the mechanical response measurements, enabling more accurate measurements to be made.

The analysis software used for the mechanical response measurements written by Cullen was extended to accommodate these changes in the experimental method. These changes included adding the ability to analyse mechanical response signals from microphones placed on both side of the lips, using either one of the microphone signals or calculating the acoustic pressure difference across the lips and performing the analysis using this value. Further extensions to the software were made enabling the use of different microphone signal conditioning amplifiers, and also enabling analysis of the results from measurements made on the artificial lips during playing.

With these improvements to the experimental method and analysis software, measurements were taken to investigate the effects of the acoustic impedance of

the instrument on the mechanical response of the lips. In measurements shown in Section 3.3.6 it has been found that by measuring the mechanical response, both with and without a mouth overpressure, and comparing this with the note played by the lips and the acoustic resonance of the pipe, a clear picture of the inward or outward striking characteristics of the lips can be seen. As is expected using the one mass model and from previous experiments, the lips behave as an inward striking reed when the playing frequency well is below the acoustic resonance of the instrument, and as an outward striking reed when the playing frequency is well above the resonance frequency of the instrument. These two cases can be seen in the experiment for the shortest and longest pipe lengths respectively. However, in the intervening area between these two clear cases there is a region where the lips cannot be described purely as inward or outward striking. Rather there is a coupling between two resonant modes of the lips, one of them inward and the other one outward. This type of behaviour cannot be modelled using the simple one mass model but needs a more complicated model such as the one suggested by Richards [44].

Mechanical response measurements were also performed to allow a comparison between the results obtained with the driving acoustic field on either the upstream or downstream side of the lips. These results confirm the assumption that at the acoustic pressure levels used for these measurements, the lips respond to the pressure difference across them and are not affected to any large extent by the absolute pressure or effects caused by non-linear flow between the

lips. Although mechanical response measurements made using downstream driving of the lips compare more directly with how the lips are driven under playing conditions, the upstream driving method was still preferred due to the greater experimental simplicity and the fact that the instrument cannot be directly attached to the mouthpiece when using the downstream driving technique. For this reason, downstream driving of the lips was only used where it was necessary for the measurement such as in the case of the studies of mouth volume.

7.2 Playing measurements of artificial and brass player's lips

Two main experiments were performed on the artificial lips to examine playing characteristics. These involved looking at the effect of the mouth cavity volume on the playing of brass instruments and some comparisons between the artificial lips and real players.

The first of these experiments, looking at the effect of mouth volume on the playing characteristics of the lips, was done in two stages. The first stage was to look at how the mechanical response of the lips, driven from the downstream side, changed with a variation in the mouth cavity volume. Changes in mouth volume were made by partially filling the mouth cavity with water and then allowing a known quantity of the water to drain out between measurements. The

results in Section 4.3.1 show that a distinct change in the mechanical response of the lips can be seen as the mouth volume is changed. The frequency at which this change in mechanical response is observed corresponds to the frequency of the Helmholtz resonance of the mouth. The effect of this Helmholtz resonance is to decrease the amplitude response of the lips, due to the loading effect that occurs when the impedance maximum of the mouth falls at the same frequency as one of the resonance frequencies of the lips. This is very similar to the effect caused by the instrument resonances falling at the same frequency as a lip resonance when performing mechanical response, driving from the upstream side. The second part of this experiment aimed to determine whether the effects seen in the mechanical response curves can also be observed in the note produced by the instrument when it is played. Although fundamental changes in the note (such as the playing frequency) cannot be expected to occur due to mouth volume changes, a study showing the relative strength of the harmonics of the note produced by the instrument revealed some systematic changes. Measuring these changes over a range of mouth volumes showed a progressive change in relative acoustic pressures of the different harmonics of the note produced at the bell of a trombone. This means that each different mouth volume leads to a slightly different tone in the note produced.

The second experiment studying the playing characteristics of the lips used a method suggested by Ayers [4] for measuring the lip resonance of real players. Using this method with both real players and with the artificial lips enabled direct

comparison between the playing of the artificial lips and a human player. These measurements showed that the artificial lips can produce results which are similar to those obtained from a real player and any differences between the artificial lips and real players seems to be less than the difference between one player and another. This confirms the impression, obtained from extensive work using the artificial lips, that they behave in many ways like the lips of a novice brass player producing reasonable notes and playing characteristics, but without the precise control of an experienced player who is able to create a better sound. Real players are also able to produce many of the higher notes, well beyond the second and third mode of a trombone which the artificial lips are able to play convincingly with the range of embochure control available in the current experiments.

7.3 Development of Lattice Boltzmann simulation

Computational simulation of fluid flow was done using the Lattice Boltzmann method. The program used to perform these simulations was written using the FORTRAN 90 programming language and developed from a previous version used by Buick [10]. The code used in this thesis was configured such that there is a rectangular simulation grid with the inflow point at the left side of the grid and the outflow at the right. The dimensions of the grid, the inflow parameters

and the boundary shape to be simulated were read in from a file on disk. The generation of these initialisation files was handled by another program written in C++ utilising the QT class libraries. This program provided a graphical interface through which initial and inflow parameters could be set and the boundary profile and grid size defined. Use of this graphical interface provided a simple way to make changes to the simulations which were performed.

The Lattice Boltzmann code was tested against two known flow types. The first of these flows was the development of a Poiseuille flow in a straight pipe. An inflow condition giving equal flow velocity across the pipe entrance was applied at the inflow boundary and measurements of the velocity cross section at different distances along the pipe measured. The second test flow was the expansion of a free jet created by having a pipe containing a rapid expansion with a high expansion ratio. The width of the jet downstream of the expansion was measured and compared with the theoretical result. Both of these test flows gave results which compared well with the expected theoretical results, and previous simulations.

7.4 Simulations of fluid flow through brass player's lips

Having developed and tested the Lattice Boltzmann simulation code, simulations were run on a variety of different boundary profiles. These simulations fell into

three categories: step channel expansions, static lip models and static lip models followed by a mouthpiece.

Three varieties of step expansions were simulated, all with the same expansion ratio and inflow parameters but with different corner shapes at the expansion. These were a sharp edged corner, a rounded edged corner where the radius of the rounded edge was equal to half of the initial channel width, and a rounded edged corner with the radius equal to the full initial channel width. These simulations were run with a Reynolds number in the initial channel section of 820. The results of these simulations show that there is a jet created at the expansion which travels downstream with little expansion until turbulent breakup of the jet occurs. The different corner profiles have the effect of changing the stability of the jet with the larger rounded corner producing the least stable jet and thus the most rapid onset of turbulent dissipation.

The second two categories of simulation involved examining the flow through static lip models. For this purpose a set of seven static lip models where used, based on those used by Hofmans [38]. In a similar way to the step expansions these simulations show that there is a jet formed as the flow passes between the lips which then travels downstream breaking up into turbulence. The effect of the lip profile is to change the stability of the jet with some lip profiles giving a jet which stays coherent for a considerable distance downstream of the lips while other profiles lead to rapid onset of turbulence or even an angling of the

jet to one side due to the Coanda effect in which the jet attaches to one of the lips. The presence of the mouthpiece backbore downstream of the lips in most cases causes the breakup of the jet to occur at roughly the same point for all the different lip models other than the one case where the jet is not directed towards the mouthpiece throat. Considering these flow patterns in terms of the playing of brass instruments shows that the Bernoulli forces on the lips are comparable if not greater than those caused by the acoustic pressure variations in the mouthpiece at threshold playing levels.

7.5 Further Work

Extensions to the current work could be done both for the experimental work and the Lattice Boltzmann simulations.

One of the main extensions to this work is to develop the models of the lips to a greater extent than those done by Cullen [21], so that the results obtained from the current experimental work can be obtained from mathematical models of the lips. In addition extension to the measurements comparing the artificial lips with real players could provide valuable insight. This could be done by using a greater number of real players to obtain a more representative idea of the differences between players and how the artificial lips compare with these players.

There is great scope for further development of the Lattice Boltzmann tech-

niques used here for studying flow between the lips and in the mouthpiece. This is becoming more practical due to the rapid increase in computational power available. Two immediate areas of interest would be to create an outflow condition to the simulation which could provide a reflection of the flow representative of a real instrument and to have non-static lip models. The non-static lip models could either follow a pre-determined oscillation path as determined by the experimental measurements or the motion of the lips could be in response to the flow around them. If both of these extensions could be achieved a full working simulated model of a brass instrument could be made giving considerable insight into the workings of the lips and the coupling between the lips, the air flow and the acoustic pressure fields in a brass instrument.

Appendix A

Experimental analysis programs

Analysis of the data from the mechanical response measuring apparatus was mainly done using the program 'auto.c'. In addition to this program, various other programs were written to enable quick manipulation of the experimental data into usable forms.

A.1 Mechanical response analysis

A flow diagram outlining the operation of the 'auto.c' program can be seen in figure A.1. The program reads in either a two or three column data file with each of the columns containg sampled data from the microphones or lip opening detector. The program outputs separate files containing the amplitude (.mag file extension), the phase response (.ang file extension) and the frequency spectrum

of the signal in the first column of the input file (file called freq).

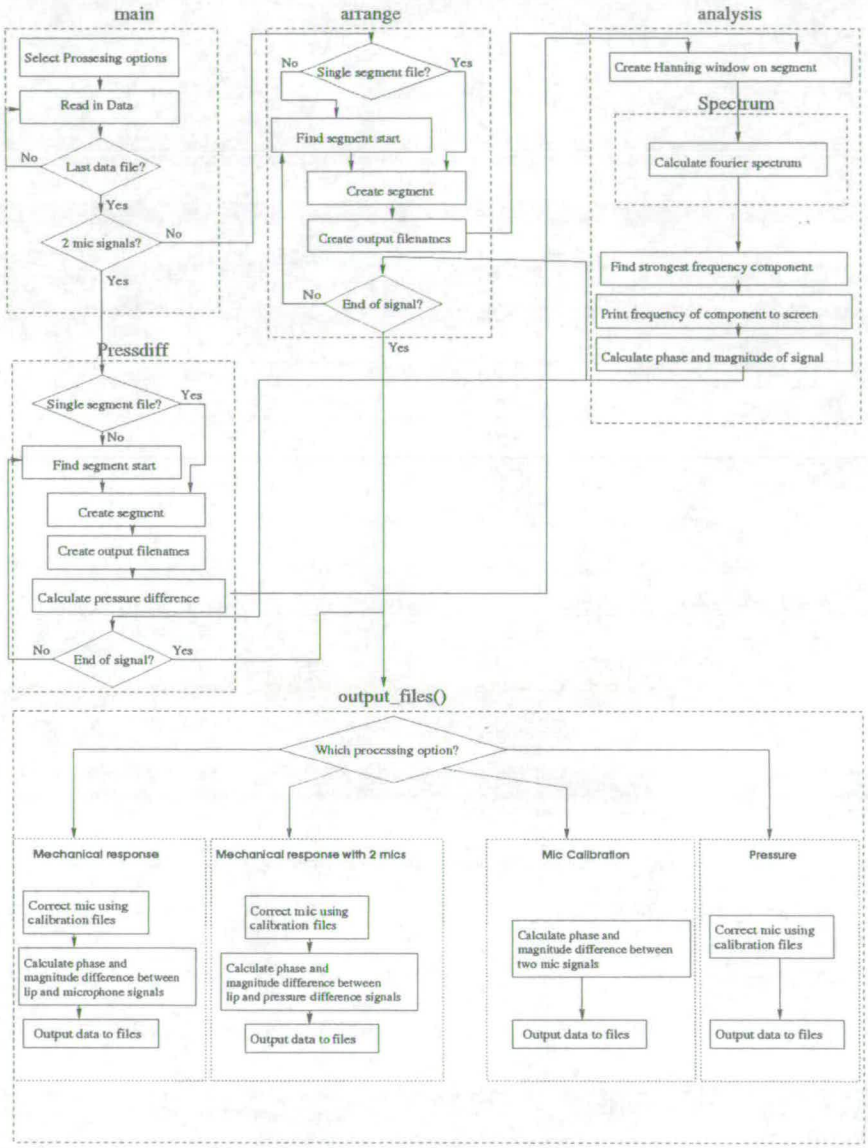

Figure A.1: Flow diagram showing the opperation of the auto.c program.

This program has a selection of four different processing options which are:

1. Analysis of the mechanical response of the lips using a microphone on one side of the lips measuring the driving signal and the diode measuring the

lip opening.

2. Analysis of the mechanical response of the lips using microphones on both sides of the lips and the diode measuring the lip opening.

3. Calibration of a microphone using one reference microphone and one uncalibrated microphone.

4. Pressure amplitude of the fundimantal frequency of a microphone signal.

Complete listing of the auto.c program is available in appendix C.

A.2 Other programs

A number of other short C programs were written to enable the quick manipulation of experimental data into the correct form for analysis using the auto.c program, or to convert the output from the auto.c program into a suitable form for display using graphing packages. A complete listing of these programs is available in Appendix C. The following is a list of these programs with a brief discussion of the operations which they perform.

- reorder.c: Reads in a four column data file and converts to a two column data file using two of the original columns as specified by the user.

- threereorder.c: Reads in a four column data files and converts to a three column data file using columns from the input file as specified by the user.

- reord3.c: Reads in a three column data file and converts to a two column data file using two of the origional columns as specified by the user.
- remtime.c: Reads in a two column data file and converts to a two column data file with time from the start of measurment as the first column and the first column from the original file as the second column.
- phasediff.c: Reads in a two column data file and calculates the phase difference between the two signals at a single frequency.
- impedmax.c: Reads in a two column data file containing frequency and amplitude and writes out the frequency of the largest amplitude.
- addtime.c: Reads in a two column data file and outputs a three column file with elapsed time from the start of measurement as the first column.
- addfreq.c: Reads in a two column data file and outputs a three column data file with frequency as the first column.

Appendix B

Lattice Boltzmann programs

B.1 Lattice Boltzmann simulation program

The Lattice Boltzmann simulation program was written in the fortran 90 programming language. A flow diagram showing the operation of this program can be seen in Figure B.1.

As can be seen from the flow diagram in Figure B.1 the simulation program takes as input two files containing the necessary information: grid.dat and in.dat.

The grid.dat file is an ascii text file which has the grid size on the first line, followed by the grid boundary specification in the form of a three column file with the x position as the first column, the y position as the second column and either a '1' or a '0' in the third column where the '1' indicates a boundary grid

point and the '0' indicates a fluid grid point.

The in.dat file contains the simulation parameters giving the initialisation values and the inflow values over the running time of the simulation. Values are also read in for how many output data files should be created and how many timesteps there should be between the output of each data file. An example 'in.dat' file is shown below:

```
Tau:
0.512
d_0
0.5
Initial_density:
1.0
No_of_output_rounds:
20
Number_of_time_steps_per_round:
1500
Initial_inflow_velocity_to_pipe:
0.0075
Time_of_initial_flow_(in_steps):
800
```

```
Final_flowrate:
0.0075
Number_of_timesteps_before_output_is_writen:
5
```

These files can either be edited using a standard text editor or can be created using the graphical interfacing program 'picsim'.

A complete listing of the Lattice Boltzmann simulation code is given in appendix C.

B.2 Graphical interface

The graphical interface program was written in the C++ programming language utilising the QT graphical interface libraries from Troltech. A flow diagram showing the full operation of this program can be seen in figure B.2.

The program reads in the data from the in.dat file and an image is saved as a bitmap (.bmp), and writes out the grid.dat and in.dat file in suitable format for the Lattice Boltzmann simulation program to read. The program creates three different windows: the edit window, the picture window and the grid window. The edit window contains two pages, each with five lines containing descriptions and an edit box for each of the variables in the file 'in.dat'. In addition there are

'Cancel' and 'Apply' buttons at the bottom of the window. The 'Cancel' button closes all the windows and exits the program whereas the 'Apply' button saves the data to file and opens up the picture window. The picture window displays the bitmap graphic which is to be converted into a text file suitable for reading by the Lattice Boltzmann program as well as providing a pull down menu. The pull down menu allows the user to load up a new image, grid and save the image or quit the program. When the grid option is selected the grid window is opened which allows the user to enter the X and Y size of the simulation grid required. The 'OK' button in the grid window causes the program to process the image and write the data to file.

A complete listing of the picsim program is given in appendix C.

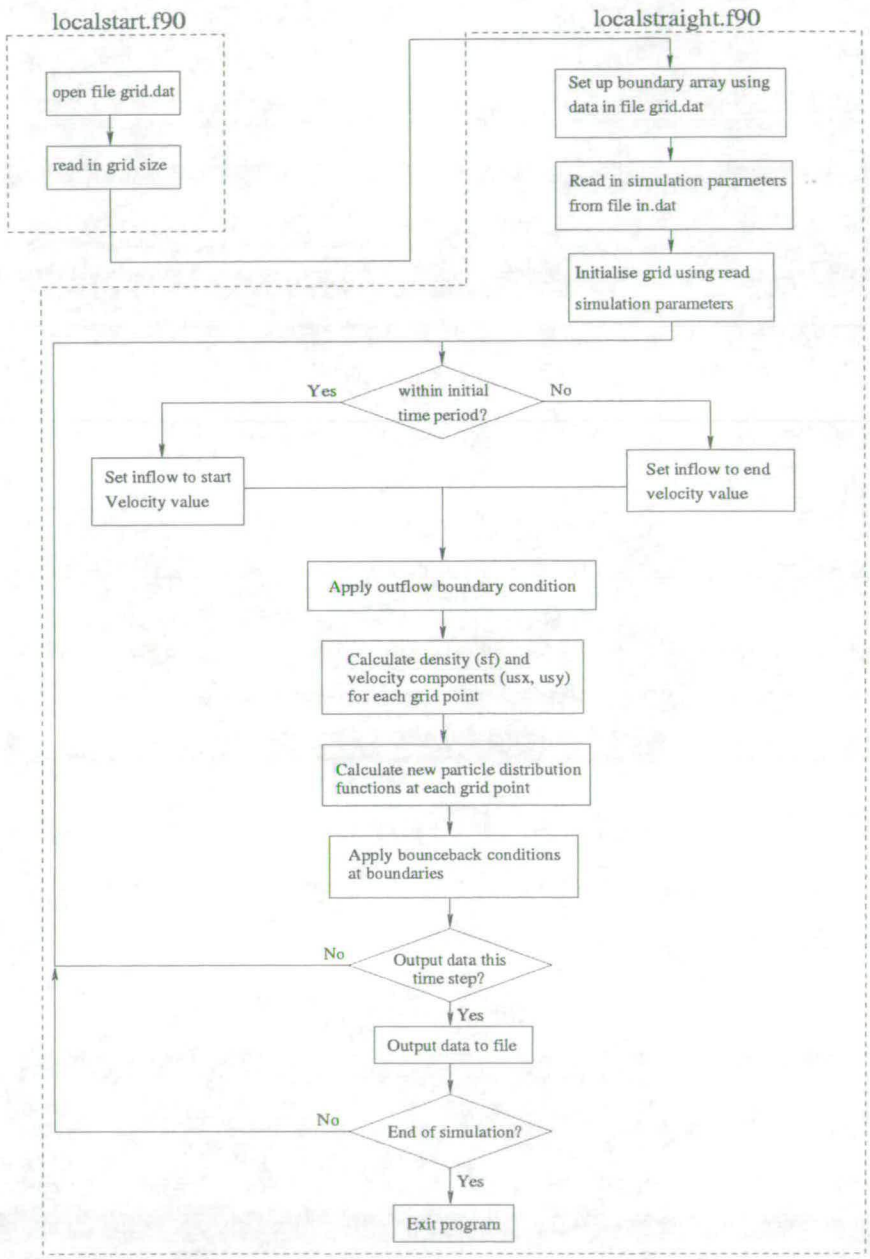

Figure B.1: Flow diagram showing the operation of the Lattice Boltzmann simulation program.

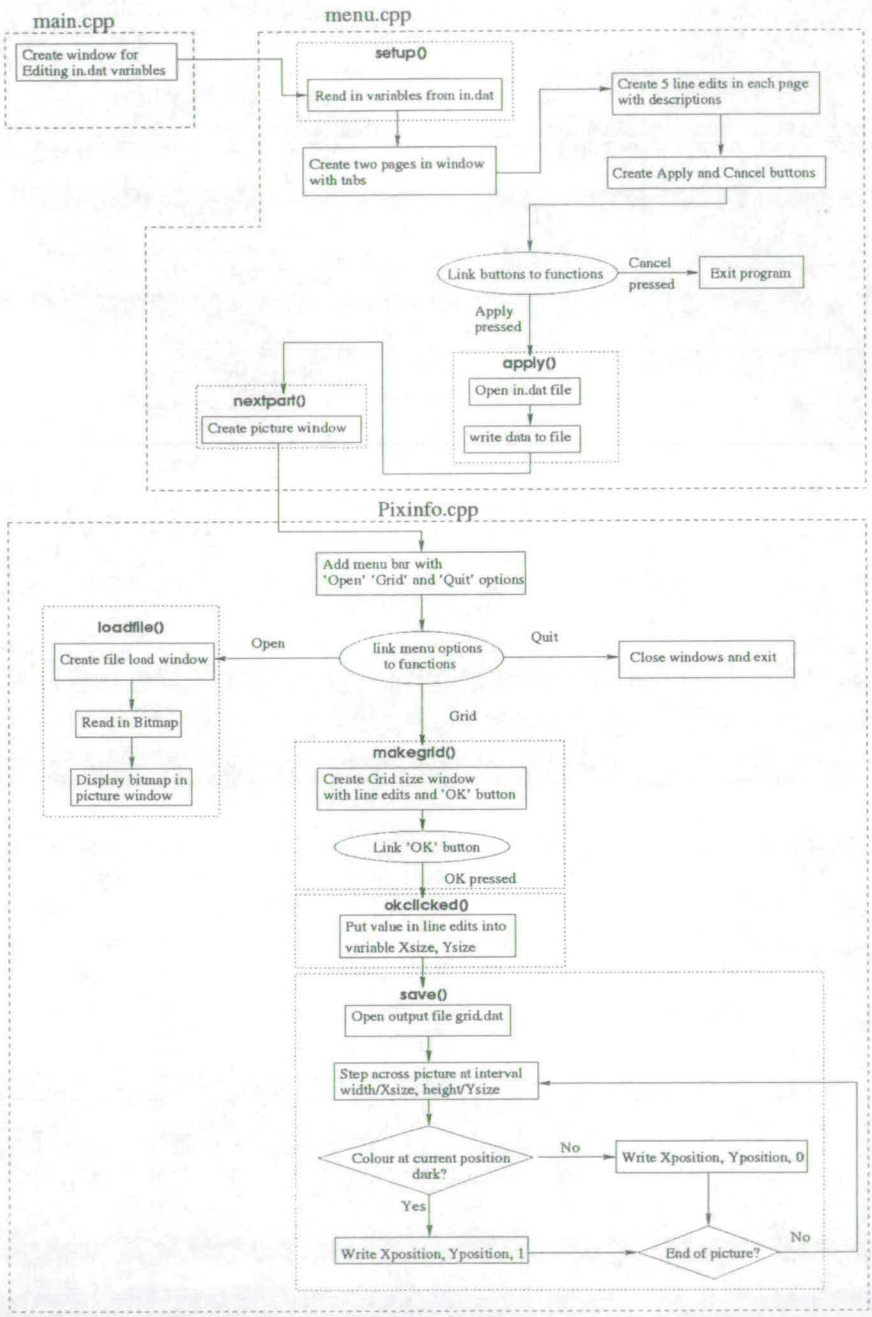

Figure B.2: Flow diagram showing the operation of the Lattice Boltzmann graphical interfacing program.

Appendix C

Program listings and simulation animations

Complete listing of the experimental analysis programs auto.c, reorder.c, three-reorder.c, reord3.c, remtime.c, phasediff.c, impedmax.c, addtime.c and addfreq.c along with the Lattice Boltzmann programs and graphical interface programs are included on the attached CD.

Animations showing the developing of the flow for each of the results shown in chapter 6 are also on the attached CD. These animations show the vorticity magnitude in the same form as shown in the diagrams in chapter 6.

Bibliography

[1] S. Adachi and M. Sato. Time-domain simulation of sound production in the brass instrument. *J.Acoust.Soc.Am.*, 97:3850–3861, 1995.

[2] S. Adachi and M. Sato. Trumpet sound simulation using a two-dimensional lip vibration model. *J.Acoust.Soc.Am.*, 99:1200–1209, 1996.

[3] N. Allenborn, K. Nandakumar, H. Raszillier, and F. Durst. Further contributions on the two-dimensional flow in a sudden expansion. *Journal of Fluid Mechanics*, 330:169–188, 1997.

[4] D. Ayers. Basic tests for models of the lip reed. In *Proc. ISMA 2001*, pages 83–86, Perugia, Italy, Sept 2001.

[5] J. Backus. Input impedance curves for the reed woodwind instruments. *J.Acoust.Soc.Am.*, 56:1266–1279, 1974.

[6] J. Backus. Input impedance curves for the brass instruments. *J.Acoust.Soc.Am.*, 60:470–480, 1976.

[7] A.H. Benade. On the propagation of sound waves in a cylindrical conduit. *J. Acoust. Soc. Am.*, 44:616–623, 1968.

[8] A.H. Benade. *Fundamentals of Musical Acoustics.* Oxford University Press, New York, 1976.

[9] D. A. Berry, H. Herzel, I.R. Titze, and K. Krischer. Interpretation of biomechanical simulations of normal and chaotic vocal fold oscillations with empirical eigenfunctions. *J. Acoust. Soc. Am.*, 95:3595–3604, 1994.

[10] J.M. Buick. *Lattice Boltzmann Methods in Interfacial Wave Modelling.* PhD thesis, The University of Edinburgh, 1997.

[11] J.M. Buick and C.A. Greated. Lattice boltzmann modeling of interfacial gravity waves. *Physics of Fluids*, 10:1490–1510, 1998.

[12] J.M. Buick, C.A. Greated, and D.M. Campbell. Lattice bgk simulation of sound waves. *Europhysics Letters*, 1:1, 1998.

[13] D.M. Campbell. Cornett acoustics: Some experimental studies. *Galpin Soc. Journal*, 49:180–196, 1996.

[14] D.M. Campbell. Nonlinear dynamics of musical reed and brass wind instruments. *Contemporary Physics*, 40:415–431, 1999.

[15] D.M. Campbell and C. Greated. *The musician's guide to acoustics.* Dent, 1987.

[16] S. Chen, W.H. Martinez, and W. Matthaeus. Lattice boltzmann model for simulation of magnetohydrodynamics. *Phys. Rev. Lett.*, 67:3776, 1991.

[17] S. Chen, Z. Wang, X. Shan, and G.D. Doolen. Lattice boltzmann computational fluid dynamics in three dimensions. *Journal of Statistical Physics*, 68:379–400, 1992.

[18] S. Chen and G. Weinreich. Nature of the lip reed. *J. Acoust. Soc. Am.*, 99:1227–1233, 1996.

[19] J.J. Connor and C.A. Brebbia. *Finite Element Techniques for Fluid Flow.* Butterworth, 1976.

[20] D.C. Copley and W.J. Strong. A stroboscopic study of lip vibrations in a trombone. *J. Acoust. Soc. Am.*, 99:1219–1226, 1996.

[21] J.S. Cullen. *A Study of Brass Instrument Acoustics using an Artificial Reed Mechanism, Laser Doppler Anemometry and other techniques.* PhD thesis, The University of Edinburgh, 2000.

[22] J.S. Cullen, J. Gilbert, and D.M. Campbell. Brass instruments: Linear stability analysis and experiments with an artificial mouth. *Acustica*, 86:704–724, 2000.

[23] M.K. Dalheimer. *Programming with QT.* O'Reilly, 1999.

[24] S.P. Dawson, S. Chen, and G. Doolen. Lattice boltzmann computations for reaction-diffusion equations. *Journal of Chemical Physics*, 98:1514, 1993.

[25] P. Dietz and N. Amir. Synthesis of trumpet tones by physical modeling. In *Proc. ISMA 1995*, Dourdan, France, 1995.

[26] F. Durst, J.C.F Pereira, and C. Tropea. The plane symmetric sudden-expansion flow at low reynolds numbers. *Journal of Fluid Mechanics*, 248:567–581, 1993.

[27] S.J. Elliott and J.M. Bowsher. Regeneration in brass wind instruments. *Journal of Sound and Vibration*, 83:181–217, 1982.

[28] R.M. Fearn, T Mullin, and K.A. Cliffe. Nonlinear flow phenomena in a symmetric sudden expansion. *Journal of Fluid Mechanics*, 211:595–608, 1990.

[29] N.H. Fletcher. Excitation mechanisms in woodwind and brass instruments. *Acustica*, 43:63–72, 1979.

[30] N.H. Fletcher. Blowing pressure, power, and spectrum in trumpet playing. *J. Acoust. Soc. Am.*, 105:874–881, 1999.

[31] N.H. Fletcher and T.D. Rossing. *The physics of musical instruments.* Springer-Verlag, 1 edition, 1991.

[32] U. Frisch, B. Hasslacher, and Y. Pomeau. Lattice-gas automata for the navier-stokes equation. *Physical Review Letters*, 56:1505–1508, 1986.

[33] J. Gilbert, S. Ponthus, and J.F. Petiot. Artificial buzzing lips and brass instruments: Experimental results. *J. Acoust. Soc. Am.*, 104:1627–1632, 1998.

[34] D. Grunau, S. Chen, and K. Eggert. A lattice boltzmann model for multiphase fluid flows. *Phys. Rev. A*, 5:2557, 1993.

[35] H.J.F. Helmholtz. *On the sensation of tones (1877).* Translated by A.J.Ellis, reprinted by Dover, 1954.

[36] A. Hirschberg, J. Gilbert, R. Msallam, and A.P.J Wijnands. Shock waves in trombones. *J. Acoust. Soc. Am.*, 99:1754–1758, 1996.

[37] R.J. Hirschberg, J. Kergomard, and G. Weinreich, editors. *Mechanics of musical instruments.* Springer–Verlag, 1995.

[38] G.C.J. Hofmans. *Vortex Sound in Confined Flows.* PhD thesis, Technische Universiteit Eindhoven, 1998.

[39] M. Krafczyk, M. Cerrolaza, M. Schulz, and E. Rank. Analysis of 3d transient blood flow passing through an artificial aortic valve by lattice-boltzmann methods. *Journal of Biomechanics*, 31:453–462, 1998.

[40] A.H.M. Kwong and A.P. Dowling. Unsteady flow in diffusers. *ASME Journal Fluids Eng.*, 116:842–847, 1994.

[41] U. Lemmin, T. Scott, and Czapski U.H. The development from two-dimensional to three-dimensional turbulence generatied by breaking waves. *Journal of Geophysical Research*, 79:3442–3448, 1974.

[42] N.J.C. Lous, G.C.J. Hofmans, R.N.J. Veldhuis, and A. Hirschberg. A symetrical two-mass vocal-fold model coupled to vocal tract and trachea, with application to prosthesis design. *Acustica*, 84:1135–1150, 1998.

[43] C. Maganza, R Causse, and F. Laloe. Bifurcuations, period doublings and chaos in clarinet-like systems. *Europhys. Letters*, 1:295–302, 1986.

[44] M. Neal, O. Richards, D.M. Campbell, and J. Gilbert. Study of the reed mechanism of brass instruments using an artificial mouth. In *Proc. ISMA 2001*, volume 1, page 99, 2001.

[45] D.R Noble, S Chen, J.G. Georgiadis, and R.O. Buckius. A constant hydrodynamic boundary condition for the lattice boltzmann method. *Phys. Fluids*, 7, 1995.

[46] J. Saneyoshi, H. Teramura, and S. Yoshikawa. Woodwind and brasswind instruments. *Acustica*, 62:194–210, 1987.

[47] D.B. Sharp and D.M. Campbell. Leak detection in pipes using acoustic pulse reflectometry. *Acustica*, 83:560–566, 1997.

[48] P. Stansell and Greated C.A. Lattice gas automation simulation of acoustic streaming in a two-dimensional pipe. *Physics of Fluids*, 9:3288–3299, 1997.

[49] Trol Tech. *www.troltech.com.*

[50] D.J. Tritton. *Physical Fluid Dynamics.* Oxford Science Publications, 1998.

[51] C. Vergez and X. Rodet. Model of the trumpet functioning: real time simulation and experiments with an artificial mouth. In *Proc. ISMA 1997 in Proc. Institute of Acoustics*, volume 19, pages 425–432, Edinburgh, UK, 1997.

[52] S. Yoshikawa. Acoustical behavior of brass player's lips. *J. Acoust. Soc. Am.*, 97:1929–1939, 1995.

[53] F.J. Young. The natural frequencies of musical horns. *Acustica*, 10:91–97, 1960.

Publications

M.A. Neal, D.M. Campbell. Study of the reed mechanism of brass instruments using an artificial mouth. In *Proc. ISMA 2001*, Perugia, Italy, September 2001.

J.M. Buick, M.A. Neal, J.A.Cosgrove, D.M. Campbell, C.A. Greated. The Lattice Boltzmann Model and its Application to Acoustics. In *Proc. 17th ICA 2001*, Rome, Italy, September 2001.

M.A. Neal, O. Richards, D.M. Campbell, J. Gilbert. Study of the reed mechanism of brass instruments using an artificial mouth. *Proc. of Institute of Acoustics Spring Conference*, Salford, UK, March 2002.